Fall 2015

Microbial Arsenic Transformation in Near Subsurface Environments

Robert James Reiter

MICROBIAL ARSENIC TRANSFORMATION IN NEAR SUBSURFACE ENVIRONMENTS

A Thesis

Submitted to the Bayer School of Natural and Environmental Sciences

Duquesne University

In partial fulfillment of the requirements for

the degree of Doctorate of Philosophy

By

Robert Reiter

December 2015

MICROBIAL ARSENIC TRANSFORMATION IN NEAR SUBSURFACE ENVIRONMENTS

By

Robert Reiter

Approved November 6, 2015

_____	_____
Dr. John F. Stolz Professor of Biology (Committee Chair)	Dr. Peter Castric Professor of Biology (Committee Member)
_____	_____
Dr. Nancy Trun Associate Professor of Biology (Committee Member)	Dr. Partha Basu Professor of Chemistry (Committee Member)

_____

Dr. Philip Reeder
Dean and Professor
Bayer School of Natural and Environmental Sciences

ABSTRACT

MICROBIAL ARSENIC TRANSFORMATION IN NEAR SUBSURFACE ENVIRONMENTS

By

Robert Reiter

December 2015

Dissertation supervised by Dr. John F. Stolz.

In the first part of this study, environmental bacterial arsenic transformation was investigated in anthropogenically arsenic contaminated subsurface sediments from the former Vineland Chemical Company in Vineland, NJ. Subsurface sediments from the vadose (371 mg/kg arsenic) and aquifer (81 mg/kg arsenic) zones and an off-site surface sediment (0.7 mg/kg arsenic; control) were used as inocula for enrichment cultures with selective media to assess for microbial arsenic metabolic activity. Arsenite (As(III)), monomethyl arsenic acid (MMA) and dimethyl arsenic acid (DMA) were provided as electron donors, while arsenate (As(V)) was provided as an electron acceptor. An anion exchange chromatography method with conductivity and UV/Vis detection was developed and utilized to investigate arsenic transformations under each selective condition.

While demethylation and arsenite oxidation were not observed, there was strong As(V) reduction to As(III) activity in the enrichments amended with lactate and As(V). Polymerase chain reaction (PCR) was used to amplify *arrA* and *arsC* genes, followed by cloning and sequencing. Both vadose and aquifer enrichments gave positive results for *arrA* (respiratory arsenate reductase) and *arsC* (arsenic resistance), while only *ars*C amplified from the off-site. Both 16S rRNA genes and the ribosomal intergenic spacer (RIS) genes were used to assess community diversity. The results indicate a diverse community with As(V) respiring bacteria.

In the second part of this study, the utility of ion chromatography (IC) in speciating inorganic (As(V), As(III)) and organic (MMA, DMA) was assessed. The As(V) and roxarsone respiring *Alkaliphilus oremlandii* OhILAs was cultured and the spent medium analyzed. Under the conditions used, OhILAs failed to produce any As(III) and As(V) when grown on roxarsone and lactate; however, As(V) to As(III) reduction was observed when grown in the presence of lactate and As(V).

In the third part of this study, microcosms were used to assess bacterial arsenic transformation in cores from a coal ash impoundment. A medium was formulated based on the water chemistry of the system. As(V) respiration was detected at all four depths tested (0-2m; 2-4m, 4-6m, and 8-10m), with the surface sediments showing the greatest rates.

DEDICATION

I would like to dedicate this work to my beloved and late father, Robert Reiter.

ACKNOWLEDGEMENTS

I would like to thank Dr. Stolz and the entire Stolz lab for allowing me to experience years of lab research in such a fascinating field of study and great working environment. More specifically, I would like to thank Rishu Dheer, Lucas Eastham, Jennifer Rutter, Samir Joshi and Oliver Dugas for their assistance in multiple facets of my thesis research. I would like to thank my committee members, Dr. Basu, Dr. Castric and Dr. Trun for all the support, helpful advice and guidance they provided. I would also like to thank Dr. Chuck Welsh for being such a supportive mentor and friend during my time working under him as a lab instructor. Additionally, I would like to thank Dr. Kyle Bibby from the University of Pittsburgh for allowing me to perform high-throughput 16S rDNA sequencing in his laboratory. Lastly, thank you to the Duquesne University Department of Biological Sciences for funding my education, teaching and research, as well as all of the faculty and staff within the department that have provided me with teaching, support and guidance.

TABLE OF CONTENTS

LIST OF TABLES

LIST OF FIGURES

Chapter I. Arsenic Background

A. Chemistry of Arsenic

Arsenic is a metalloid that is widespread in nature despite its low crustal abundance (0.001%) and can be found the air, soils, sediments, and water bodies as well as within many living organisms [1-3]. Occurring in both inorganic and organic forms, its common oxidation states are As(-III), As(0), As(III) and As(V) with the latter two being the most prevalent [2-6]. Volatile inorganic and methylated As(-III) containing arsines (H_3As, CH_5As, C_2H_7As, C_3H_9As) can occur in trace amounts in some anaerobic environments while elemental arsenic [As(0)] is extremely rare [1-3,6-8]. As(III) most commonly exists in anoxic environments in the form of the compound known as arsenite ($H_2AsO_3^-$ or $HAsO_3^{2-}$), while As(V) is predominantly found as arsenate ($HAsO_4^{2-}$ or $H2AsO_4^-$) in aerobic environments [2,6]. Arsenate adsorbs to several common minerals including aluminum and iron containing sediments which renders it largely hydrologically immobile, while arsenite commonly exists in the aqueous phase and is, thus, the more mobile of the two [2,3,6]. Methylated arsenicals (methylarsenic) are commonly found in nature, largely as the result of a highly conserved inorganic arsenic methylation pathway (which will be discussed in greater depth later) and primarily possess arsenic in the trivalent [As(III)] or pentavalent [As(V)] oxidation states[1-3,6-8]. Trivalent methylarsenicals include monomethylarsonous acid [MMA(III)] and dimethylarsinous acid [DMA(III)], while the pentavalent varieties include monomethylarsonic acid [MMA(V)] and dimethylarsinic acid [DMA(V)].

The anionic charge of inorganic and methylated arsenicals in nature is dependent upon the pKa of the hydroxyl group(s) and, thus, varies according to the pH of the environment in which they are present. Acidic environments (pH < 7) will favor the protonated forms of the hydroxyl groups (OH) while deprotonated forms will be favored under basic conditions (pH > 7). The pK_a of several arsenicals can be found in **Table 1.1** **Figure 1.1** demonstrates the structures of these compounds assuming a neutral pH (7).

B. History of Arsenic

Arsenic has been historically used by humans for a variety of purposes, some dating back thousands of years ago. In ancient times, arsenicals were utilized as metallurgic tools for the purification of iron from its ores during smelting operations [9]. Copper-arsenic alloy, also referred to as "arsenic bronze" resulting from the smelting of copper ores was extensively used during this time period in the production of glass, mirrors and statues [10]. The arsenic containing mineral arsenic trisulfide (As_2S_3), commonly referred to as "orpiment" or "orphiment" was commonly used as an ornamental pigment included in many paintings, household items and decorations due to its brilliant yellow color highly reminiscent of that displayed by gold [10]. Another sulfur containing arsenical, tetraarsenic tetrasulfide (As_4S_4), commonly referred to as "realgar" was used for similar purposes due to its red color found appealing by many [10]. Orpiment and realgar also became widely popular in a multitude of ancient civilizations as an externally applied medicinal agent used for the treatment of variety of skin conditions such as ulcers, fungal infections, as well as the removal of unwanted hair [10,13].

Arsenical	pKa_1	pKa_2	pKa_3	Reference
As(V)	2.3	6.7	11.6	[11]
MMA(V)	2.6	8.2	N/A	[12]
DMA(V)	6.2	—	—	[11]
TMAO	3.6	—	—	[12]
As(III)	9.2	12.1	13.4	[12]

Table 1.1. pKa values of several common arsenic oxyanions.

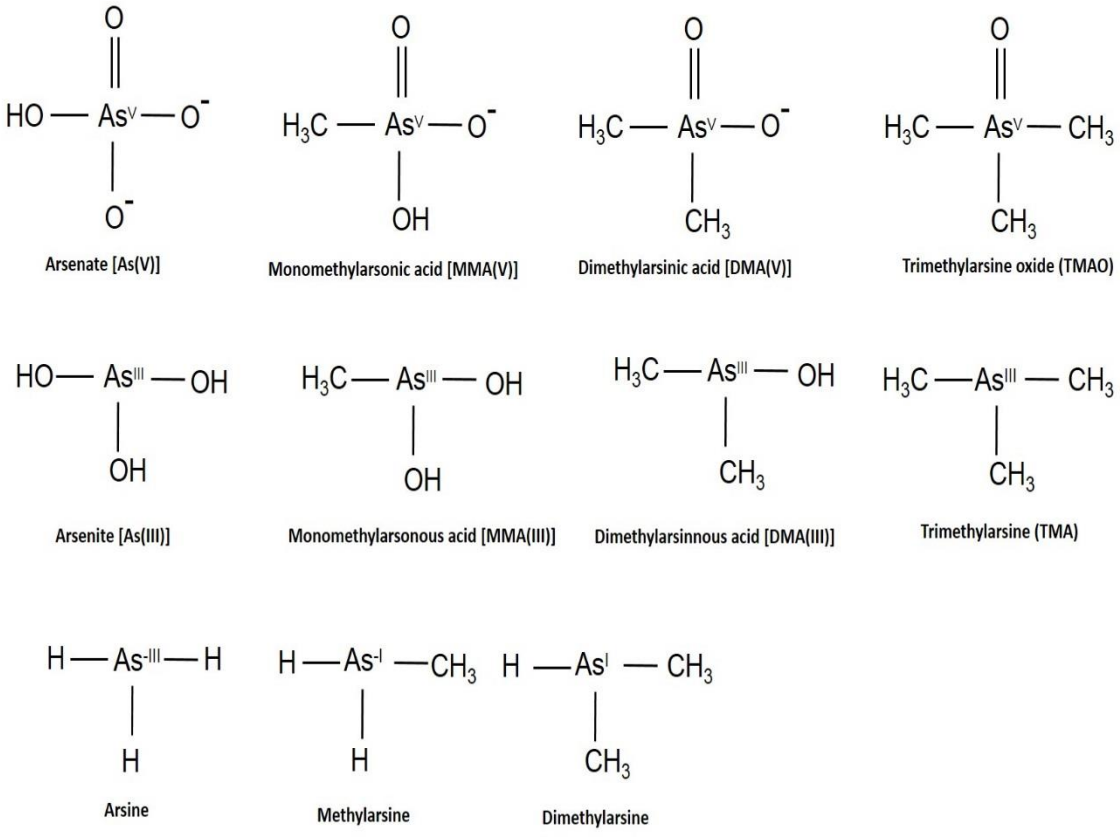

Figure 1.1. Structures of several arsenicals. Superscripts on As atoms indicate oxidation states. Charges of compounds reflect a neutral pH (7.0).

Metallic (elemental) arsenic was not discovered or distinguished from mineral arsenic (i.e. orpiment, realgar) until the medieval period during the 13th century[10]. It was during the medieval period that arsenic gained its notoriety for being a potent poison and homicidal agent. The As(III)-containing compound known as arsenic trioxide (As_2O_3) or "white arsenic" **(Figure 1.2)** was discovered and its odorless, tasteless, colorless and, therefore, undetectable nature made it ideal for suicide or murder – which led to the murders of many prominent political figures and unsuspecting husbands of unhappy wives[14]. The symptoms suffered by poisoned victims (i.e. vomiting, diarrhea, nausea, etc.) resembled those of many common diseases of the time period, making it difficult to attribute their deaths to arsenic poisoning [14]. Thus, numerous murderers walked away unscathed by the legal system after committing such crimes, prompting nicknames for arsenic such as the "poison of kings" and "king of poisons." [15] However, in 1836, James Marsh published an effective technique for post-mortem arsenic poisoning testing, later referred to as the "Marsh Test" that could prove when arsenic was used as a murdering tool, preventing the future possibility of such a crime going unpunished [16]. Briefly, the forensic sample of interest, suspected to contain arsenic was added to a U-tube apparatus filled with dilute sulfuric acid and a piece of zinc metal. If the sample is indeed arsenic positive, the reaction will generate H_2 (hydrogen gas) and H_3As (arsine gas), with the latter being detected by flaming the gas and exposing the flame to a ceramic glass filled with cold water, on which a black residue of elemental arsenic will form, readily capable of being detected by the naked eye [17].

Intentional arsenic poisonings have, unfortunately, still been committed after the Marsh Test surfaced however, with the most recent case occurring in 2003 where an individual allegedly laced coffee with arsenic at a church meeting in Maine which resulted in the death of a man [18].

The discovery of elemental arsenic created a boom in the number of inorganic and organic arsenicals being synthesized and characterized, thus increasing the variety of arsenicals used in medicine [10]. Throughout the 18th century, a variety of medicinal arsenicals were prescribed by physicians to be administered topically, internally (inhalation, ingestion, rectal administration), intravenously and hypodermically as sedatives, antiseptics, antipyretics, caustics, tonics among other things [13,19]. In the 18th century, a tonic composed of arsenic trioxide dissolved in potassium bicarbonate was prepared by Dr. Thomas Fowler, which rapidly gained popularity with doctors for its therapeutic value. This solution, which became known as "Fowler's solution" was widely utilized in the treatment of a variety of human conditions including leukemia, integumentary system disorders (i.e. psoriasis, dermatitis, eczema), disorders of the oral cavity (gingivitis, stomatitis), epilepsy, anemia, asthma, convulsions, heart palpitations, rheumatism as well as several other diseases [19,20]. While Fowler's solution was successfully used in the treatment of an extensive list of human ailments (most notably leukemia) between the 18h and 20th centuries, the risks associated with long-term usage of this medicine became increasingly clear, as patients receiving Fowler's solution over extended periods of time developed diseases such as cancers of the skin, liver, lung, nasopharynx, bladder, and lymphatic tissue [20-22].

This evidence, along with the emergence of innovative cancer therapeutic techniques such as radiotherapy and cytotoxic chemotherapy, led to the discontinuation of Fowler's solution by the late 20th century [13,19,23]. In the early 20th century, Dr. Paul Ehrlich developed an organic arsenical known as arsphenamine ($C_{12}H_{12}As_2N_2O_2$) or "Salvarsan" **(Figure 1.3)** that proved to be highly effective in the treatment of protozoan trypanosome infections (trypanosomiasis) and the potentially deadly sexually transmitted disease, syphilis [13,24-26]. This was the most common treatment for syphilis in the 20th century prior to the discovery of the now highly popular and commonly used antibiotic drug, penicillin [13,19,23]. Although Fowler's solution has been discontinued in modern days to its intrinsic toxicity, arsenic trioxide (the active ingredient in Fowler's solution) has been studied more carefully and is currently an approved and highly successful treatment administered intravenously at low doses to patients suffering from newly diagnosed or relapsed acute promyelocytic leukemia (ACL)[27-31]. While acute and chronic doses of arsenic at higher concentrations have undeniably shown to be extremely toxic and deadly to humans, more minuscule doses actually have very powerful medicinal and therapeutic properties.

C. Arsenic in the Environment

Arsenic can be found in air, waters, soils, sediments, as well as inside of living organisms. While arsenic is only the 20th most common element found within the Earth's crust, it has found a multitude of ways to spread throughout our surroundings [1]. The accumulation of arsenic in our environment can be attributed to two causes: (1) natural release and (2) anthropogenic contamination.

Natural sources of arsenic distribution on the planet include volcanic eruptions, downhill weathering and forest fires, and can pose a significant risk to human health across the globe. . However, it has been suggested that anthropogenic sources of arsenic accumulation in the environment outweigh those caused by nature by as much as three-fold [1,29]. Dating back to ancient times, arsenic, which was a common constituent of copper, gold and lead ores was released in copious amounts into the environment in smoke during the metallurgic smelting of these metals [10]. Arsenic, both inorganic and organic, has been produced and sold industrially in products such as pesticides, herbicides, medicines, paints, dyes, wood preservatives, desiccants and chemical warfare agents, all of which have contributed to its presence in the environment [1,3]. While most of these products (notably inorganic arsenic) have been discontinued due to the risks they bestow on the environment and human health, there are still chemicals currently being produced industrially that are organoarsenical based. One such example is the chemical included in broiler chicken feed known as roxarsone (**Figure 1.4**; 3-nitro-4-hydroxybenzene arsonic acid). The continued use of this compound in chicken feed presents a significant environmental threat, as it is passed to soils in stool and subsequently biodegraded by fecal and soil bacteria into highly toxic inorganic arsenic [30]. Methylarsenicals are currently being used in various herbicidal chemicals available commercially. While the EPA has ordered the production of these herbicides to cease following December 31, 2013 [31], products of this nature currently remain on the market.

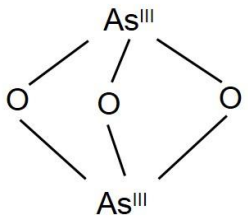

Figure 1.2. Arsenic trioxide structure.

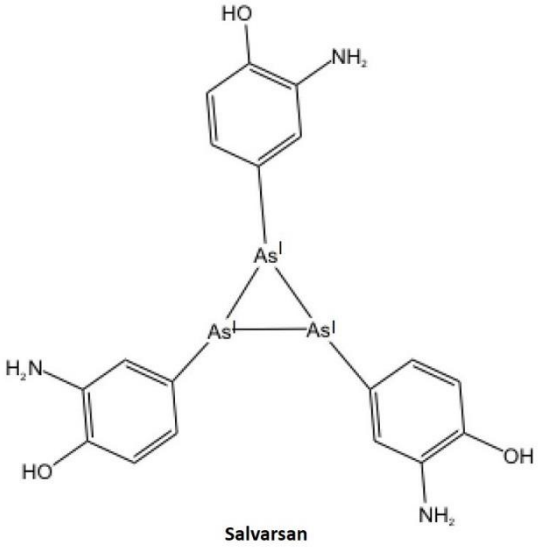

Figure 1.3. Salvarsan structure.

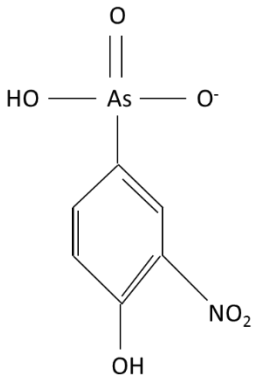

Figure 1.4. Roxarsone structure.

The MMA(V)-based compound Monosodium methylarsonate (MSMA) herbicides are currently being used to control weeds on various golf courses in the United States [32]. This poses a risk to aquifer groundwater systems surrounding these areas, as arsenic has been shown to migrate to the lake water and subsurface sediments in the golf courses [32]. Recent data has been published demonstrating that, similar to the fate of roxarsone in chicken litter, the methylarsenic in this herbicide is biotransformed in soil into a highly toxic methylated form [1]as well as inorganic arsenite by bacteria, making the use of this herbicide a potential risk to the environment and human health [33].

D. Arsenic Toxicity

Arsenic is widely infamous for being highly poisonous and lethal to human beings. Most people who have heard of arsenic typically associate the element with death, largely attributed to its title as the single most common homicidal poisoning agent in the history of man; thus, it comes as no surprise that arsenic is toxic to all forms of life at certain levels [1,7,29,34,35]. Humans can be exposed to arsenic through contaminated air, food or water with the latter being the most prevalent route[1,36,37]. Acute arsenic exposure in humans can lead to symptoms such as gastrointestinal (GI) tract discomfort, nausea, vomiting, diarrhea, bloody stool as well as anemia[36,37]. Long-term exposure to arsenic has occurred most prevalently through the ingestion of contaminated drinking which is the leading cause of chronic arsenic poisoning, often referred to as "arsenicosis", in the world [36]. Unfortunately, arsenicosis can detrimentally affect virtually every organ system in the human body [1,7,36]. One of the hallmark symptoms of arsenicosis is integumentary system disruption (skin disorders) [1,29,35-37].

Lesions of the skin are highly common and can manifest in the form of keratosis (growths) and/or pigmentation (spots) [1,7,36,38]. Coinciding with the abnormalities of the skin, arsenicosis sufferers have also been shown to experience diabetes mellitus, cancers of various organs as well as pulmonary, liver, cardiovascular, gastrointestinal, hematological, neurological and immunological diseases [1,7,36]. The reproductive system is also affected by arsenicosis; thus, embryonic development can occur irregularly and create stillbirths and birth defects in newborn infants [37].

The acute and chronic toxicity of arsenic varies in severity and mechanism depending on its oxidation state and chemical form [29,35,39]. As(V) strongly mimics phosphate structurally and chemically and replaces phosphate in many key intracellular pathway [29,35,40]. The substitution of As(V) for phosphate deactivates several compounds in the cell and leads to their rapid hydrolysis, a process referred to as "arsenolysis." [40] Such an event inhibits critical intracellular processes such as substrate-level and oxidative phosphorylation, depriving cells of ATP required for normal functioning and leading to cell death [2,3,35,40] (**Figure 1.5a**). In humans, As(V) exposure causes severe ATP depletions in erythrocytes, creating morphological impairments that can lead to a variety of chronic vascular diseases[41]. As(III), on the other hand, operates under an entirely different toxicity mechanism, targeting and binding thiol (SH) groups of enzymes and/or their SH-containing cofactors, causing an impairment of their function [2,3] (**Figure 1.5b.**). As(III) has a strong binding affinity for the pyruvate dehydrogenase enzyme which is crucial to the citric acid cycle, consequently preventing ATP production[42-46]. As(III) has also been shown to inhibit the expression of critical genes in DNA damage repair pathways, which can contribute to carcinogenesis[47].

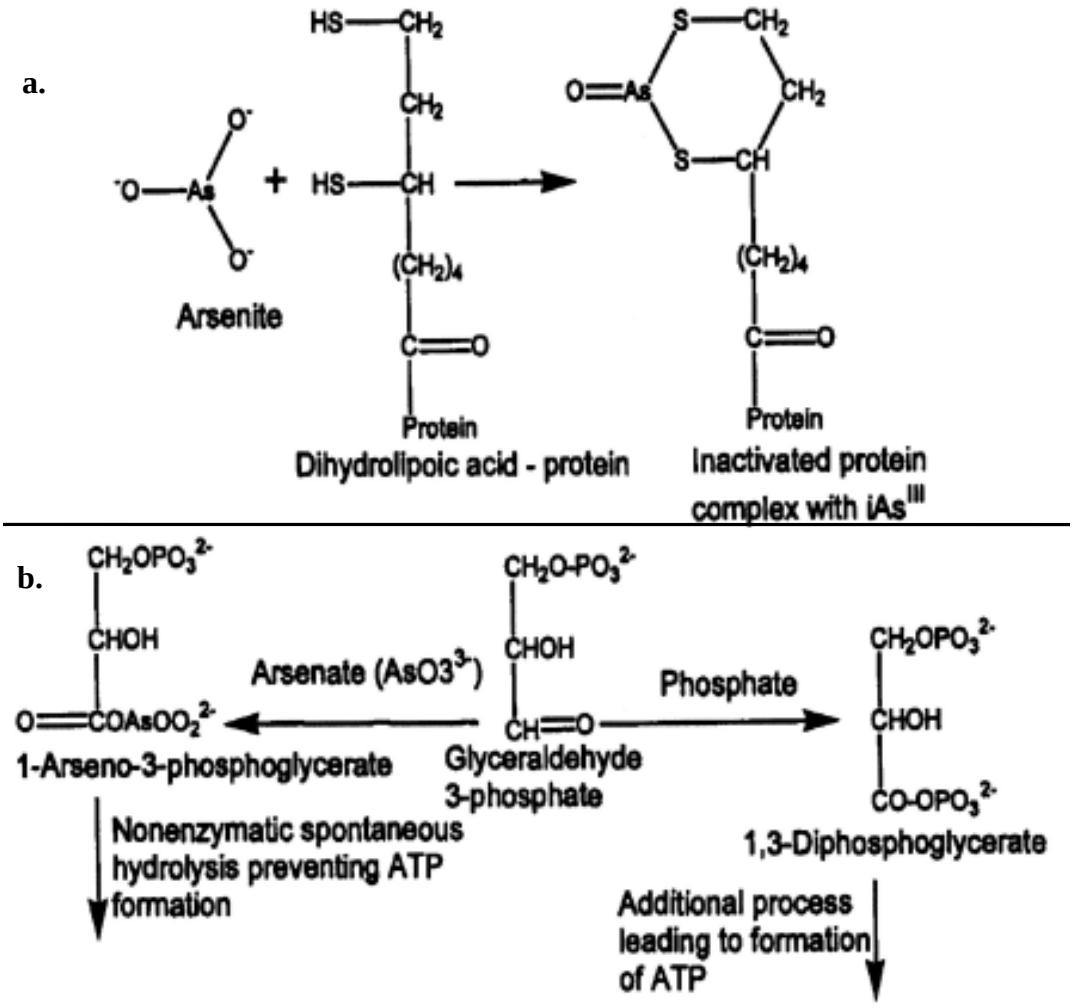

Figure 1.5. Mechanisms of inorganic arsenic toxicity. As(III) binds sulfhydryl groups of proteins and/or cofactors and inhibits them (**a**)**.** As(V) mimics phosphate thus preventing ATP formation during glycolysis and cell respiration (**b**). Adapted with permission from Akter, 2005 [29].

Inorganic arsenic methylation, which will be discussed later, is a highly conserved pathway in bacteria, fungi and animals that for years was depicted as a detoxification pathway [48,49]. Therefore, methylarsenicals have historically been known as safer varieties than their inorganic parent compounds. However, it was revealed that trivalent methylarsenicals [MMA(III) and DMA(III)] are greater inhibitors of glutathione (GSH) reductase as well as thioredoxin reductase *in vitro* than their inorganic [As(III)] or pentavalent [MMA(V) and DMA(V)] counterparts, raising questions about the validity of the original theory suggesting a "detoxification" purpose for the methylation cascade[47,48]. Additional research conducted in the early 21st century indicated that both *in vitro* and *in vivo*, MMA(III) has a higher acute toxicity value (lower LC_{50}) than As(III) [49,50]. Thus, there are key intermediates in the arsenic methylation cascade are actually more toxic than their inorganic predecessors, contradicting the initial belief that this mechanism operates strictly for detoxification purposes. More recent publications provide evidence suggesting As(III)-based methylarsenicals may be more toxic than the inorganic species and suggests the following toxicity hierarchy: MMA(III) = DMA(III) > As(III) > As(V) > MMA(V) = DMA(V) [29,51]. Recently, the mechanisms underlying the highly carcinogenic properties possessed by trivalent arsenicals [As(III), MMA(III), DMA(III)] have been heavily explored. Current research suggests that the carcinogenicity of these arsenicals can be attributed largely to the generation of reactive oxygen species (ROS), rather than direct binding of As(III) with sulfhydryl groups of proteins [14]. Excessive generation of ROS can cause chromosomal aberrations, DNA mutations, DNA repair inhibition, altered DNA methylation, loss of normal apoptosis and deficiencies in cellular signal transduction pathways [14].

Compound`	**LC_{50} (µM)**	**Cell Type**	**Reference**
As(V)	571	Human epidermoid carcinoma A431 cells	39
As(III)	5.49	Human epidermoid carcinoma A431 cells	39
MMA(III)	6	Chang human hepatocytes	49
DMA(III)	2.16	Human epidermoid carcinoma A431 cells	39
MMA(V)		N/A	N/A
DMA(V)	843	Human epidermoid carcinoma A431 cells	39

Table 1.2. LC_{50} values of several arsenic oxyanions of toxicological interest.

Regardless of which arsenic species reigns superior as being the most deadly, exposure has been shown to be mutagenic, carcinogenic, and teratogenic in nature [11,7]. The LC_{50} values of arsenicals of toxicological interest can be found in **Table 1.2**. As previously discussed, the most common cause of arsenicosis in human beings is through the ingestion of contaminated water. Over 30 countries throughout the world have documented arsenicosis cases resulting from arsenic-enriched groundwater that is relied upon by the human population for drinking purposes [1, 27, 38-38, 52]. The most massive and lethal case of arsenicosis outbreak in the world's history occurred in South Asia in Bangladesh and West Bengal, India, where aquifers relied upon by the human population for drinking water have become heavily enriched with arsenic [3,55,56]. The World Health Organization (WHO) recommends that groundwater sources maintain an arsenic maximum contaminant level (MCL) of 10 µg/l (ppb) [27]. The United States Environmental Protection Agency (EPA) has abided by this guideline, while Bangladesh has set their limit to 50 ppb [27, 31]. Groundwater arsenic concentrations in West Bengal and Bangladesh have been measured at levels heavily exceeding the aforementioned governmental MCL guidelines – reaching arsenic concentrations up to 2,500 and 3,200 ppb, respectively [27,28]. With millions of people relying on this groundwater as a drinking supply, this catastrophic contamination has led to disease and death from arsenicosis in thousands of human beings populating these South Asian territories [1, 27]. This contamination is not the result of an anthropogenic source, but rather from the release of naturally occurring arsenic bound to subsurface sediments into the groundwater supplies [3, 27]. Subsurface As(V) is commonly adsorbed to a variety of minerals, including apatite, pyrite as well as aluminum and iron (hydr)oxides [27].

A variety of (bio)geochemical processes can lead to the release of aqueous arsenic from its solid phase and several hypotheses have been presented aimed at fully understanding how such a contamination has occurred at these two locations [139]. These hypotheses will be discussed in further detail in the section discussing bacterial arsenic mobilization and include mechanisms such as reduction of Fe(III) containing minerals, reduction of As(V) bound to Fe(III) and Al(III)-containing minerals, release from sulfide minerals, as well as release from apatite during bacterial nutrient acquisition. It is likely that a combination of multiple (bio)geochemical processes have contributed to this devastating phenomenon and millions of people in Southeast Asia drinking from these water wells currently remain exposed. Other countries with documented groundwater arsenic contaminations due to various anthropogenic and natural sources include Vietnam, Thailand, Taiwan, Cambodia, China, Hungary, Mongolia, Argentina, Chile, Brazil, Mexico, Germany, Spain, Greece, United Kingdom, Ghana, United States and Canada [1, 37].

Once arsenicosis has been diagnosed, treatment options are available to limit any further health manifestations induced by the arsenic poisoning. First and foremost, the source of contamination must be immediately eliminated (most commonly the discontinued ingestion of contaminated water). Once the point source is identified and eliminated, it is necessary to prevent any further detrimental physiological effects that may be introduced by the remaining arsenic in the system. To neutralize the arsenic, chelating agents are often used as a therapeutic strategy [37]. Chelating drugs used for such purposes include dimercapto succinic acid (DMSA) and dimercapto propanol [37]. Other treatment strategies include disease specific therapies, such as various chemotherapies for cancer that may have resulted.

E. Arsenic metabolism

Although arsenic's notorious reputation of being a potent killer precedes it, its biochemical transformation is a feat shared by life forms spanning both the prokaryotic and eukaryotic kingdoms, ranging from unicellular bacteria and yeast to fungi, mammals and human beings [1,2,4-6,55]. While all eukaryotes and many prokaryotes perform these reactions merely as a resistance strategy, multiple representatives of the latter have been described that metabolize toxic arsenic for energy acquisition and growth [2-6]. Examples of common biological arsenic transformations include methylation, reduction, oxidation, demethylation and others. Arsenic transforming organisms are dispersed throughout the prokaryotic kingdom and include members of Gram positive, Archaea, and Proteobacteria groups [2]. Arsenic transforming prokaryotes can be categorized based on the nature and biochemical role of each reaction occurring.

i. Methylation

The notion that living organisms are capable of metabolizing such a toxic metalloid stemmed from the work of 19th century biologists who observed that certain fungi produce a peculiar garlic-like odor when grown in the presence of arsenic [52]. During 1800's, bright-green wallpapers containing the compound copper arsenite ($CuHAsO_3$) were produced industrially and present in the majority of homes [52]. Unfortunately, this practice led to the fatalities of a slew of homeowners exposed to arsenic through the accidental inhalation of volatilized particles emanating from these wallpapers [52].

The foul smelling odor was always present in the rooms in which accidental and fatal poisonings occurred, suggesting that perhaps fungal microorganisms were responsible for the liberation of gaseous arsenicals contaminating these homes [52]. The Italian physician, Bartolomeo Gosio, further investigated the hypothesis that microorganisms were responsible for the volatilization of arsenic from copper arsenite containing wallpapers by developing a microbiological test for the presence of arsenic in a material. He incubated the material with the fungus *Scopulariopsis brevicaulis* and determined arsenic was present if the garlic odor resulted, which would later be coined as "Gosio gas." [52]. Frederick Challenger and his associated would later identify "Gosio gas" as the volatile arsenical trimethylarsine (TMA) [52]. Challenger and his coworkers showed that inorganic arsenic was being biologically converted to volatile TMA by the fungus *S. brevicaulis* by a distinct methylation pathway **(Figure 1.6)**. Years of subsequent research have strongly supported this conclusion [1,6,29,52,53,53-55].

Challenger and his associates demonstrated the methylation of arsenate to TMA with intermediates including As(III), MMA(III), MMA (V), DMA(III) , DMA(V), as well as TMAO [52,53,55]. This sequential methylation is a multi-step reaction, with reductions of As(V) containing intermediates followed by oxidative methylation of the resulting As(III) containing compounds [6,52,53,55]. In 1985, the methyl group donor in the process (and oxidizing agent) was shown to be S-adenosylmethionine (SAM\ [56]. During the methylation cascade SAM liberates a single methyl group and is converted to S-adenosylhomocysteine. **Figure 1.7** shows a modern model of the original Challenger pathway with the inclusion of SAM as the methyl donor.

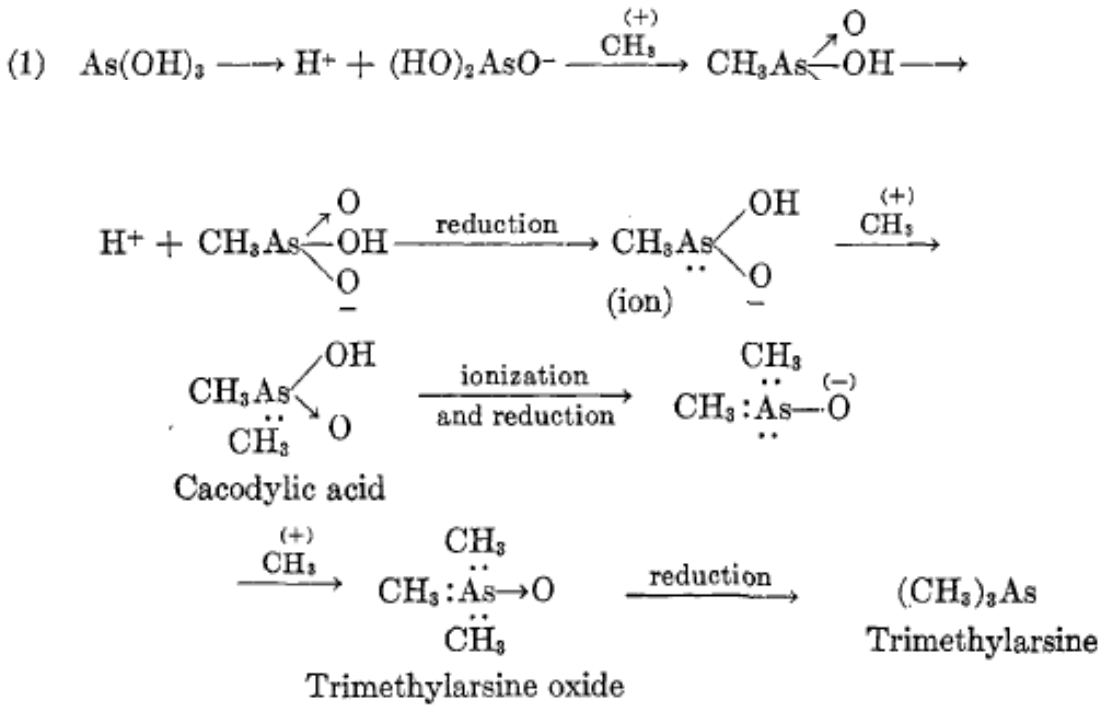

Figure 1.6. Challenger pathway of biological arsenic methylation. As(V) is first reduced to As(III) (not shown) and then oxidatively methylated. The resulting methylated pentavalent arsenical is reduced and the cycle repeats – reduction followed by oxidative methylation. The entire pathway if completed yields volatile TMA from As(V). Adapted with permission from Challenger, 1945 [53].

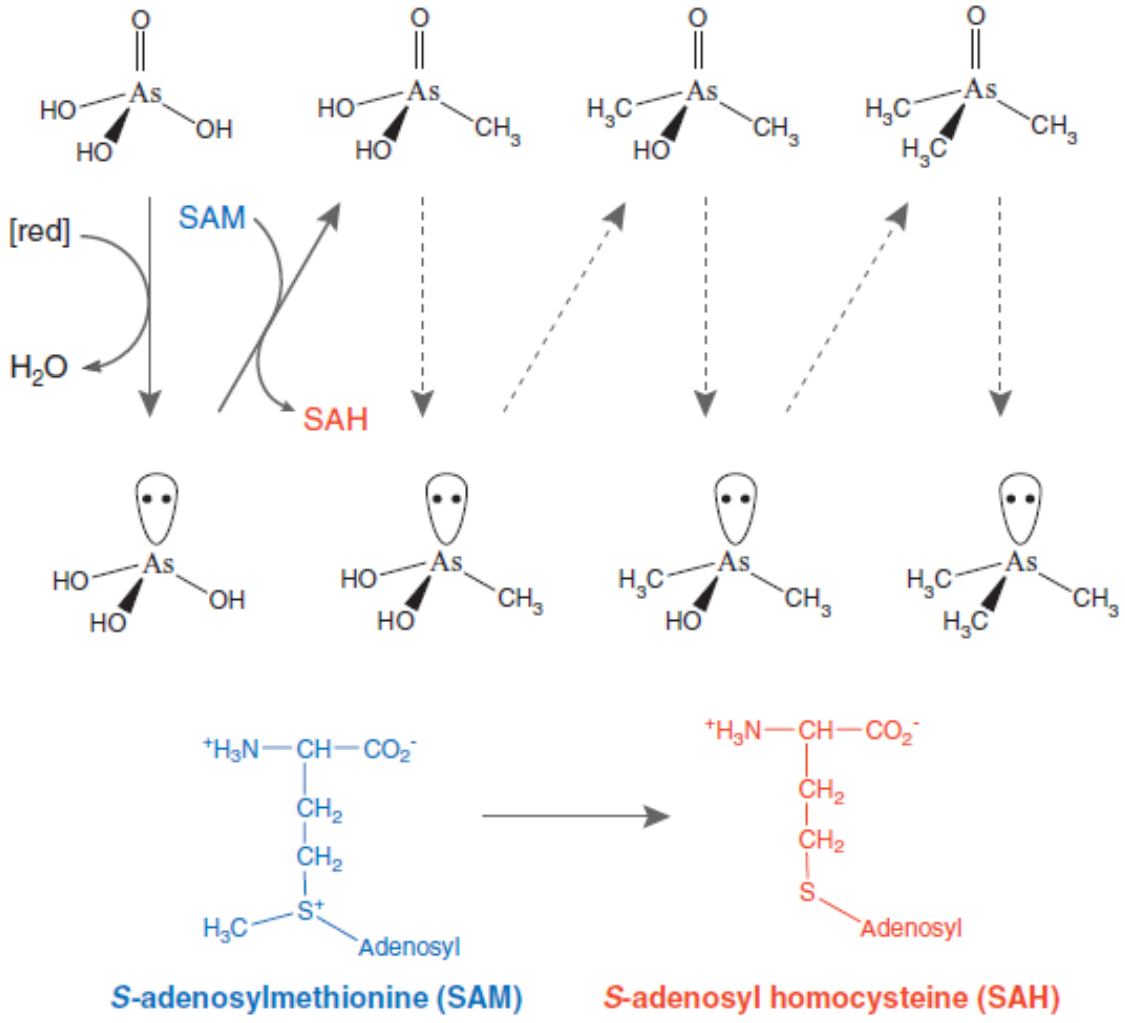

Figure 1.7. Challenger pathway of biological arsenic methylation with the inclusion of SAM as the methyl donor. The liberation of the single methyl group converts SAM to SAH. Adapted with permission from Stolz, 2006 [6].

While Challenger and his coworkers were only able to obtain evidence of arsenic methylation by a fungal species, decades of additional research conducted by other researchers verified that arsenic methylation is an extremely conserved pathway spanning multiple phylogenies of life including many prokaryotes as well as higher eukaryotes such as many plants and animals, as well as all human beings [14,52,53,57-62]. As previously discussed, this highly conserved pathway was originally thought to be solely for detoxification purposes but recent data conflicts with this widely supported hypothesis, as some of the intermediates produced are more toxic than the highly toxic As(III) parental compound (references While the methylation pathway has become well established over the years and understood in eukaryotes (i.e. yeast, fungi, humans), recent work has been devoted to understanding the bacterial enzymes and chemical mechanisms underlying the process [51,63]. The presence of MMA(V), DMA(V) and multiple volatile arsenic species including TMA have been detected (arsine, mono- and dimethylarsine) when aerobic and anaerobic bacteria were fed inorganic arsenic as well as MMA(V) and DMA(V) [51,52,63]. It is also worth noting that in bacterial systems other methyl donors have been implicated including methylcobalamin and cysteine [52]. The enzyme implicated in bacterial arsenic methylation has been identified as an As(III) S-adenosylmethionine methyltransferase (SAM methyltransferase) known as ArsM, which is a homolog of the human Cyt19 enzyme, which is also an As(III) SAM methyltransferase [51,52,63].

This enzyme has been found in the genomes of over 120 bacterial species and has been demonstrated as a necessity in the conversion of inorganic arsenic to volatile methylated and inorganic arsines, which are products of the methylation pathway[57]. Since the discovery of highly conserved methylation cascade, several microorganisms have been characterized over the past couple decades capable of performing a variety of arsenic transforming activities including reduction, oxidation, demethylation which will now be discussed [2,3,6,29,54,64].

ii. Arsenate reduction

a. Arsenic resistant microbes

Arsenic resistant microbes (ARMs) are extremely common and are characterized by their ability to import arsenate into their cytoplasm, reduce it to arsenite using a thiol-containing compound as an electron donor (i.e. glutathione, thioredoxin) and export it out of the cell as a mechanism of coping with high concentrations of arsenate in the environment [2-6]. Bacteria do so via a specific set of genes comprising the *ars* operon, which can be found in chromosomal DNA (i.e. *E. coli)* as well as in plasmids (i.e. *Staphylococcus*) [2-6]. Arsenate has a high structural similarity to phosphate, allowing it to enter the cell via ATP-dependent (PhoS, PstC, PstB) or potential-coupled (Pit) phosphate transport systems, where it is subsequently reduced to arsenite via ArsC, a cytoplasmic arsenate reductase enzyme [6,54,64,65]. The resulting arsenite in the cytoplasm is then exported from the cell through arsenite-specific ATP-dependent or independent transporters such as ArsAB in *E. coli* and ArsB in *Staphylococcus aureus*, respectively [2,6,54,64]. Another lesser characterized class of arsenite transporter, Acr3p, has also been found in bacteria [66].

Expression of the *ars* operon is regulated by *arsR* and *arsD*, trans-acting repressor genes that encode protein products (ArsR, ArsD) that bind the *ars* promoter and arsenite [6,67,68]. Variations of the genes comprising the *ars* operon (i.e. the arsenite export genes) exist among individual bacterial species, but *arsR*, *arsB* and *arsC* appear essential to all ARMs [5,54,65].

b. Dissimilatory arsenate reducing prokaryotes

The anaerobic respiration of As(V) is a feat accomplished by multiple phylogenies of prokaryotes, including ε-, γ- and δ-Proteobacteria, Gram positive bacteria and Archaea [2-6]. The evolution of this process is energetically favorable, as the redox potential of the {As(V) → As(III)} reaction is +135 mV, which when coupled to the oxidation of organic compounds such as lactate is very exergonic thermodynamically [2,4]. These organisms are referred to as dissimilatory arsenate-reducing prokaryotes (DARPs) and examples include *Chrysiogenes arsenatis*, *Sulfurospirillum barnesii* strain SES-3, *Bacillus selenitireducens* strain MLS 10, and *Alkaliphilus oremlandii* strain OhILAs [2-6]. DARPs are able to respire As(V) via the services of respiratory arsenate reductase (Arr) enzymes. Highly conserved and localizing in either the periplasm (i.e. *C. arsenatis*) or membrane (i.e. *B. selenitireducens*) of the cell, the enzymes belong to the dimethyl sulfoxide (DMSO) reductase family and exist as heterodimers consisting of a larger, catalytic ArrA subunit and smaller, electron transferring ArrB subunit [2,4-6]

iii. Arsenite oxidation

Many bacterial species have been described that oxidize As(III) to As(V), be it for resistance or energy acquisition [2-6].

Coined as heterotrophic arsenite-oxidizing bacteria (HAOs), some bacteria oxidize As(III) without profiting energetically from the process and require an organic carbon source. Examples include *Thermus aquaticus* YTI, *Thermus thermophiles* HB8 and *Alcaligenes faecalis* [2-6]. Others known as chemoautotrophic arsenite-oxidizing bacteria (CAOs) have the ability to use arsenite as an electron donor (oxidation to arsenate) to reduce oxygen or nitrate and use the energy generated to drive CO_2 fixation into organic cell material [2-6]. Examples of such include *Rhizobium* strain NT-26 and *Alkalilimnicola ehrlichii* strain MLHE-1, which respire oxygen and nitrate during this process, respectively [6,69,70]. CAOs and HAOs achieve arsenite oxidation via conserved enzymes known as arsenite oxidases (Aox, Aso, Aro) [2,4-6]. A member of the dimethyl sulfoxide (DMSO) reductase family, Aox is heterodimeric structurally, composed of a large catalytic AoxB subunit and a smaller AoxA subunit and has been shown to localize in the both the periplasm and cell membrane [2,4-6]. Interestingly, an arsenite oxidase enzyme known as Arx (*arx* gene) has recently been identified in the arsenite oxidizing bacteria *A. ehrlichii* strain MLHE-1 and *Ectothiorhodospira* strain PHS-1 [71,72]. Also a member the DMSO reductase family, this enzyme was originally thought to be a bidirectional respiratory arsenate reductase as its sequence shares a higher degree of homology with ArrA than it does with AoxB [71,73]. **Figure 1.8** presents a summary of some of the major arsenic transport and transformation events that occur in the cell.

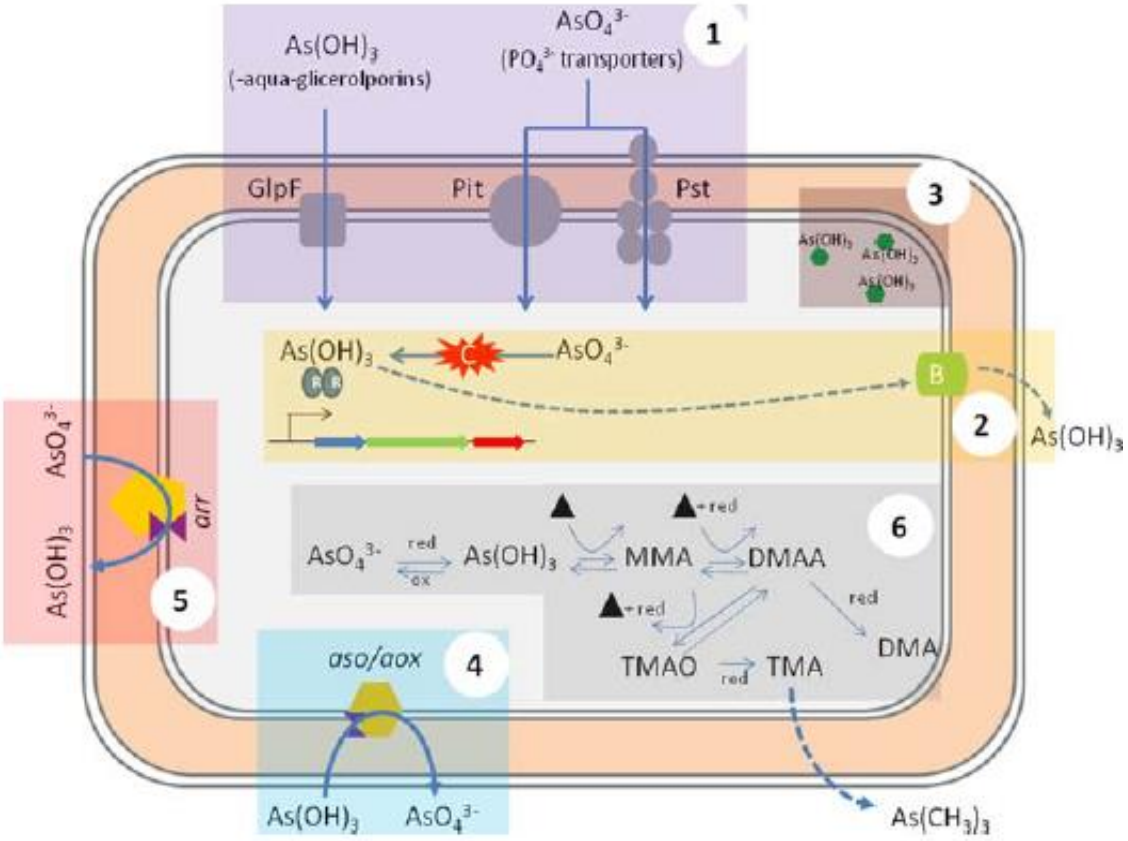

Figure 1.8. Microbial arsenic transport and transformation pathways. 1) As(V) enters through phosphate transporters; 2) ARMs reduce As(V) to As(III) via ArsC and export the As(III) through the ArsB transporter; 3) As(III) can be sequestered into vacuoles and thus detoxified as in *Saccharomyces cerevisiae* (Ghosh et. al, 1999) 4) HAOs and CAOs use As(III) as an electron donor during respiratory growth, where it is oxidized to As(V) via the Aso/Aox/Aro enzyme; 5) DARPS use As(V) as the terminal electron acceptor during respiratory growth, reducing it to As(III) via the Arr enzyme complex; 6) As(V) can be methylated by a different class of ARMs via ArsM (not shown) to yield a variety of methylated trivalent and pentavalent arsenicals. Adapted with permission from Paez-Espino, 2009 [54].

iv. Methylarsenic demethylation

The methylarsenic demethylation process was originally suggested by Challenger and coworkers, who observed that the fungi *S. brevicaulis* and *Penicillium notatum* could convert $ClCH_2CH_2AsO(OH)_2$ to TMA, which is indicative of As-C bond cleavage [6,53]. The next documented account of demethylation of methylarsenic was published in 1968 when Von Endt and coworkers enriched microbes that degraded MSMA to inorganic arsenic from various soil samples [74]. Since then, there has been a growing body of literature citing species-specific examples of bacterial demethylation of methylarsenic. Various *Pseudomonas* species were enriched from Lake Kahokugata and shown to degrade DMA(V) to MMA(V), arsenate and arsenite, and could grow on the compound as a sole carbon source [75,76]. Bacteria from this same genus (*Pseudomonas*) were isolated from organoarsenical contaminated environmental soils (exposed to organic arsenic-containing chemical warfare agents) from Ohkunoshima Island, and were capable of degrading MMA(V) to inorganic arsenic[76]. Another bacterial species, *Mycobacterium neoaurum*, has been shown to demethylate MMA(V) and MMA(III) to mixtures of arsenate and arsenite, but is incapable of transforming DMA(V) [77]. Environmental anaerobic sludge samples incubated with DMA(V) and MMA(V) have demonstrated biological transformation to MMA(V) and MMA(III), respectively, but not under denitrifying conditions [78]. The most recent account of methylarsenic demethylation has indicated microbial demethylation of MMA(V) to inorganic arsenite {As(III)} in simulated golf soil samples treated with MMA(V) [33]. While there have clearly been numerous accounts of biotransformation of methylarsenic to the inorganic form, the chemical and enzymatic mechanisms underlying the process have yet to be elucidated.

It has been proposed that this pathway may follow a "Reverse Challenger" mechanism, during which S-adenosylhomocysteine (SAH) acts as the methyl group acceptor (and reducing agent) during reductive demethylation steps of As(V) containing intermediates, followed by subsequent oxidation of the resulting As(III) containing compounds [6]. This pathway was supported in *M. neoaurum*, which showed the conversion of MMA(V) to arsenite during its early growth stages, followed by the transition to arsenate during the stationary phase [77]. However, more recent data published has shown that microbial demethylation of MMA(V) can occur in a two-step process [33]. In this study, bacterial strains from the *Burkhoderia* and *Streptomyces* genus were isolated capable of reducing MMA(V) to MMA(III) and demethylating MMA(III) to arsenite, respectively [33]. In mixed culture, the two were capable of MMA(V) reductive demethylation to As(III), but individually failed to do so [33]. This suggests that, contrary to a "Reverse Challenger" pathway in which reduction and demethylation occur simultaneously, the cleavage of the As-C bond may require two independent stages and cycling of methylarsenic species between multiple organisms **(Figure 1.9)** [33]. Therefore, there is an expanding body of evidence that supports the notion of a bacterial demethylation process, but more research must be devoted to this pathway to uncover its mechanism of operation.

v. Bacterial arsenic mobilization

As previously mentioned, As(V) is commonly found in more oxic conditions and is commonly bound to several subsurface minerals. These minerals are most commonly iron and aluminum (hydr)oxides.

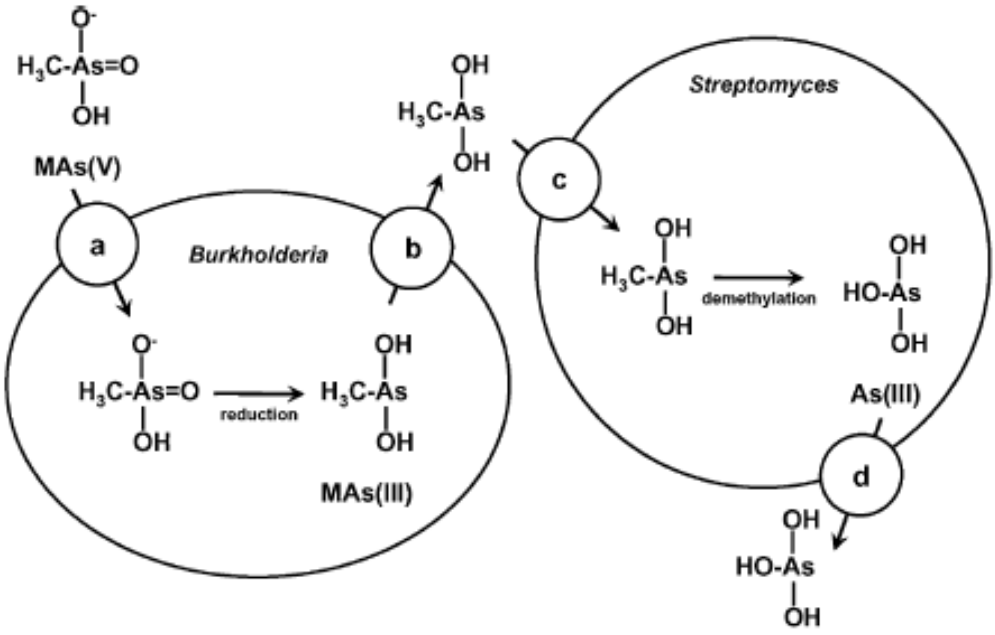

Figure 1.9. Proposed MMA(V) two-step demethylation pathway. *Burkholderia* imports MMA(V) into the cell where it is reduced to MMA(III0. MMA(III) is then exported from the cell and imported into *Streptomyces* where it is demethylated to As(III) by a mechanism unknown. The As(III) is then exported, likely through Ars(A)B complexes. Adapted with permission from Yoshinaga, 2011 [33].

As(III), which is much more toxic than its oxidized counterpart, is most commonly found in anaerobic environments in the aqueous phase. For years, geochemical processes contributing to the release of aqueous As(III) from As(V) in the solid phase have been researched, due largely in part to the arsenic contamination occurring in South Asia. However, more recently, the role of bacteria in these chemical processes, causing what is known as biogeochemical arsenic transformation, has become a topic of extensive study. Thus, the groundwater contamination in West Bengal and Bangladesh has led to a series of geochemical and biogeochemical hypotheses explaining how arsenic is mobilized from subsurface sediment particles to groundwater.

It has recently been discovered that both As(V) and Fe(III) reducing bacteria may play a pivotal role in arsenic mobilization and speciation in subsurface systems. Similar to the case of arsenic, the more reduced form of iron (Fe(II) or ferrous iron) has much greater hydrological mobility than the more oxidized form (Fe(III) or ferric iron) [3]. Ferric iron (hydr)oxides bind As(V) tightly while ferrous iron (hydr)oxides do not, and As(III) has a much lesser binding affinity for Fe(III) containing minerals than does As(V) [131]. Thus, redox reactions involving iron and arsenic in subsurface environments appear to strongly influence solubility and speciation of both metals.

Experiments conducted using microcosms generated from subsurface sediments extracted from the Aberjona Watershed in Massachusetts, which possesses a high concentration of sedimentary arsenic due to wastes previously generated at an industrial complex producing arsenical pesticides, showed that dissimilatory reduction of As(V) from ferric arsenate minerals drove an accumulation of As(III) in the aqueous phase [131].

Similar results were obtained using sterile sediment pure cultures of the first DARP ever characterized, strain MIT-13 [131].

It was experimentally demonstrated that dissimilatory iron reducing bacteria (DIRB) greatly impact the mobility of arsenic, as the DIRB bacterium *Shewanella alga* strain BrY (a facultative anaerobe isolated from sediments of the Great Bay Estuary, New Hampshire[129]) was shown to release aqueous As(V) from ferric arsenate solely via the reduction of Fe(III) to the poorly adsorptive Fe(II) species [89]. Similar results were obtained by microcosms (growth media bottles inoculated with environmental sediment) generated from sediments of the arsenic-contaminated Lake Coeur d'Alene in Idaho, as they too demonstrated the ability to mobilize As(V) via dissimilatory ferric iron reduction[89]. Furthermore, a pure culture of the DIRB and DARP, *Sulfurospirillum barnesii* strain SES-3 (isolated from Massie Slough marsh in Nevada[91]) was shown to catalyze Fe(II) and As(III) mobilization from Fe(III) and As(V), respectively, in ferric arsenate sediments[90]. This strain was capable of releasing As(III) from an aluminum arsenate sediment by dissimilatory arsenate reduction activity [90]. It is worth noting that during experimentation with SES-3, separate abiotic data suggested that ferric iron readily adsorbs arsenic in the +3 oxidation state [90]. This is contradictory to the notion that As(III), once formed will remain in the aqueous phase, and that its ability to readsorb appears to be contingent upon the availability of iron remaining in the ferric state. Furthermore, much of the SES-3 catalyzed generation of As(III) from As(V) either remained adsorbed to the ferric iron sediment or was readsorbed following its mobilization into the aqueous phase, further supporting this hypothesis [90].

While the aforementioned findings strongly support the hypothesis that subsurface microbial dissimilatory reduction of arsenic and iron greatly influences the mobility of and speciation (i.e. oxidation state) of both elements, it appears as if non-respiratory reduction of As(V) via the services of ARMs cannot occur on solid-phase substrate and requires aqueous arsenate. Incubation experiments conducted with the glucose-fermenting ARM, *Clostridium sp*. strain CN8 showed complete arsenate reduction activity on aqueous As(V) in the presence of ferrihydrite (a ferric oxide sediment) but no dissolution or reduction of the iron contained in the mineral [130]. Additionally, dissimilar to the activity observed by strain SES-3, all of the solid-phase arsenic remained as As(V) with no additional As(III) being mobilized into the aqueous phase [130]. Additionally, aqueous As(V) that became adsorbed to the ferrihydrite remained in the +5 oxidation state and did not appear to dissolute into the aqueous phase [130].

More light was shed on this topic following the discovery that ARMs, unlike DARPs, were incapable of reducing adsorbed As(V) [130]. Research in the early 21st century clarified the explanation behind this observation, as the respiratory arsenate reductase catalytic subunit, known as ArrA, is situated in the periplasm rather than in the cell (unlike the cytoplasmic arsenate reductase, ArsC.) While ARMs individually are incapable of mobilizing solid-phase As(V), if present in a complex community of DARBs and DARPs, they can greatly impact the speciation of the aqueous phase arsenic that enters the groundwater, thus rendering them potentially hazardous to the safeness of the groundwater. **Figure 1.10** demonstrates how a mixed community of DARPs, DARBs and ARMs can significantly impact arsenic mobilization and speciation in an aquifer environment.

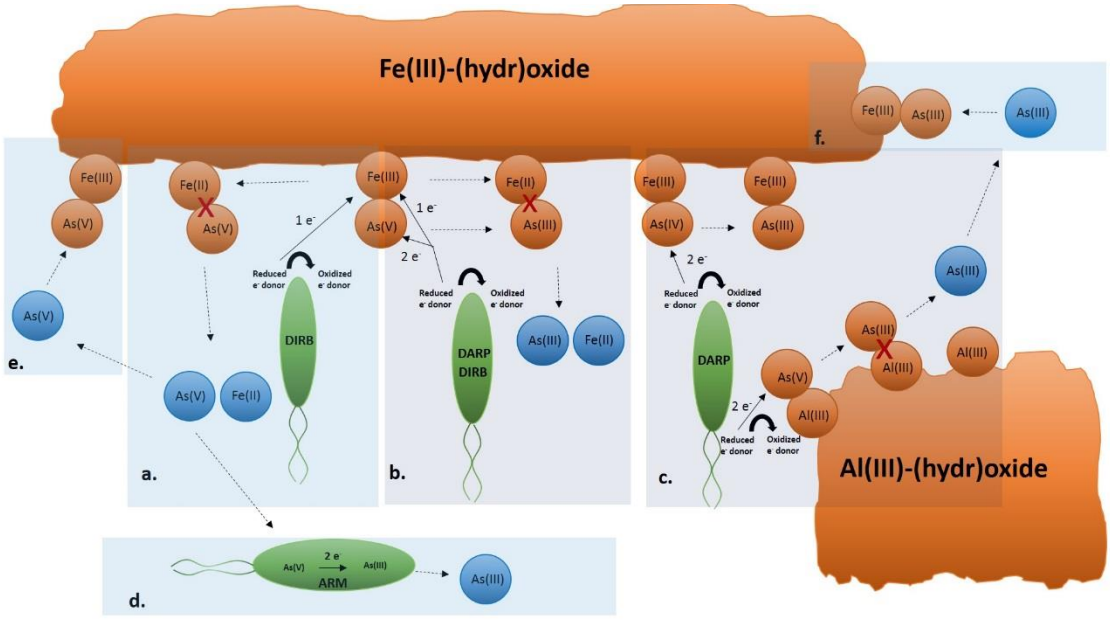

Figure 1.10. Three possible mechanisms by which arsenic can be mobilized from sediments in subsurface environments. Multiple organic and inorganic electron donors are utilized to respire solid-phase Fe(III) and/or As(V), driving the mobilization process. (a) Adsorbed As(V) is released by DIRB activity (i.e. *Shewanella alga* strain BrY). (b) As(III) and Fe(II) are released by a DARP & DIRB strain, respectively (i.e *Sulfurospirillum barnesii* strain SES-3). (c) As(III) is released by DARP activity (i.e. *Sulfurospirillum barnesii arsenophilum* strain MIT-13). (d) ARMS can reduce aqueous AS(V) to As(III))(i.e. *Clostridium sp.* strain CN8). (e) As(V) and (f) As(III) can be following their release.

Chapter II. Development of Thermo Scientific/Dionex ICS-1100 anion exchange chromatography method

A. Abstract and Hypotheses

Hypothesis: A Thermo Scientific/Dionex ICS-1100 ion exchange chromatography system can detect and quantify As(V), As(III), monomethylarsonic acid [MMA(V)], dimethylarsinic acid [DMA(V)] as well as other useful anions involved in bacterial metabolism.

In this study, a Thermo Scientific/Dionex (Bannockburn, IL) ICS-1100 system was optimized to detect and quantify oxyanions of arsenic [As(V), As(III), MMA(V), DMA (V)] and other anions common to bacterial metabolic pathways. Initial studies using conductivity detection yielded promising results with As(V), MMA(V), lactate, acetate, nitrate, nitrite and sulfate all showing relatively sensitive detectability. However, this detection method alone was insufficient for comprehensive analyses of arsenic transformation, as As(III) and DMA(V) were not detectable using conductivity. Installation of a UV/Vis 4-channel detector rectified this problem and readily and sensitively detected As(V), As(III), MMA(V), MMA(III), lactate, nitrate and nitrite. Lactate and acetate showed highly similar retention times, creating quantitation issues when analyzing solutions containing a mixture of both of these compounds, especially when the lactate concentration exceeded that of acetate. This complication was resolved by decreasing the amount of lactate in the As(V)/lactate enrichment cultures from 10 mM to 2.5 mM. This system proved to be highly versatile and useful as an analytical tool for microcosm, enrichment culture and pure culture analyses.

B. Background

Arsenic speciation is most commonly measured using various forms of liquid chromatography, with separation and detection techniques selected based on individual sensitivity requirements [79]. The seemingly most popular and effective technique implemented to separate and measure arsenic species is high performance liquid chromatography combined with inductively coupled plasma mass spectrometry, or HPLC-ICP-MS. Extremely sensitive with recorded detection limits (DL) as low as 0.04 μg/l or ppb [79], this technique has been used extensively and successfully for inorganic and organic arsenic speciation from sources such as environmental waters, drinking water, human urine, animal tissues, bacterial cultures, rice and animal feed [79-83]. High performance liquid chromatography using an anion-exchange column with U.V. detection has also been an effective and widely practiced technique for measuring arsenic [79,84,85]. More importantly, this technique has been used extensively for arsenic speciation in slurry-derived bacterial cultures [86-88]. The DL of a U.V. detector has been shown to range from 0.1-1.2 mg/l or ppm [74] which is quite sensitive when analyzing cultures of extremophiles that can metabolize high concentrations of arsenic. Dionex Corporation (now part of Thermo Fisher Scientific) provides a variety of analytical instruments that can be powerful tools when analyzing microbial arsenic transformation.

C. Materials and Methods

i. **Dionex ICS-1000 system features**

The Dionex ICS-1100 anion exchange chromatography system was used for all analytical work included in this dissertation.

To maximize time efficiency during analyses, an AS/DV autosampler with a 50 sample capacity was used for sample introduction into the chromatography system. The eluent used was a mixture (after diluting the 100x stock eluent 100-fold, making the final concentration 1X) of 4.5 mM sodium carbonate and 1.4 mM sodium bicarbonate prepared in NANOpure water. Once injected into the ICS-1100 via a 15 μL injection loop, the sample passes through an AG22 (2 x 50 mm) guard column followed by an AS22 (2 x 250 mm) anion exchange separator column. An ASRS-300 2mm suppressor was used to negate any signal generated by the eluent during analyses involving conductivity detection. The first detector included in the system was an Ultimate 3000 Diode Array UV/Vis detector capable of 4-channel simultaneous detection. The second detector was a heated DS6 heated conductivity cell that was set at a constant 30° C. All data was processed using the Chromeleon LE 7.0 software, which will be described below. A general diagram of all of the external components of the Dionex ICS-1100 system is shown in **Figure 2.1**.

ii. Chromeleon LE 7.0 software

a. Chromeleon Console

The Chromeleon Console is the main control panel that is immediately visible upon opening the Chromeleon software. There are three main tabs, each of which control the AS-DV Autosampler, ICS-1100 and Diode Array Detector control panels, respectively. Prior to utilizing any of these control panels, each component must be connected to the computer separately by simply clicking "connect."

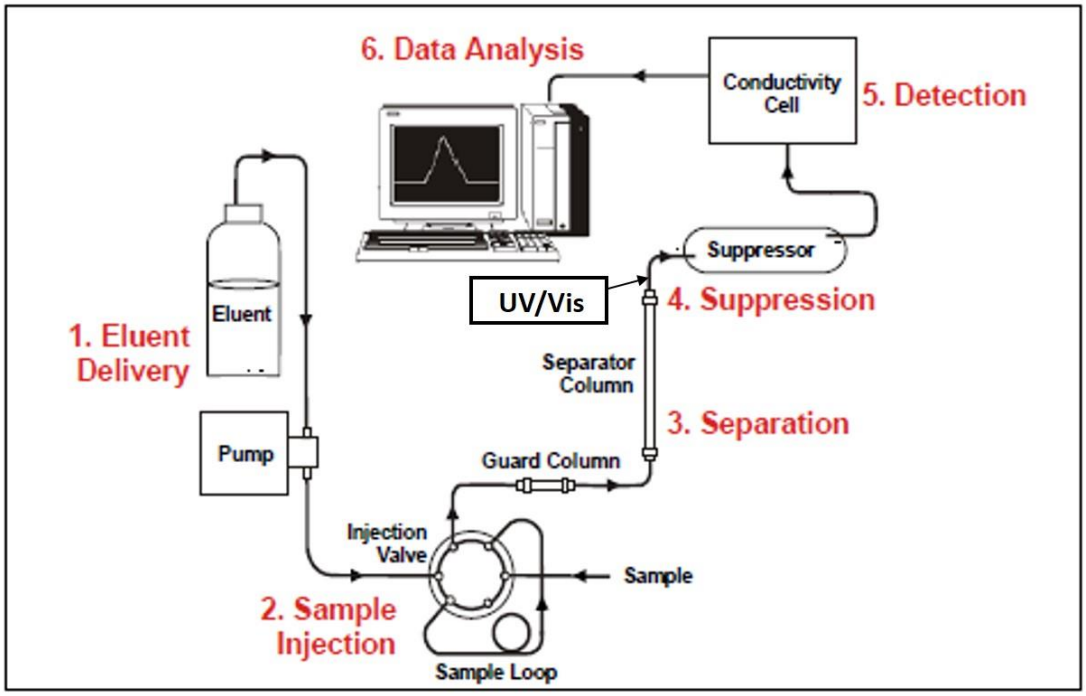

Figure 2.1. Schematic diagram of the Dionex ICS-1100 system. An autosampler is used to deliver all samples to the injection valve. The bicarbonate/carbonate based eluent is delivered through a dual headed pump and flows continuously through the system. Upon injection into the injection valve the sample passes through a guard column to remove metals and is separated by cationic column. The UV/Vis detector then detects individual anions based on their absorbance properties and sends a signal to the Chromeleon software. Any background signal from the anionic properties of the eluent are inhibited by the suppressor and the conductivity cell then detects each individual anion in the sample and sends a signal to the Chromeleon software. Analyses can then be done based on the information generated from the UV/Vis 4-channel detector and conductivity cell. Adapted (and modified) from: Thermo Scientific/Dionex. Figure 1-1: Ion Analysis Process. *Dionex ICS-1100 Ion Chromatography System Operator's Manual*. 2012: 2. http://www.dionex.com/en-us/webdocs/73269-Man-IC-ICS1100-Operators-Oct2012-DOC065289-03.pdf.

The AS-DV Autosampler control panel allows the user to control the deliver speed and deliver volume, as well as perform commands such as “move to vial,” “deliver sample,” “reset memory,” “raise needle,” and “stop.” The operating status, deliver status and volume remaining in each vial are also shown while using this control panel. Also displayed is the run-time progress of the current sample in analysis. The ICS-1100 control panel displays pressure (psi), signal (μS) and cell temperature (°C), and gives the user the ability to turn the suppressor and pump on and off. The flow rate (ml/min) applied by the pump can be adjusted from this panel as well as the current (mA) applied by the suppressor. In order to check for stability in pressure as well as conductivity and UV/Vis signals, a “monitor baseline” option is available. The Diode Array Detector control panel allows the user to control the wavelengths at which each channel is performing acquisitions, and allows the UV and Vis bulbs to be turned on and off manually.

In order to start analyzing samples, a “sequence” must be created that can be fully customized. While creating a sequence, it’s necessary to create a fully customizable “instrument method” that controls the run time, flow rate, strength of the suppressor, eluent type used, detection channels, wavelengths of UV/Vis detection (if used), etc. Also an option while creating an instrument method is a series of commands that instruct the autosampler to rinse the needle prior to withdrawing and delivering the sample to the ICS-1100 system. The “script editor” option allows the user to perform manual commands before, during or after each sample is analyzed (i.e. turning off the pump and suppressor at the conclusion of each run).

Once the instrument method is designed, a "processing method" must be selected. Choosing "default" will allow the user to design a custom processing method and rename it later, which will be discussed below. Once an instrument method is created and the "default" processing method is selected, the sequence is created and samples can now be entered. The first step to running a sample in the sequence is providing its name, numerical position in the autosampler (i.e. 1-50), injection volume (15 µl in this system), type and status. The type of sample can be "unknown," " blank," "check standard," "calibration standard," "matrix," "spiked" or "unspiked" and the status of any given sample can be "idle," "interrupted," or "finished." New samples entered into the sequence must be listed as "idle" in order for any injection to occur. Once all of the aforementioned information is entered into the sequence, hitting the "resume" button will signal the autosampler to inject samples into the ICS-1100 system, which will generate a series of chromatograms from which data can be obtained.

b. Calibrating standards

Once a sequence has been created with an appropriate instrument method, external standards must be prepared and analyzed. Standard preparation will be discussed in the section below. When entering each standard sample into the sequence, "calibration standard" must be selected as the sample type. Once this has been done, levels must be selected for each standard that was prepared (i.e. 500 µM As(V) is level 1, 250 µM As(V) is level 2, 100 µM As(V) is level 3, etc.). This will allow each level to represent a separate data point on the calibration curve that will be generated automatically.

After running each standard, in the "Data processing" side tab, which will be discussed in more detail below, the information and data on each standard must be entered into the "component table" which is found when clicking the "Calib. & PM" icon on the upper task bar. This table allows you to enter the standard name, average retention time, window, channel, levels (these levels must match up with the levels previously set while editing the sequence), evaluation type, concentration unit, etc. Once this information is entered, calibration curves are automatically generated that will be used to quantify all samples (**Figure 2.2**). The graphs are labeled with the name of the standard, the type and the channel on which it was analyzed.

c. Data Processing

While running samples, chromatograms are generated with various peaks that need to be detected and quantified based on the standard calibrations previously performed. As previously described, upon opening the "Data Processing" side tab there is a "Calib. & PM" icon with a calibration table in which numerical standard values are entered. To the left of the "Calib. & PM" icon is another icon called "Results." Results can be displayed in various fashions including views of single or multiple chromatograms (overlapping or stacked doublet views).

iii. Standard preparation

Prior to running any standards, a multianion solution (Sigma-Aldrich) consisting of 3 ppm (mg/l) fluoride, 10 ppm chloride, bromide, nitrate, phosphate and sulfate was run to test for retention times.

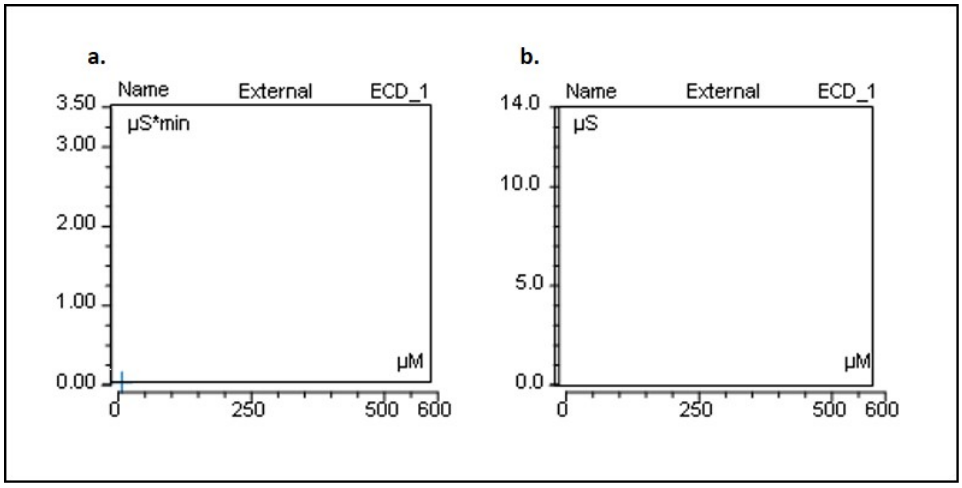

Figure 2.2. Blank templates of standard curves generated with Chromeleon LE 7.0 software using **a.** Peak area and **b**. Peak height during quantification. "External" refers to external standard and "ECD_1" refers to electronic conductivity detector 1. The concentration of the sample is displayed on the X-axis and can be modified to measure in any unit the user desires (µM in this case).

a. Vineland enrichments

Previously prepared anaerobic stock solutions of each anion were used as a starting point for all dilutions (See Chapter 3, **Table 3.1**), with the exception of a 1,000 ppm (21.73 mM) standard nitrite solution provided by Invitrogen (Carlsbad, CA). Standards solutions of As(V), As(III), DMA(V), MMA(V), lactate, acetate and nitrate were prepared in NANOpure water at 500, 250, 100, 50, 25 and 10 µM concentrations using a mass serial dilution technique with an analytical scale for greater precision when determining exact dilution factors. Sterile tubes (15 ml) were used to prepare each standard solution, with initial and final masses of each standard sample being recorded to calculate ACTUAL concentrations to be entered in the calibration table of the Chromeleon program for higher linearity of curves. Five ml aliquots of each standard solution were transferred to 5 ml Polyvials provided by Dionex, capped using Dionex Polyvial caps which were pre-soaked in deionized water, and placed in the autosampler.

b. Coal combustion byproduct disposal site microcosms

For the microcosm analyses discussed in Chapter 4, all standard solutions were prepared as described above using serial mass dilutions as previously described. Dilutions were performed using basal media (discussed in Chapter 4) with only 50 mg of yeast extract that was diluted twenty-fold in NANOpure water. The previously prepared stock solutions indicated in **Table 3.1** were used as starting points for each dilution set. Standard solutions of As(V), As(III), DMA(V), MMA(V), lactate, acetate and sulfate were prepared at 500, 100, 50, 25 and 10 µM concentrations. Each solution was loaded into the autosampler as described above.

c. *Alkaliphilus oremlandii* OhILAs cultures

For the OhILAs analyses (Chapter V), all standard solutions were prepared by mass serial dilution described on the previous page in OhILAs basal media (pg. 147) with the exception of adding only 50 mg of yeast extract. The previously prepared stock solutions indicated in Table **3.1** were used as starting points for each dilution set. Standard solutions of As(V), As(III), DMA (V), MMA(V), lactate and acetate were prepared at 500, 100, 50, 25 and 10 µM concentrations. Each solution was loaded into the autosampler as described above.

D. Results

i. System optimization

The ICS-1100 system with conductivity detection demonstrated the ability to clearly separate and detect multiple anions, as indicated by the chromatogram generated with the multianion solution tested (**Figure 2.3**). Upon testing the four arsenic species of interest when using the conductivity cell alone for detection, As(V) and MMA(V) were detected while As(III) and DMA(V) did not generate any visible peaks (**Figure 2.4**). Following the installation of the UV/Vis detector, however, all four arsenical anions were readily detectable **(Figure 2.5).** As(V) had optimal detection at 200 nm wavelength, As(III) showed the most significant peak at 205 nm, while MMA(V) and DMA(V) were most sensitively detected at 195 nm. When solutions were prepared in NANOpure water, lactate and acetate had very similar retention times, with lactate being the most conductive of the pair (**Figure 2.6**).

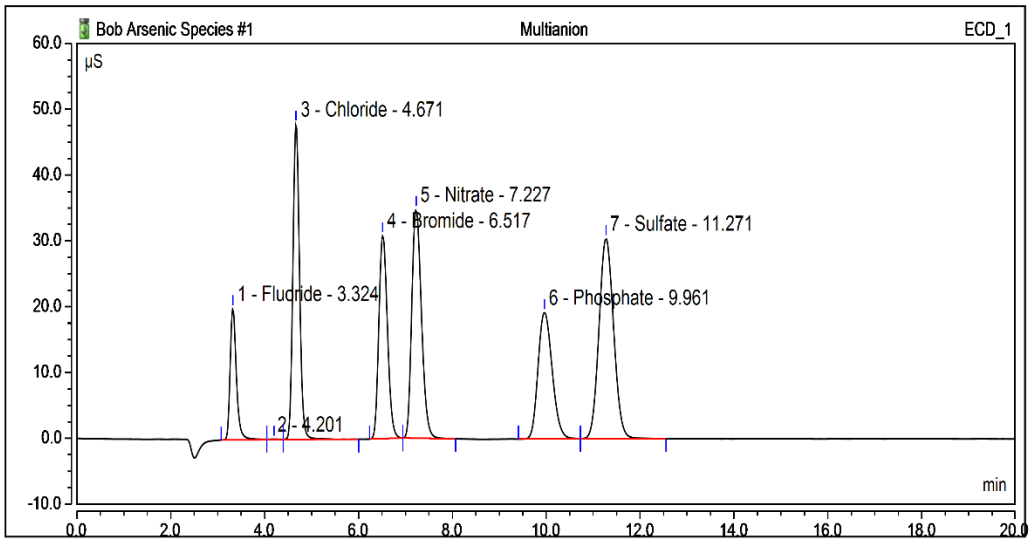

Figure 2.3. ICS-100 conductivity chromatogram of a multi-anion solution (Sigma-aldrich) consisting of (ppm): fluoride (3), chloride (10), bromide (20), nitrate (20), phosphate (30) and sulfate (20).

When comparing separate chromatograms, if the lactate concentration outweighs that of acetate by two-fold during analyses, there was an inability to detect acetate (**Figure 2.7**). This retention time overlap was even more severe when the two compounds were run together at equimolar amounts (10 mM) in SES-3 DARP media (bacterial media described in Chapter 3) diluted 50-fold. Under these conditions, acetate was unable to be detected (**Figure 2.8**). When dropping the eluent concentration down to 0.1X, the standards in NANOpure consisting of equimolar amounts of lactate and acetate were able to be separately detected and quantified, which a large shift in retention times being noted (**Figure 2.9**). However, other anions such as sulfate and As(V) could not be eluted from the separator column when ran in SES-3 DARP media under these conditions. When time-course samples of SES-3 DARP bacterial cultures amended with As(V) and lactate were analyzed at 1X and 0.1X eluent strengths, the 0.1 X eluent was able to show the disappearance of lactate and appearance of acetate over time (**Figure 2.10**), while the 1X eluent could only show the loss of lactate (**Figure 2.11**). Therefore, it was determined that the 1X eluent will be used for all bacterial culture analyses.

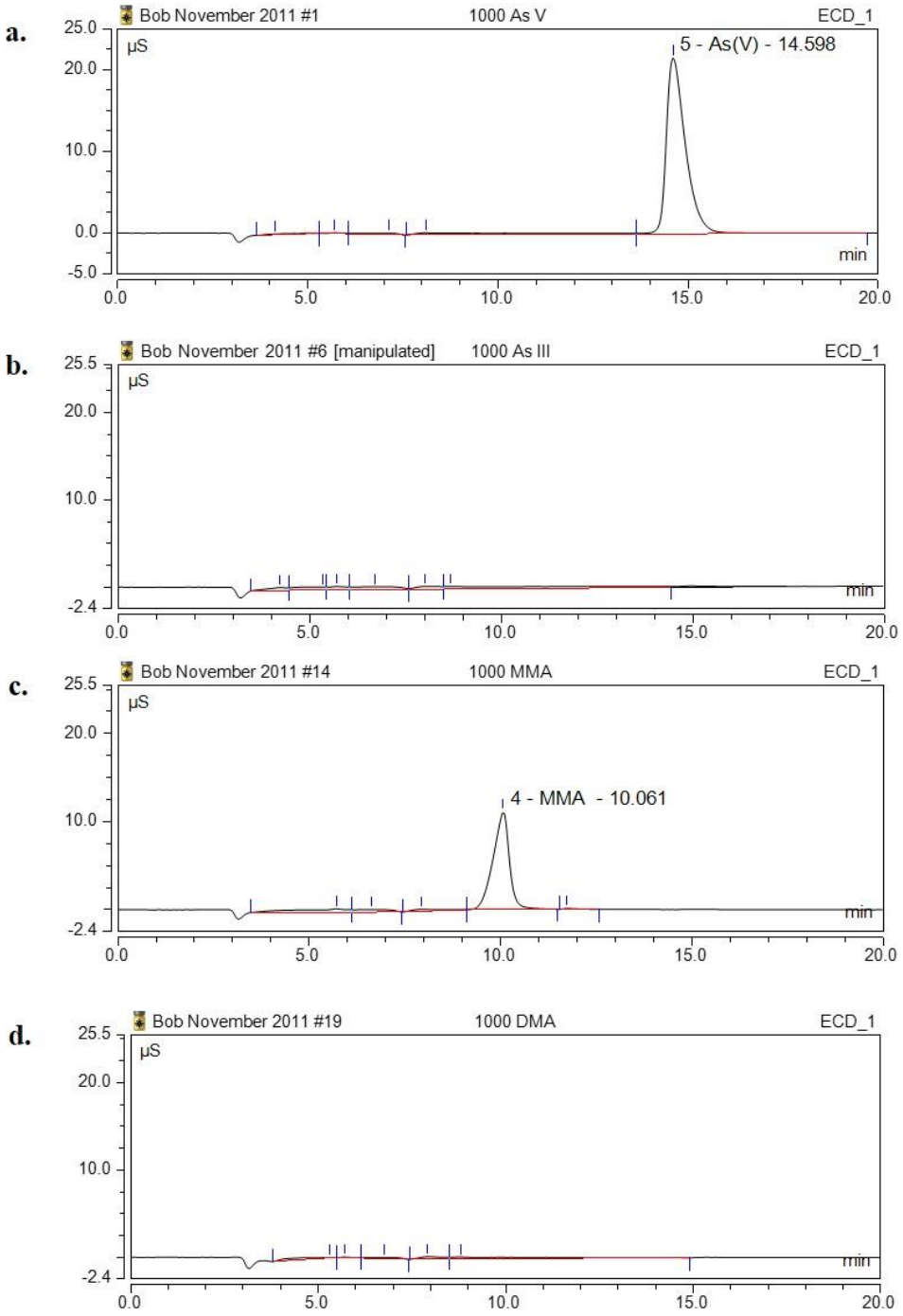

Figure 2.4. Chromatograms of 1 mM a. As(V), b. As(III), c. MMA(V) and d. DMA(V) in NANOpure water analyzed on the ICS-1100 with conductivity detection.

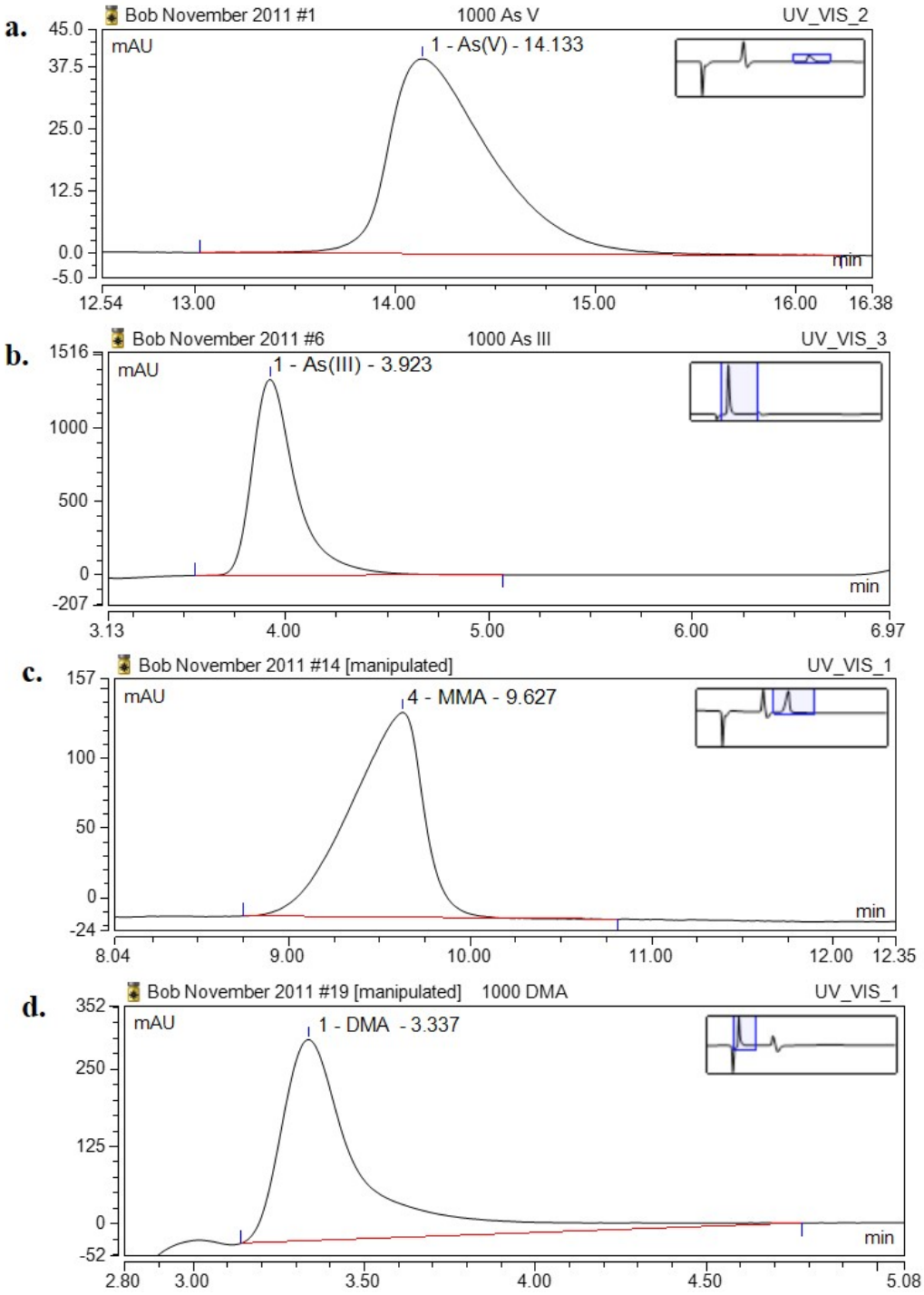

Figure 2.5. Chromatograms of 1 mM a. As(V), b. As(III) c. MMA(V), and d. DMA (V) in NANOpure water analyzed on the ICS-1100 with UV/Vis detection. As(V) was analyzed at 200 nm wavelength, As(III) at 205 nm, MMA(V) and DMA (V) at 195 nm.

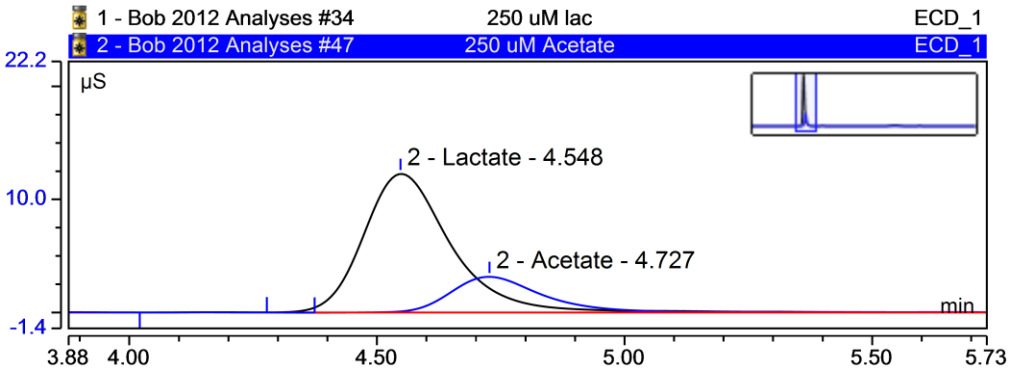

Figure 2.6. Overlaid ICS-1100 conductivity chromatograms of equimolar amounts of lactate and acetate (250 µM) in NANOpure water.

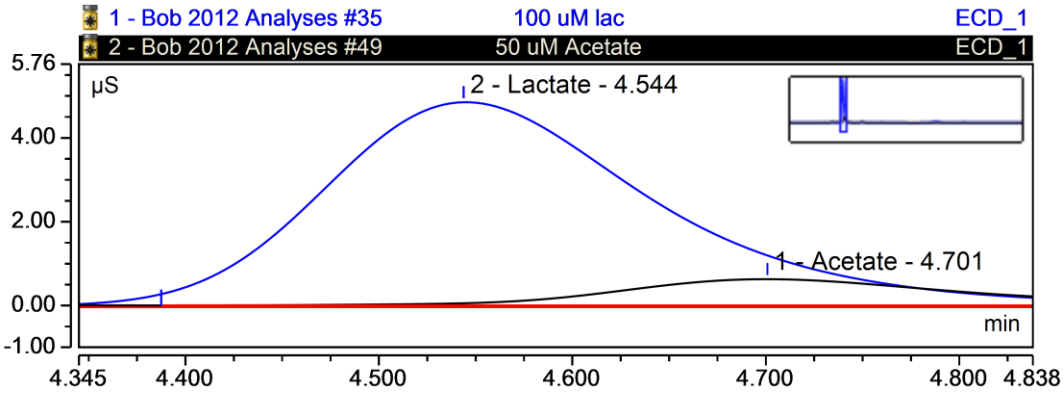

Figure 2.7. Overlaid ICS-1100 conductivity chromatograms of lactate (100 µM) and acetate (50 µM) in NANOpure water.

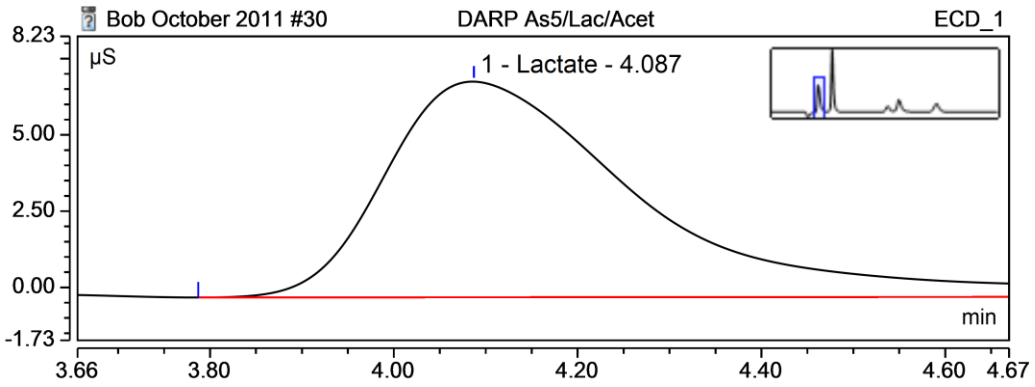

Figure 2.8. ICS-1100 conductivity chromatogram of equimolar lactate and acetate (250 µM) together in 50-fold diluted SES-3 DARP media (discussed in Chapter 3). Acetate did not generate a distinguishable and segregated peak.

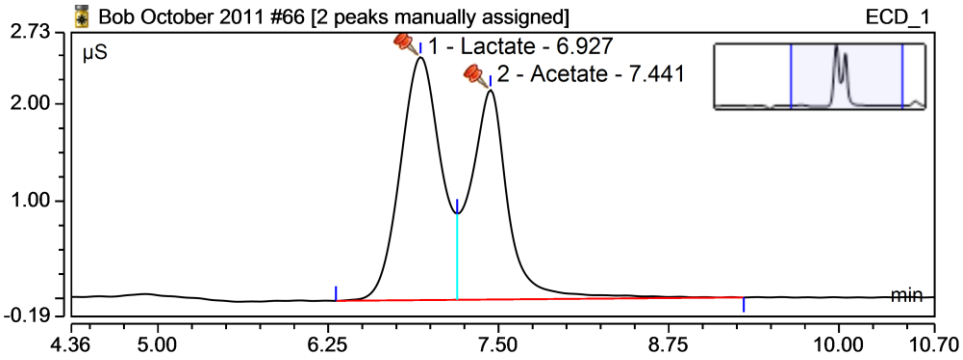

Figure 2.9. ICS-1100 conductivity chromatogram of equimolar amounts of lactate and acetate (100 uM) together in NANOpure water with 0.1 X eluent. The red pin icons indicate the peaks were assigned manually.

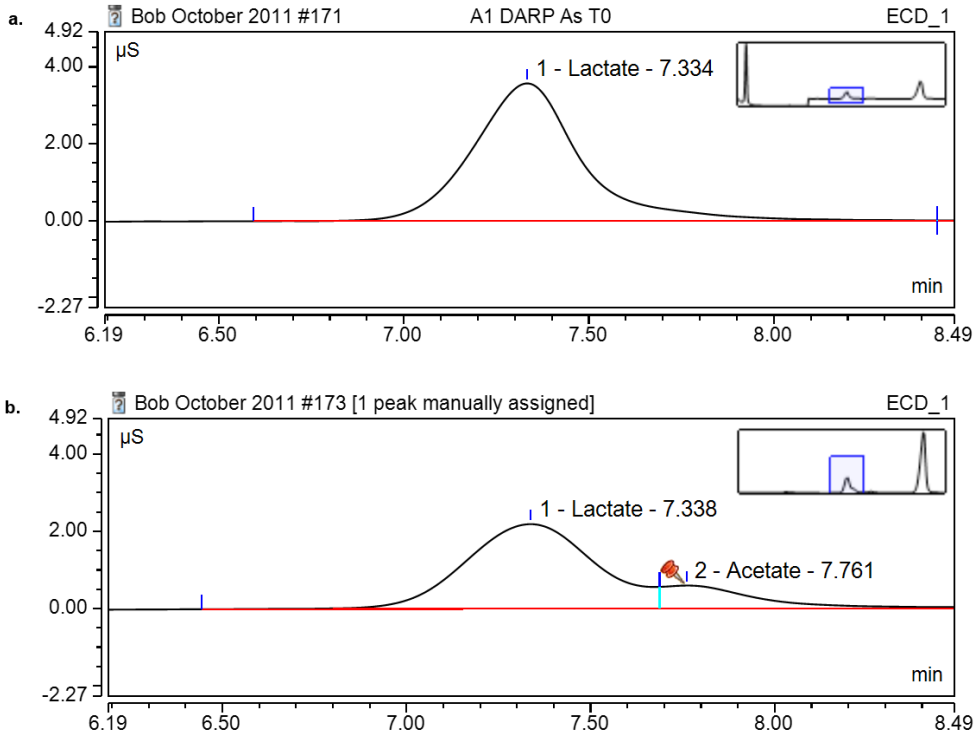

Figure 2.10. ICS-1100 conductivity chromatograms of SES-3 DARP bacterial culture filtrates at a. 0 and b. 24 hours of 37°C incubation using 0.1X eluent at 20-fold dilution. The red pin icon indicates the peak was assigned manually.

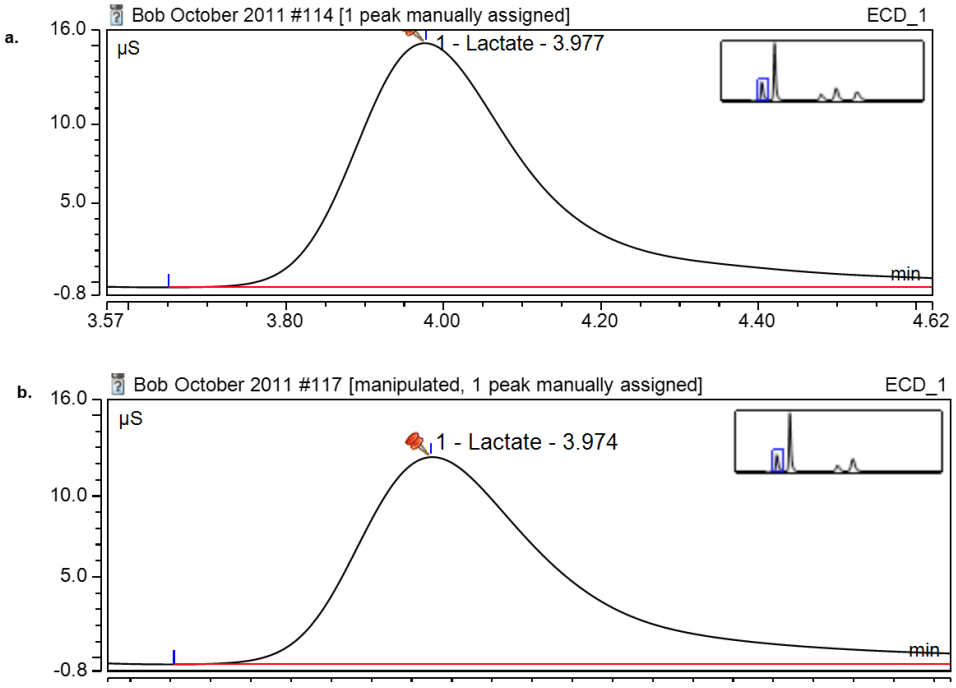

Figure 2.11. ICS-1100 conductivity chromatograms of SES-3 DARP culture filtrates at a. 0 and b. 24 hours of 37°C incubation using 1X eluent at 20-fold dilution. The red pin icon indicates the peak was assigned manually.

ii. Standard Preparation

Standards of As(V), MMA(V), DMA(V), lactate, acetate and nitrate were successfully prepared in NANOpure water. **Table 2.1** shows the detection properties of all anion standards prepared for the Vineland enrichments. The standard curves associated with each standard run can be found in **Figures 2.12** and **2.13** (nitrate data not shown). The properties and curves associated with the standard solutions prepared for the CCB disposal site microcosms and the OhILAs cultures can be found in chapters IV (pages 191-194) and V (211-214), respectively.

G. Discussion

While using the stock Thermo Fisher/Dionex ICS-1100 ion chromatography system with the stock components (conductivity cell detector only) is flawed for bacterial arsenic metabolism analyses, the introduction of the 4-channel UV/Vis detector can make this a powerful and relatively cheap tool for such purposes. The ability to properly detect and quantify As(III) and DMA(V), which are two very common and important arsenical metabolites in a variety of bacterial arsenic transformation pathways, was critical to the various research projects described in this dissertation. Since neither As(III) nor DMA(V) possess conductivity properties, using only the conductivity cell alone as a detection method in this chromatography system proves to be insufficient, as these compounds cannot be detected. Inserting the UV/Vis detector prior to the suppressor in the ICS-1100 system allows for these two arsenicals to be quantified and provides a novel method to investigate bacterial arsenic metabolism.

Compound	Detection Method	Average Retention Time (min.)	Detection Limit (DL)
As(V)	Conductivity	19.438	<10 µM
As(V)	UV 200 nm	18.780	<50 µM
As(III)	UV 205 nm	3.970	<10 µM
MMA	Conductivity	9.979	~10 µM
MMA	UV 200 nm	9.479	<50 µM
DMA	UV 200 nm	3.613	<25 µM
Lactate	Conductivity	4.548	<10 µM
Lactate	UV 200 nm	4.090	<50 µM
Acetate	Conductivity	4.928	<10 µM
Nitrate	Conductivity	8.275	<10 µM

Table 2. Detection properties of anion standards prepared for Vineland enrichments. Each standard was prepared in sterile NANOpure water.

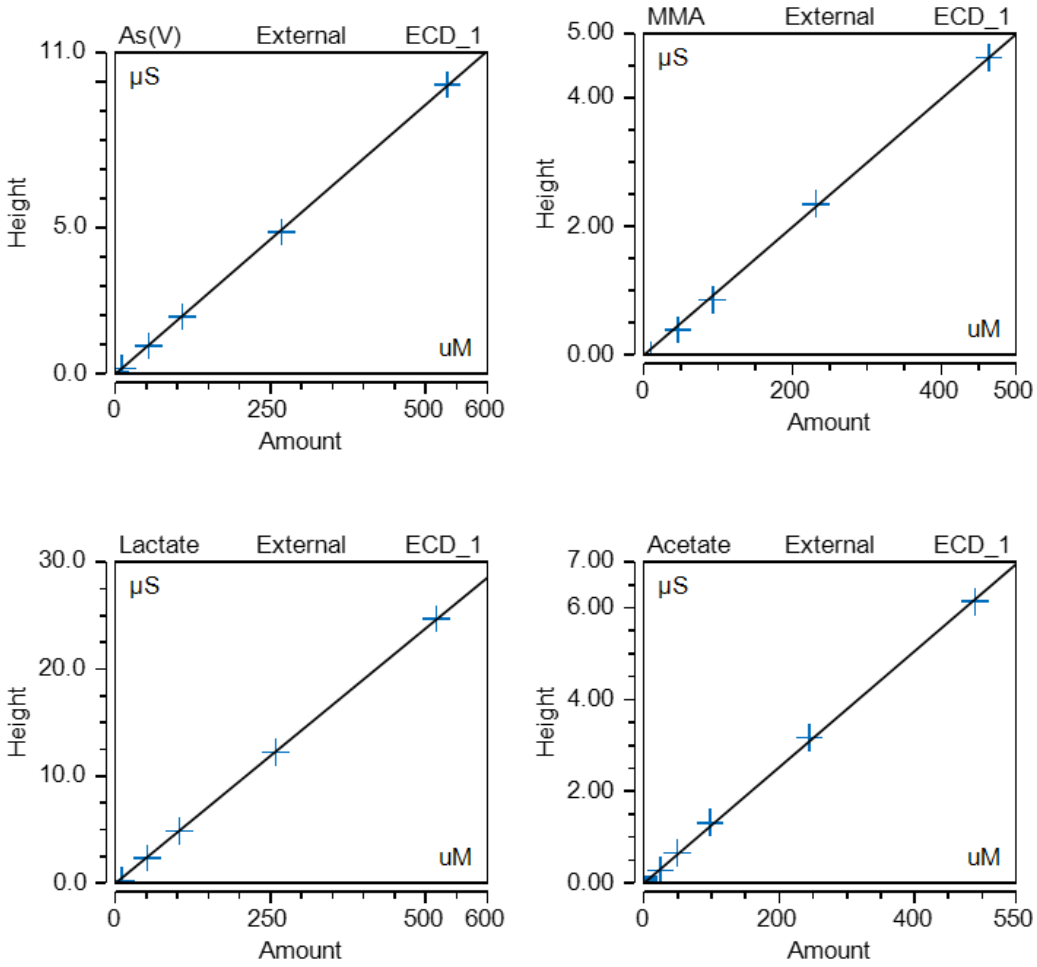

Figure 2.12. Chromeleon LE 7.0 generated standard curves of standard solutions prepared in NANOpure water and run on the ICS-1100 using conductivity detection. The names of each compound can be found on the top left of each graph. Peak height was used for quantification of each standard.

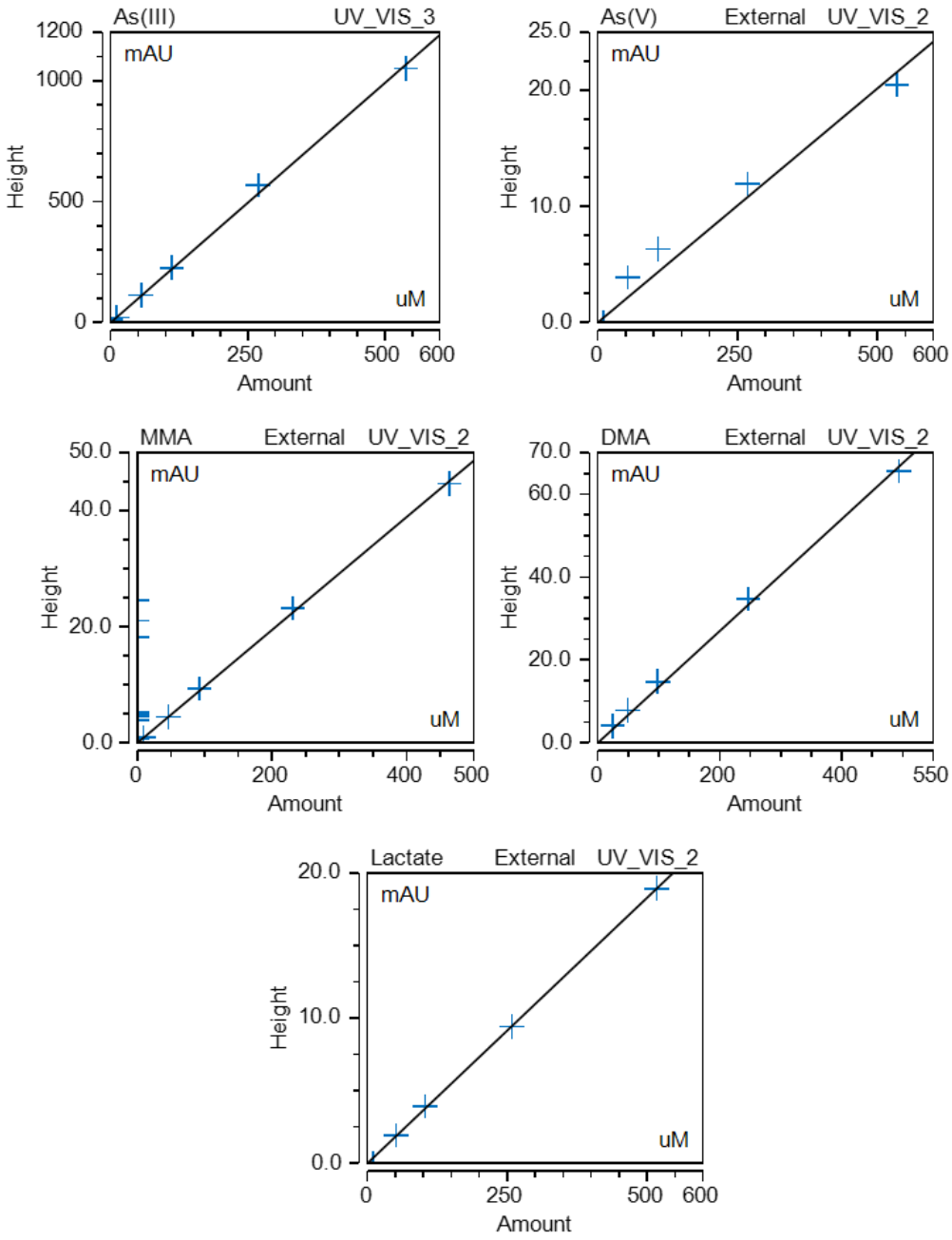

Figure 2.13. Chromeleon LE 7.0 generated standard curves of standard solutions prepared in NANOpure water and run on the ICS-1100 using UV/Vis detection. The name of each compound can be found on the top left of each graph. Peak height was used for quantification of each standard. Top right of graph: UV_VIS_2 is 200 nm wavelength [used for detection of As(V), MMA(V), DMA(V)]; UV_VIS_3 is 205 nm wavelength [used for detection of As(III)].

Highly sensitive methods such as HPLC-ICP-MS have DL values much lower than those obtained with this system and are highly effective at detecting extremely low concentrations of arsenic (<0.1 µM), such as those found in water and urine. However, this novel method is highly effective for analyzing bacterial arsenic transformations, as the levels of arsenic included in bacterial media prepared for this type of research commonly ranges from the hundreds of micromolar to millimolar range. Therefore, this method can be used to separate, detect and quantify four major arsenic anions [As(III), As(V), MMA(V), and DMA(V)] and can be an effective analytical tool in the study of bacterial arsenic metabolism.

Chapter III. Vineland Chemical Company enrichment culture analyses

A. Abstract and Hypotheses

Hypothesis: The anthropogenic arsenic contamination caused by Vineland Chemical Company has selected for a robust community of bacteria capable of arsenic transformation at various levels.

H^1: Microbial methylarsenic demethylation is occurring.

H^2: Microbial respiratory arsenite [As(III)] oxidation is occurring.

H^3: Microbial respiratory arsenate [As(V)] reduction is occurring.

In this study, environmental bacterial arsenic transformation was investigated in anthropogenically arsenic contaminated subsurface sediments from the former Vineland Chemical Company location in Vineland, NJ. Subsurface sediments from the vadose (371 mg/kg arsenic) and aquifer (81 mg/kg arsenic) zones at this location were extracted, including an off-site (0.7 mg/kg arsenic) control. Enrichment cultures were established using a series of selective media conditions with elevated arsenic. An anion exchange chromatography method with conductivity and UV/Vis detection was developed and utilized to investigate arsenic transformations under each selective condition. While methylarsenic demethylation and arsenite [(AsIII)] oxidation were not evident, [As(V)] reduction activity to As(III) was exhibited in all enrichments amended with lactate and As(V).

The rapid As(V) reduction kinetics and balanced 2:1 As(V):lactate disappearance stoichiometry observed in the on-site aquifer and vadose enrichments and lack thereof in the off-site enrichment suggest a dissimilatory As(V) respiratory mechanism using lactate as the electron donor is followed only in the experimental cultures, while the off-site control is reducing the As(V) as a resistance mechanism. To investigate this possibility further, polymerase chain reaction (PCR), using previously designed degenerate primers, was used to amplify *arrA* (the respiratory As(V) reductase) and *arsC* (the non-respiratory As(V) reductase) genes, followed by cloning and sequencing. Sequencing results revealed that both on-site enrichments possessed *arrA*, while the off-site control did not. All *arrA* gene fragments sequenced from the vadose and aquifer on-site enrichments showed the highest similarity to that of *Desulfosporosinus* Y5, a Gram-negative anaerobic bacterium isolated from the sediment of Onondaga Lake in Syracuse, NY capable of dissimilatory As(V) respiration with lactate as the electron donor. Both on-site enrichments and the off-site enrichment appear to possess *arsC* based on PCR amplicons of expected lengths (353 bp). These molecular findings further support the notion of a respiratory As(V) reduction mechanism in the on-site sediments vs. a resistance pathway in those from the off-site location. PCR was also used to amplify the 16S rRNA gene and ribosomal intergenic spacer (RIS) region, the results of which demonstrated mainly endospore forming *Clostridium* and *Bacillus* species from the Firmicutes (Gram-positive low G+C) phylum and high bacterial community diversity, respectively.

The findings here suggest that the anthropogenic arsenic contamination at this location has selected for potentially environmentally hazardous subsurface dissimilatory arsenate respiring prokaryotes (DARPs).

B. Background

Vineland, New Jersey is home to a location formerly occupied by The Vineland Chemical Company, which commercially produced DSMA-(disodium methylarsonate (MMA(V)-based) and MSMA-based herbicides during its operation from 1950-1994 [31]. During this time span, arsenic containing by-product salts were irresponsibly and improperly disposed of in piles and enclosures formerly used as chicken coops, leading to their contact with rainfall and the contamination of local surface and subsurface sediments, ground water, the Maurice River, the Union Lake, and the Blackwater Branch [31]. Around 57,000 people in the area rely on the groundwater for their drinking water source [31], making the arsenic contamination a serious environmental issue, given the potential for adverse human health consequences. This anthropogenic arsenic contamination forced the Environmental Protection Agency (EPA) to intervene and enforce the Comprehensive Environmental Response, Compensation and Liability Act of 1980 (Superfund Act) as of September 1, 1984 [31]. The clean-up efforts regulated by the EPA remain in effect.

The evolution of bacterial communities capable of performing the aforementioned arsenic transformations in the arsenic contaminated subsurface sediments of the former Vineland Chemical Company location in Vineland, NJ may have contributed to and could further exacerbate the arsenic contamination of the region, posing a serious environmental threat to the neighboring human and animal populations.

DARPs in subsurface sediments have been shown to mobilize immobile As(V) from aluminum and iron containing minerals via respiratory reduction to As(III) [2,89,90] (**Figure 3.1**) suggesting that sediment-bound arsenic in the vadose and aquifer zones in Vineland may be chemically modified and moved into the aqueous state by microbial activity, which could subsequently cause an arsenic contamination in the groundwater. By analyzing the arsenic transforming capacity of the bacterial communities present in these subsurface zones, an understanding of the type of biogeochemical cycling occurring at this site may be reached, providing an explanation for the accumulation of inorganic arsenic in various regions surrounding the former chemical plant. The insight gained from this project will also contribute to the field of biogeochemical arsenic cycling and can be applied to other scenarios in which anthropogenic arsenic contaminations have occurred.

C. Methods and Materials

i. Sediment Excavation

Subsurface sediments from the vadose zone (374 mg/kg total As) and aquifer zone (81 mg/kg total As) from the former Vineland Chemical Company site, including those from an off-site location (0.7 mg/kg As) were aseptically excavated into anaerobic Wheaton bottles. They were stored at 30° C in the dark until analyses were performed.

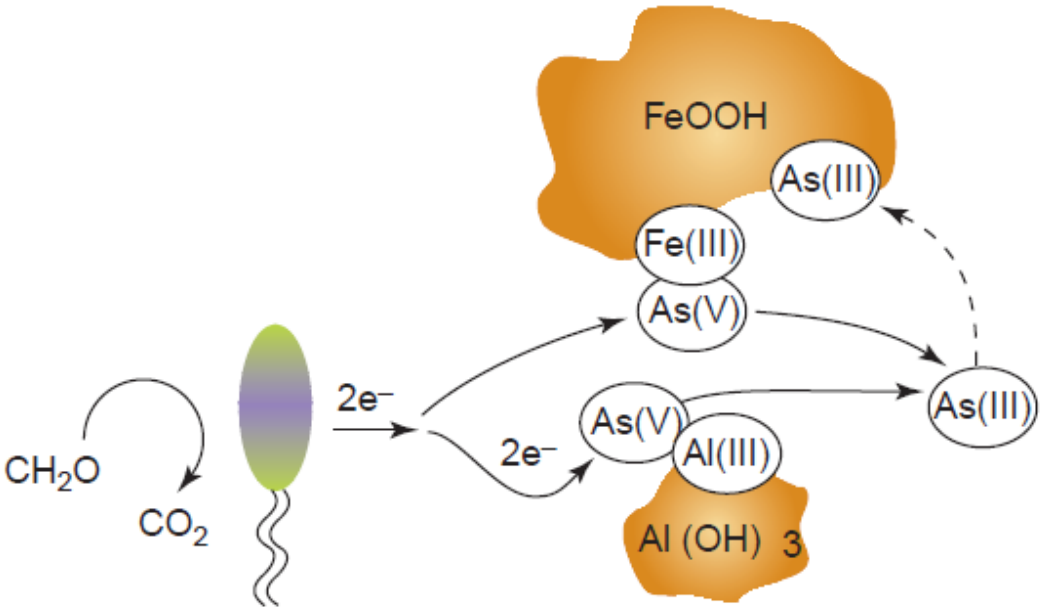

Figure 3.1. Model of subsurface As mobilization via DARP reduction of As(V) to As(III). Adapted from Oremland and Stolz 2005 [3].

ii. Media preparation

a. First set of experiments

In order to culture bacterial communities within the extracted sediments, "SES-3" base media was prepared as follows[91] (grams per 1000 mL): K_2HPO_4 (0.225), KH2PO_4 (0.225), NaCl (0.46), $(NH_4)_2SO_4$ (0.225), $MgSO_4$7H20 (0.117), yeast extract (1), $NaHCO_3$ (4.2), and Na_2S-7$H_2$0 (0.1), followed by 2 mL of 500X vitamin and trace element solutions [86]. The 500X vitamin solution was prepared as follows (grams per 1000mL): biotin (.01), folic acid (.01), pyridoxine (.05), hydrochloride (.05), riboflavin (.025), thiamine (.025), nicotinic acid (.025), pantothenic acid (.025), p-aminobenzoic acid (.025), thioctoc acid (.025) and vitamin B-12 (.0005). The mixture was then filter sterilized (Fisher 0.2 µm PES filter) and stored at 4°C. The 500X trace element solution was prepared as follows (grams per 1000mL): Nitrilotriacetic acid (7.55), magnesium sulfate (15), manganese chloride (2.55), sodium chloride (5), ferric chloride (0.5), calcium chloride (0.5), cobalt chloride (0.5), zinc sulfate (0.5), cupric sulfate (.05), aluminum potassium sulfate (.05), boric acid (.05), sodium molybdate (.125), nickel chloride (.125), and sodium tungstate (.125). Nitrilotriacetic acid, it was dissolved by rigorous stirring and the addition of NaCl pellets until the pH reached 6.5. All additional components were added after this pH was achieved. The solution was then filter sterilized and stored at 4°C. The SES-3 solution was then adjusted to a final pH of 7.3 by the addition of concentrated HCl and allocated in 50 or 100 mL quantities into Wheaton bottles [91]. The bottles were degassed with CO_2 and N_2 at a 3:2 ratio in the liquid media for five minutes followed by the air space for a minute. The bottles were sealed with a butyl stopper, crimp topped and autoclaved.

b. Second set of experiments

For the second round of microcosms and enrichment cultures, four different SES-3 media variations were constructed in order to attempt to grow bacteria capable of metabolizing arsenic in a vvariety of ways. The first media formulation was named "SES-3 DARP" and included the same ingredients indicated above with the exception of 0.5 g/l yeast extract and 2.1 g/l $NaHCO_3$. The second media formulation was named "SES-3 CAO" and consisted of the same ingredients indicated above with the exception of yeast extract. The third media formulation was named "SES-3-HAO" and consisted of the same ingredients above with the exception of 5 g/l yeast extract, 0.5 g/l $NaHCO_3$, and a N_2 alone degas. The fourth media formulation was named "SES-3-D" and consisted of the same ingredients indicated above with the exception of no yeast extract, 0.5 g/l $NaHCO_3$ and N_2 alone degas.

iii. Stock solution preparation

Stock solutions of Na_2HAsO_4 (sodium arsenate), $AsNaO_2$ (sodium arsenite), $(CH_3)_2AsO_2H$ (dimethylarsinic acid), $CH_3AsNa_2O_3$ (disodium methylarsonate) $NaC_3H_5O_3$ (sodium lactate), CH_3COONa (sodium acetate), and $NaNO_3$ (sodium nitrate) were prepared according to **Table 3.1.** The stock solutions were prepared volumetrically and transferred to asterile Wheaton bottles, where they were degassed under 60:40 CO_2:N_2 for 5 minutes. The asterile solutions were sealed with a butyl stopper, crimp topped, and then filter sterilized into a separate, degassed, sealed and autoclaved Wheaton bottle and stored at 4°C for future use.

iv. Microcosm and enrichment culture establishment

a. First set of experiments

The sediments previously excavated and stored as described above were aseptically added in ~5 g amounts to 100 mL of anaerobic SES-3 basal media. The sediments were quickly added to the media followed by resealing the bottles with a butyl stopper and crimp top. The head spaces of the sealed microcosms were purged with filtered N_2 gas for 5 minutes to eliminate potential O_2 contamination resulting from the sediment transfer. Separate microcosms were prepared using vadose, aquifer and off-site sediments as inoculums. Each microcosm was placed in a 30° C incubator in the dark to stimulate microbial growth. After macroscopic turbidity was witnessed in the aquifer, vadose and off-site microcosms, 1 mL of each was transferred to fresh SES-3 media bottles amended with different combinations of electron donors and acceptors in order to establish several growth conditions. (**Table 3.2**). Amendments were performed by aseptically and anaerobically transferring set volumes from each stock solution into media bottles to reach the desired final concentrations of each. Viable cultures were maintained by 1 mL transfer into fresh, appropriately amended media bottles on a biweekly basis.

b. Second set of experiments

Microcosms were prepared as described above and transferred to a new set of enrichment conditions. For the second set of enrichments, different media compositions were used for each selective condition (**Table 3.3**). Cultures were maintained by incubating at 30° C in the dark and aseptically transferring 1 ml to fresh media every two weeks.

Compound	Concentration
Sodium arsenate	500 mM
Sodium arsenite	500 mM
Dimethylarsinic acid	500 mM
Disodium methylarsonate	20 mM
Sodium lactate	1 M
Sodium acetate	500 mM
Sodium nitrate	2 M

Table 3.1. Stock solutions prepared for amendment into media. All were prepared in sterile NANOpure water.

Growth Condition	Electron Donor	Electron Acceptor
1	Lactate (10 mM)	As(V) (5 mM)
2	As(III) (5 mM)	NO_3^- (20 mM)
3	Lactate (10 mM)	DMA (5 mM)
4	DMA (5 mM)	NO_3^- (20 mM)

Table 3.2. Growth conditions established for initial enrichment cultures. A variety of electron donor/acceptor combinations were utilized to select for different categories of arsenic transforming bacteria. Growth condition 1 selects for DARPs, condition 2 selects for CAOs and conditions 3 and 4 select for methylarsenic demethylating strains.

Media Type Used	Electron Donor	Electron Acceptor
SES-3 DARP	10 mM Lactate	5 mM As(V)
SES-3 DARP	10 mM Acetate	5 mM As(V)
SES-3 CAO	5 mM As(III)	5 mM NO_3^-
SES-3 HAO	5 g Yeast Extract	5 mM As(III)
SES-3 Dem	10 mM DMA	10 mM NO_3^-
SES-3 Dem	10 mM DMA	None

Table 3.3. Growth conditions established for second enrichment culture set. The type of bacteria selected for is indicated in the nomenclature of each media type: SES-3-DARP media selects for DARPS, SES-3 CAO selects for CAOs, SES-HAO selects for HAOs and SES-Dem selects for methylarsenic demethylating bacteria.

At various time points, a sterile syringe flushed with O_2-free N_2 gas was used to extract 1 ml of raw culture for growth analyses and 1 ml of filtered culture (0.22 µM PES) for chemical analyses. Following culture extractions, each tube was placed at -80° C for future use. Growth was quantitated by thawing the raw culture extracts and analyzing the optical density (O.D.) on a Perkin-Elmer Lambda 2 dual-beam spectrophotometer at 600 nm wavelength[30,87,92]. SES-3 media identical to that used during the inoculations was used as a standard to zero the instrument prior to quantitating each sample. Analytical aliquots were thawed, diluted 20-fold in NANOpure water and analyzed as previously described on the Dionex ICS-1100 anion chromatography system.

v. Molecular Methods

a. Genomic DNA Extraction

All genomic DNA extractions for molecular analyses were performed using a modified and optimized Phenol/Chloroform technique. The technique was developed by combining various techniques that were documented and available in the Stolz lab. Cultures were grown to log-phase (12-24 hours of incubation), transferred to a 50 ml centrifuge tube and centrifuged at 7,000 rpm for 10 minutes. The supernatant was discarded and 1 ml of a modified buffer (1 mM Tris pH 8.0; 500 mM EDTA pH 8.0) was added. The pellet was then resuspended via vigorous vortexing and transferred to a 1.5 ml microfuge tube. The resulting solution was then centrifuged at 7,000 rpm for 10 minutes, with the resulting supernatant being discarded. The pellet was then resuspended and washed in 494 µL of TE buffer via vortexing.

Thirty µl of 10% sodium dodecyl sulfate (SDS) , 72 µL of lysozyme working solution (100 mg/ml prepared fresh each time in TE buffer), and 1.2 µl of RNase working solution (10 mg/ml prepared in sterile NANOpure water) were added to give final concentrations of 0.5%, 12 mg/ml and 20 µg/ml of each, respectively. The resulting solution was mixed by micropipetting and incubated for 1 hour at 37° C with light shaking. Three µl of proteinase K working solution (20 mg/ml prepared in sterile NANOpure water) was added, mixed by micropipetting, and incubated for 45 minutes at 37°C with light shaking. Six hundred µl of a 1:1 volumetric ratio working solution of Tris-buffered phenol/chloroform was added. The Tris-buffered phenol was prepared by adding (volumetrically) 1 part Tris pH 8.0 to 1 part pure liquid phenol and shaking/inverting rigorously for phase separation. The solution was inverted several times and centrifuged for 10 minutes at 12,000 rpm. The aqueous phase of the resulting biphasic solution transferred to a fresh 1.5 ml tube. The phenol/chloroform working solution was again added to the fresh tube at a 1:1 volumetric ratio, followed by another 10 minute centrifugation step at 12,000 rpm. The aqueous phase was removed from the resulting biphasic solution and placed in a fresh 1.5 ml microfuge tube. Pure chloroform was added at a 1:1 volumetric ratio to the tube followed by a final 12,000 rpm spin in the centrifuge. The final aqueous phase was transferred to a fresh 1.5 mL tube. Sodium chloride (5M NaCl) was added to achieve a final concentration of 5M as well as 0.6 volumes of room temperature isopropanol (the volumes of NaCl and isopropanol were dependent upon the amount of aqueous phase withdrawn during the final chloroform extraction step).

The DNA precipitated out of solution and became visible as a white stringy substance after inverting the tube several times. This stringy precipitate was pelleted by briefly centrifuging (~1 minute) at room temperature at 12,000 rpm. The supernatant was carefully removed and the resulting DNA pellet washed (without vortexing or pipetting to mix) using 1 ml of room temperature 70% ethanol, followed by a 5 minute spin at room temperature. The supernatant was then carefully removed and the tube was placed in a speed vacuum for 10-15 minutes using medium heat. When the ethanol was fully evaporated, the dry pellet was resuspended in 50 ml of sterile NANOpure water by gently flicking and incubating at 4°C for several hours. To verify the presence of RNA-free DNA, 5 µl of the resulting resuspended solution was electrophoresed on a 0.8% agarose gel for 45 minutes at 120 V (procedure described below) and quantified using the Qubit Fluorometer (described below).

b. Agarose gel electrophoresis

For all agarose gel electrophoresis experiments, a 1000 ml stock solution of 50X TAE buffer was prepared. The 50X TAE stock solution was prepared by adding 242 g of Tris base, 57.1 ml of glacial acetic acid and 18.61 g of EDTA and taking the solution to 1000 ml with deionized water. A working solution of 1X TAE was prepared by adding 20 ml of 50X TAE to 980 mL of deionized water. To prepare the agarose gels, the desired amount of agarose powder was added to 100 mL of 1X TAE buffer working solution in a 250 ml beaker (i.e. 2 g of agarose added makes a 2% gel). The solution was mixed briefly by hand swirling and microwaved for 60-90 seconds to fully dissolve the agarose.

Following cooling at room temperature briefly, 0.5 µL of a 50 mg/ml ethidium bromide solution was added to achieve a final ethidium bromide concentration of 2.5 µg/ml.

The solution was briefly swirled by hand to mix and poured into a Thermo Scientific Owl EasyCast horizontal gel unit. The gel was given 45-60 minutes to solidify and 1X TAE working solution was poured over the gel up to the fill line. Samples were prepared by mixing the DNA of interest with 6X loading dye to achieve a final loading dye concentration of 1X and loaded into the gel using a micropipette. Electrophoresis was performed at varying voltages between 50-120 mV depending on the type of analyses being performed.

c. Polyacrylamide gel electrophoresis

Polyacrylamide gels electrophoresis (PAGE) was performed for ribosomal intergenic spacer analysis (RISA). For all PAGE experiments a 5X TBE stock solution was prepared by adding 54 g of Tris base, 27.5 g of boric acid, 20 ml 0.5 M EDTA (pH 8.0) and taking the solution 10 1000 ml with deionized water. The 0.5 M EDTA (pH 8.0) was prepared by adding 1.8612 g EDTA to 100 ml of deionized water. The solution was mixed on a magnetic stirring plate with NaOH gradually added to fully dissolve the mixture and adjust the final pH to 8.0. The resulting solution was autoclaved for 30 minutes for sterilization. A 1X TBE buffer working solution was prepared by adding 200 ml of 5X TBE to 800 ml of deionized water. Reagents required to prepare a polyacrylamide gel were a 40% acrylamide/bis-acrylamide solution, 10% ammonium persulfate (APS) solution, and TEMED. The 40% acrylamide/bis-acrylamide solution was prepared by adding 38.93 g acrylamide and 1.07 g of bis-acrylamide to a 200 ml jar and taking the volume to 100 ml with deionized water (stored at 4° C).

The 10% APS solution was prepared by adding 1 g of APS to a centrifuge tube and taking the volume to 10 ml with deionized water (stored at 4° C). To prepare the polyacrylamide gel (5%), 9.965 ml of deionized water and 3 ml of 5X TBE were added to a 50 ml beaker, followed by 1.87 ml of the 40% acrylamide/bis-acrylamide solution, 150 µl of 10% APS, and 15 µl of TEMED. Immediately after adding the TEMED, the gel solution was poured via 10 ml syringe into the casting plates and locked into the casting apparatus (Bio-Rad, Hercules, CA). After allowing gel polymerization to occur for at least 30 minutes, the casting apparatus was then placed in the vertical electrophoresis unit (Bio-Rad) followed by the addition of 1X TBE buffer. DNA samples and 6X loading dye were loaded via micropipette into the gel lanes in a fashion in which gave the loading dye a final concentration of 1X (i.e. 20 µl DNA, 4 µl loading dye). PAGE was then carried out at 70 mV for 1.5 hours, followed by soaking of the gel in 1µg/ml ethidium bromide solution for 30 minutes on a rocking tray.

d. DNA Quantitation

All DNA quantitation was performed using an Invitrogen Qubit Fluorometer with the dsDNA BR Assay Kit. Working solution was prepared in 1.5 mL microfuge tubes by diluting the provided dsDNA BR reagent 200-fold in the provided reaction buffer. This working solution was added to the DNA sample of interest in the provided thin-wall 0.5 ml provided PCR tubes to reach a final volume of 200 µL. Between 1 and 10 µL of DNA can be used meaning between 190-199 µL of working solution was added per tube.

Standard solutions included in the kit (Standard 1: 0 ng /µL DNA; Standard 2: 200 ng/ µL DNA) were added in 10 µL volumes to the tubes along with 190 µL of working solution for calibrations. All samples were vortexed briefly for 2-3 seconds and incubated for 2 minutes at room temperature before quantitating using the Qubit platform. Concentrations (ng/µl) were calculated automatically and displayed on the screen of the unit based on total DNA content and the volume of sample used.

f. Polymerase Chain Reaction (PCR)

Standard PCR mixture conditions for all reactions performed included the following unless otherwise specified (per 50 µL individual reaction): 50 ng DNA, 10 µL of Promega (Madison, WI) 5X GoTaq Reaction Buffer, 1 µL Promega 10 mM dNTP mix (200 µM final concentration), 0.5 uM forward and reverse primers (volumes depends on primer concentrations), 1 unit of Promega GoTaq Polymerase and sterile NANOpure water until final volume was reached. A master mix (30 µl/reaction) was prepared for all PCR reactions including (in order) sterile NANOpure water, 5X GoTaq Buffer, 10 mM dNTP mix, forward primer, reverse primer, and GoTaq Polymerase. Thirty µl of master mix was added to individual reaction tubes containing a 20 µl mixture of sterile NANOpure water and 50 ng of template DNA. Forward and reverse primer oligonucleotides were synthesized by Integrated DNA Technologies (IDT; Coralville, IA) and resuspended in 1 ml of sterile NANOpure water before being used. PCR reaction parameters varied depending on the type of analysis being performed and will be described below. All reactions were performed using a Techne Incorporated (Romeoville, IL)) Techgene thermal cycler.

g. Ribosomal Intergenic Spacer Analysis

Bacteria have specific operons in their genomes that are responsible for the production of rRNA [93] **(Figure 3.2).** Within this operon, between the 16S rRNA gene (upstream) and 23S rRNA genes (downstream) lies a region referred to as the ribosomal intergenic spacer (RIS) [93]. The length and sequence of this spacer region varies among bacterial species and strains, making its utilization during molecular analyses highly useful [93]. PCR amplification of the RIS DNA locus is known as ribosomal intergenic spacer analysis (RISA) and has been used extensively to analyze biodiversity in heterogeneous bacterial communities, including those found in environmental soils [94-96]. After PCR amplification of the RIS regions in a mixed culture of bacteria, each unique amplicon of unique length migrates a different distance during agarose or polyacrylamide gel electrophoresis, allowing for each gel band to represent a different species. This allows for a rapid and easy method of determining biodiversity in a complex bacterial community. The technique is not flawless, however, as many species and strains have multiple rRNA operons with RIS regions of different lengths in their genomes [93]. Multiple primer sets that bind to conserved regions in the 16S and 23S rRNA genes have been designed for RIS amplification. The primers ITSF and ITSReub **(Table 3.4),** which bind to conserved regions in the 16S rRNA gene (nucleotide positions 1423-1443) and 23S rRNA gene (nucleotide positions 38-23), respectively, have been shown to be very effective for RISA[97]. Therefore, the ITSF and ITSReub primer pair was chosen for all RISA work conducted.

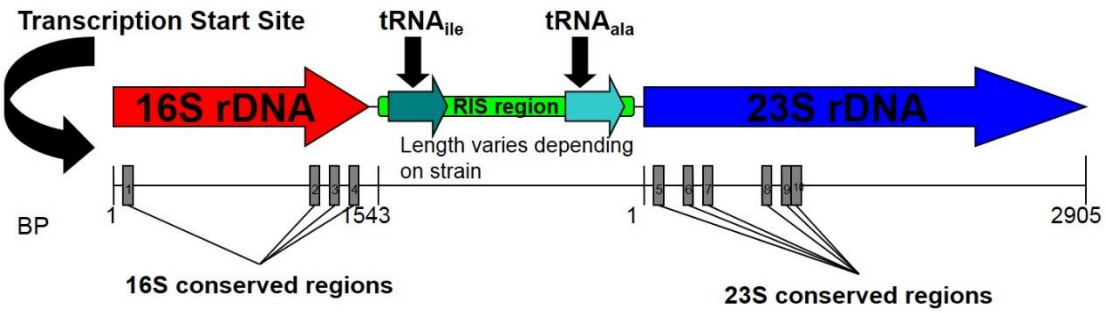

Figure 3.2. Schematic diagram of the rRNA operon (*E. coli*) found in bacterial genomes. In many cases (not always), the RIS region varies in length among individual strains. Amplifying this region using PCR, a widely used technique known as ribosomal intergenic spacer analysis (RISA), is a useful tool for determining biodiversity in a heterogeneous bacterial sample.

The PCR program known as "Touchdown" was chosen for RISA and included the parameters in **Table 3.5** [108]. The amplification reaction products were electrophoresed on a 2% super fine resolution (SFR) agarose gel for 2 hours at 70 mV. RISA products were cloned and sequenced in the initial enrichment culture experiments. In the second enrichment culture experiments, the RISA PCR products were only used to qualitatively determine bacterial biodiversity via migration patterns after agarose gel electrophoresis.

h. 16S rRNA gene amplification

The 16S rRNA gene, which encodes the 16S rRNA, possesses multiple regions that are highly conserved throughout the entire prokaryotic kingdom. These regions of homology allow for the easy PCR amplification and cloning of the gene, making its utilization a very powerful tool in molecular biology, as species identities and phylogenetic relationships can be deduced from its full sequence [98]. This technique has been widely practiced and proven to be highly useful in determining identities of unculturable bacterial species and strain isolates, as well as measuring biodiversity in heterogeneous environmental communities [70,88,91,92,99-103]. By PCR amplifying, cloning and sequencing the 16S rDNA from genomic DNA in the enrichment cultures as well as any potential culture isolates, it is possible to obtain the identities and phylogenetic distribution of the bacteria present. For 16S rDNA amplification, the 8F (anneals at nucleotide positions 8-28) and 1492R (anneals at nucleotide positions 1492-1473) forward and reverse primers, respectively were chosen and their properties are indicated in **Table 3.6** [104]. The "Touchdown" PCR program was again chosen for amplification. The amplification products were electrophoresed for 1 hour at 100 mV on a 1% agarose gel.

Gene	Name	Sequence (5'-3')	T_m,˚C	Reference
16S-23S Spacer	ITSF	GTCGTAACAAGGTAGCCGTA	N/A	97
16S-23S Spacer	ITSReub	GCCAAGGCATCCACC	N/A	97

Table 3.4. Properties of ITSF and ITSReub primers used for RISA.

Stage	# of Cycles	Temperature (°C)	Time (min.)
	1		
Initial Denaturation		94	5
	20		
Denaturation		94	1
Annealing (first)		60 (drop 0.5/cycle)	1
Annealing (last)		50	1
Extension		72	3
	15		
Denaturation		94	1
Annealing		50	1
Extension		72	3
	1		
Final Extension		72	7
	1		
Final Hold		4	Indefinite

Table 3.5. Cycle parameters for "Touchdown" PCR[108].

i. *arrA* probing

A powerful tool for detecting respiratory As(V) reduction is to probe bacterial genomes for the gene encoding the catalytic subunit of the Arr enzyme, *arrA*. Several research groups have taken advantage of the evolutionary conservation of this gene by designing degenerate PCR primers designed to amplify *arrA* fragments, allowing for detection of the respiratory As(V) reductase gene within heterogeneous bacterial DNA samples. This technique provides a concrete molecular marker for respiratory As(V) reduction and, thus, the presence of DARPs in environmental samples of unknown bacterial composition [101,102,105,106]. For this experiment, the degenerate primer sets indicated in **Table 3.7** were used to probe for the presence of DARPs in the SES-3 DARP enrichments amended with As(V) and lactate. For the primer pair ArrAfwd and ArrArev, the PCR parameters described in **Table 3.8** were used [105]. All amplification products were electrophoresed for 1 hour and 45 minutes at 80 mV on a 2% SFR agarose gel. For primer pair *arrA*F1 and *arrA*R2, the PCR parameters indicated in **Table 3.9** were established [108]. For primer pairs *arrA*F5/*arrA*R6 and *arrA*F5/*arrA*R8, the PCR parameters indicated in **Table 3.10** were established [108]. For the primer pair *arrA*F1/*arrA*R3, "Touchdown" PCR was used. All *arrA*F and *arrA*R primer set amplifications were electrophoresed on 1.5% agarose gels at 100 mV for 1 hour and 15 minutes. For the primer pairs AS1F/AS1R (Initial PCR I) and AS1F/AS2R (Initial PCR II), the PCR reaction mixtures were assembled as previously described for all reactions, with the exception of adding dNTPs at a final concentration of 100 µM, 100 ng of genomic template DNA and GoTaq Buffer at a final concentration of 1x [102]. Each reaction tube had a final volume of 25 µl [102].

Gene	Name	Sequence (5'-3')	T_m,˚C	Reference
16S rRNA	8F	AGAGTTTGATCCTGGCTCAG	52	104
16S rRNA	1492R	GGTTACCTTGTTACGACTT	54	104

Table 3.6. Properties of 8F and 1492R primers for 16S rDNA analyses [104].

Primer Name	Sequence (5'-3')	T_m,˚C	Reference
*arrA*F1	CGCCCGCCGCGCCCCGCGCCCGTCCGCCGCCCCC GCCCGTGTCAAGGHTGTACBDCHTGG	81.9	108
*arrA*R2	GTATCVATHGCTTCNTCCCA	53.1	108
*arrA*R3	GCWGCCCAYTCVGGNGT	60.3	108
*arrA*F5	CGCCCGCCGCGCCCCGCGCCCGTCCCGCCGCCCCCGC CCGADTTTGAGTTYTAYAGYGAAAC	79.4	108
*arrA*R6	TCATAGTGNGGNACAAAGGC	54.9	108
*arrA*R8	GGGTTVAWTTTNGCBACATC	51.5	108
AS1F	CGAAGTTCGTCCCGATHACNTGG	69.2	102
AS1R	GGGGTGCGGTCYTTNARYTC	63.7	102
AS2F	GTCCCNATBASNTGGGANRARGCNMT	64.2	102
AS2R	ATANGCCCARTGNCCYTGNG	62.2	102
ArrAfwd	AAGGTGTATGGAATAAAGCGTTT	N/A	105
ArrArev	CCTGTGATTTCAGGTGCC	N/A	105

Table 3.7. Properties of all primers used for *arrA* amplification.

Stage	No. of Cycles	Temperature (°C)	Time
	1		
Initial Denaturation		94	5 minutes
Loops 1-4	**2 per loop**		
Denaturation		94	45 seconds
Annealing (loop 1)		56 (drop 2/loop)	45 seconds
Annealing (loop 4)		50	45 seconds
Extension		72	1 minute
Loop 5	**20**		
Denaturation		94	45 seconds
Annealing		48	45 seconds
Extension		72	1 minute
	1		
Final Extension		72	5 minutes
	1		
Final Hold		4	Indefinite

Table 3.8. PCR cycle parameters for *arrA* probing using the ArrAfwd /ArrArev primer pair [105].

Reaction parameters named "Initial PCR I" and "Initial PCR II" indicated in **Table 3.11** were established [107]. A nested approach was taken toward the products of "Initial PCR I" and "Initial PCR II" by using 1 µl of each as a DNA template for a reamplification reaction consisting of the standard PCR mixture specifications listed previously, with the exception of 50 µM dNTP concentration, 1µM concentration of the forward and reverse primers AS2F and AS1R, respectively, and the addition of 1.5 mM $MgCl_2$. The PCR reaction parameters indicated in Table as "Nested PCR" were followed [107]. The PCR I initial and nested reactions were repeated using the standard PCR reaction mixture conditions previously described. For the nested reaction, 1 µl of PCR I product DNA was used as the template. Amplification products of each initial PCR as well as the nested reactions were electrophoresed for 1 hour and 15 minutes on a 1.5% agarose gel. The products were cloned and sequenced.

j. *arsC* probing

Degenerate primers have successfully been designed and utilized to probe for multiple genes comprising the *ars* operon such as *arsA*, *arsB* and *arsC* [66,107,109]. Detection of any gene within this operon provides direct evidence of a resistance mechanism of As(V) reduction versus that of a respiratory nature. For this experiment, the non-respiratory *arsC* gene (encoding ArsC, the cytoplasmic non-respiratory As(V) reductase enzyme) was chosen as a target for PCR probing, as its presence in heterogeneous bacterial genomic DNA provides further insight into the mechanism of As(V) reduction that is operating.

Stage	No. of Cycles	Temperature (°C)	Time
	1		
Initial Denaturation		94	5 minutes
Loops 1-7	**2 per loop**		
Denaturation		94	45 seconds
Annealing (loop 1)		54 (drop 2/loop)	45 seconds
Annealing (loop 7)		42	45 seconds
Extension		72	1 minute
	1		
Final Extension		72	5 minutes
	1		
Final Hold		4	Indefinite

Table 3.9. PCR cycle parameters for *arrA* probing using the *arrA*F1/*arrA*R2 primer pair [108].

Stage	**No. of Cycles**	**Temperature (°C)**	**Time**
Initial Denaturation	**1**	95	10 minutes
	40		
Denaturation		95	15 seconds
Annealing		50	40 seconds
Extension		72	1 minute
Final Hold	**1**	4	Indefinitely

Table 3.10. PCR cycle parameters for *arrA* probing using the *arrA*F5/*arrA*R6 and *arrA*F5/*arrA*R8 primer pairs [108].

Stage	No. of Cycles	Temperature (°C)	Time
Initial PCR I			
	1		
Initial Denaturation		94	5 minutes
	35		
Denaturation		94	30 seconds
Annealing		50	30 seconds
Extension		72	1 minute
	1		
Final Hold		4	Indefinitely
Initial PCR II			
Initial Denaturation	**1**	72	5 minutes
	35		
Denaturation		94	30 seconds
Annealing		55	30 seconds
Extension		72	2 minutes
Final Hold	**1**	4	Indefinitely
Nested PCR			
Initial Denaturation	**1**	72	2 minutes
	30		
Denaturation		94	30 seconds
Annealing		55	30 seconds
Extension		72	1 minute
Final Hold	**1**	4	Indefinitely

Table 3.11. PCR cycle parameters for *arrA* probing using the AS1F/AS1R (Initial PCR I), AS1F/AS2R (Initial PCR II) and AS2F/AS1R (nested PCR) primer sets [102].

The degenerate primers designed for *arsC* amplification listed in **Table 3.12** were chosen for this experiment. For the *arsC*F/*arsC*R forward and reverse primer set, respectively, the PCR cycle parameters listed in **Table 3.13** were followed and the reaction mixtures were assembled as previously described for standard PCR reactions [100]. For the *amlt-42-f*/*amlt-376-r* and *smrc-42-f*/*smrc-376-r* primer sets, the PCR parameters listed in **Table 3.14** were followed [107]. Standard PCR mixture conditions were used with the exception of using 0.25 µM concentrations of each primer [107]. All amplification products were electrophoresed for 1 hour and 45 minutes at 80 mV on a 2% SFR agarose gel. The products were purified, cloned and sequenced following amplification.

k. Cloning and Sequencing

All RISA product ligations and transformations from the initial experiments were performed using a Life Technologies (Grand Island, NY) TOPO® TA® cloning kit with One Shot® TOP10 electrocompetent *E. coli* cells according to the manufacturer's instructions. The pCR™2.1-TOPO TA vector **(Figure 3.3)** was used for these experiments. For transformant analyses, 1.5% LB agar plates with 100 µg/ml ampicillin were prepared by adding 10 g tryptone, 5 g yeast extract, 5 g NaCl and 15 g agar to a 1000 ml bottle and taking the solution to 1000 ml with deionized water. The solution was mixed and the pH was set to 7.0 by adding NaOH. After autoclaving for 30 minutes and allowing to cool, ampicillin was added at a final concentration of 100 µg/ml. Agar plates were poured in an aseptic fashion by an open flame, capped and solidified at room temperature for 30 minutes, and stored at 4°C.

Gene	Name	Sequence (5'-3')	T_m,˚C	Reference
arsC	*amlt-42-f*	TCGCGTAATACGCTGGAGAT	54	107
arsC	*amlt-376-r*	ACTTTCTCGCCGTCTTCCTT	54	107
arsC	*smrc-42-f*	TCACGCAATACCCTTGAAATGATC	59	107
arsC	*smrc-376-r*	ACCTTTTCACCGTCCTCTTTCGT	59	107
arsC	*arsC*F	AACAGTTGCCGCAGCATTCT	N/A	100
arsC	*arsC*R	ATGCGCTCCAGCTCACGCTT	N/A	100

Table 3.12. Properties of all primers used for *arsC* amplification.

Stage	**No. of Cycles**	**Temperature (°C)**	**Time**
Initial Denaturation	**1**	94	2 minutes
	28		
Denaturation		94	30 seconds
Annealing		55	30 seconds
Extension		72	1 minute
	1		
Denaturation		94	1 minute
Annealing		55	1 minute
Extension		72	5 minutes
Final Hold	**1**	4	Indefinitely

Table 3.13. PCR cycle parameters for *arsC* probing using the *arsC*F/*arsC*Rr primer set [100].

Stage	No. of Cycles	Temperature (°C)	Time
Initial Denaturation	**1**	95	3 minutes
	40		
Denaturation		95	15 seconds
Annealing		60	15 seconds
Extension		72	15 seconds

Table 3.14. PCR cycle parameters for *arsC* probing using the *amlt-42-f*/*amlt-376-r* and *smrc-42-f*/*smrc-376-r* primer sets [107].

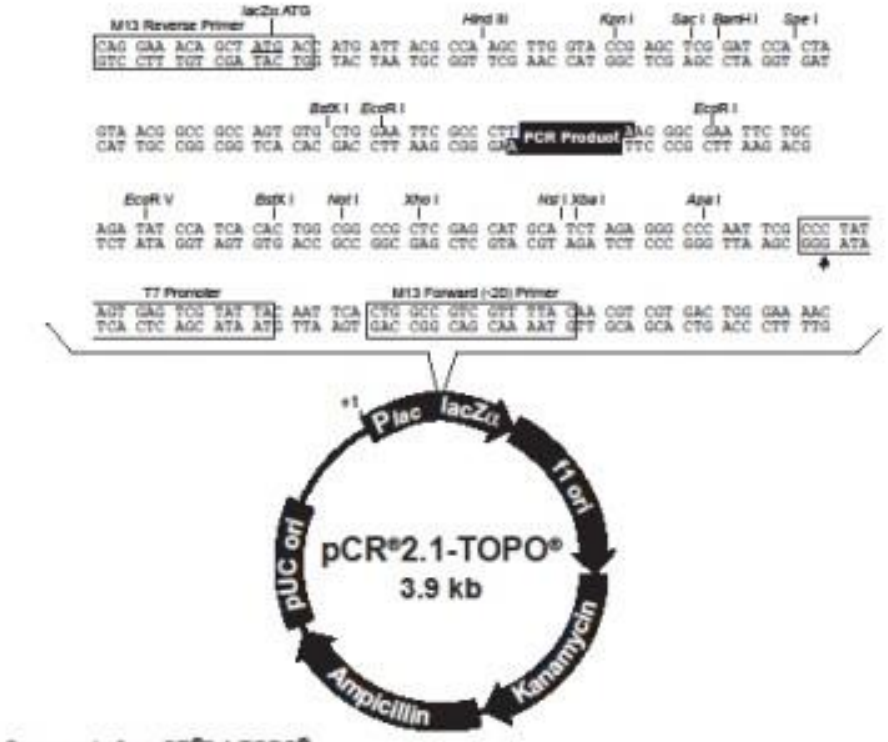

Comments for pCR®2.1-TOPO®
3931 nucleotides

*Lac*Zα fragment: bases 1-547
M13 reverse priming site: bases 205-221
Multiple cloning site: bases 234-357
T7 promoter/priming site: bases 364-383
M13 Forward (-20) priming site: bases 391-406
f1 origin: bases 548-985
Kanamycin resistance ORF: bases 1319-2113
Ampicillin resistance ORF: bases 2131-2991
pUC origin: bases 3136-3809

Figure 3.3. Map of the pCR™2.1-TOPO vector. Adapted from: Thermo Fisher Scientific. Map of pCR2.1-TOPO. *TOPO TA Cloning Kit*. 2015: 29. https://tools.thermofisher.com/content/sfs/manuals/topota_man.pdf.

Prior to their use in the transformation reactions, the plates were dried at room temperature and overlaid with 40 µl of 40 mg/ml X-gal solution in N-N-dimethylformamide. The reasoning behind this is due to the presence of the *lacZ* gene in the vector used in this experiment. This specific gene is responsible for producing the β-galactosidase protein, which creates a blue coloration in the cell when X-gal is cleaved by β-galactosidase. The insertion site of the PCR product in this specific vector disrupts the *lacZ* gene, preventing the formation of β-galactosidase. Thus, the colonies that turn blue can be interpreted as possessing empty vectors (intact *lacZ* gene) and need not be further analyzed. After the transformation reactions, only white colonies were transferred individually via sterile toothpick to separate 15 ml centrifuge tubes containing LB media. After incubating the transformants in LB media tubes, plasmid extractions were performed using a Promega plasmid extraction kit according to the manufacturer's instructions.

All ligations and transformations from the second experiments (*arrA* and *arsC* probing, 16S rDNA analyses) were performed using a Life Technologies TOPO® TA® cloning kit for sequencing with One Shot® TOP10 chemically competent *E. coli* cells according to the manufacturer's instructions. The pCR™4-TOPO TA vector **(Figure 3.4)** was used for these experiments.

Due to the DNA sequence properties of the pCR™4-TOPO TA vector, blue and white screening to identify transformants containing gene inserts versus false positives containing empty vectors was unnecessary, as lack of PCR product insertion into the ligation locus of the vector results in lethality (The intact *ccdB* gene is lethal) and prevents colony formation; thus, if a transformant contains an empty vector it will fail to grow.

Following the transformation reactions, colonies were selected and PCR product insert amplifications were performed using an optimized colony PCR protocol as follows: Each colony was carefully picked using a sterile toothpick and resuspended in 50 µl of sterile NANOpure water in a microfuge tube. After resuspending each colony, the tubes placed in the thermal cycler and heated for 2 minutes at 98° C to lyse the cells. Twenty microliters of the resuspended and lysed colonies were used as the template DNA and PCR reaction reagents, including M13 forward and reverse primers, were prepared in a master mix, yielding final reaction tube concentrations listed on page 91 for standard PCR conditions (50 µl reaction tube volumes). The "Colony PCR" program (**Table 3.15**) on the thermal cycler was selected for PCR amplifications. The resulting PCR products were purified using sephadex columns and a microcentrifuge. The Applied Biosystems (Grand Island, NY) Big Dye Terminator v3.1 Cycle Sequencing kit was utilized for sequencing according to the manufacturer's instructions but with ArrAfwd and ArrArev primers used instead of M13F and M13R. Following the sequencing reaction, the sequences were analyzed on an ABI 3100 automated sequencer according to the manufacturer's instructions.

Stage	No. of Cycles	Temperature (°C)	Time
Initial Denaturation	**1**	95	5 minutes
	30		
Denaturation		95	30 seconds
Annealing		55	30 seconds
Extension		72	2 minutes
	1		
Final Extension		72	10 minutes

Table 3.15. Cycle parameters of the "Colony PCR" program.

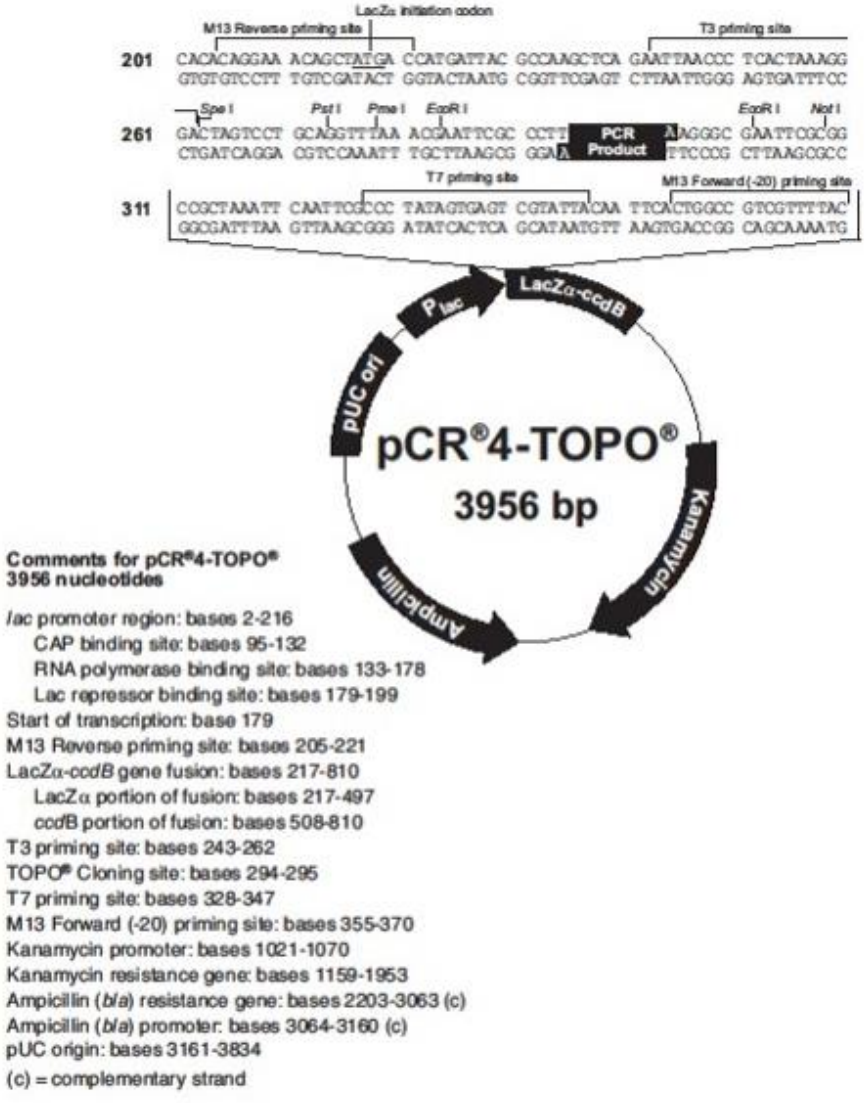

Figure 3.4. Map of the pCR™4-TOPO vector. Adapted from: Thermo Fisher Scientific. Map of pCR4-TOPO. *TOPO TA Cloning Kit for Sequencing*. 2014: 35. https://tools.thermofisher.com/content/sfs/manuals/topotaseq_man.pdf.

Once the sequences were obtained, GenBank (National Center for Bioinformatics, (http://www.ncbi.nih) nucleotide (Blast N) searches were performed to identify similarities to other sequences on the database and deduce the identity of each gene. The aforementioned cloning and sequencing protocol was followed for all molecular analyses with the exception of the 16S rDNA amplifications. For 16S rDNA analyses, whole genomic DNA samples from the vadose, aquifer and lactate enrichments grown in the presence of As(V) and lactate were sent to the University of Pittsburgh for high throughput sequencing under the supervision of Dr. Kyle Bibby.

vi. Analytical methods

All analytical work during these experiments was conducted using the Dionex ICS-1100 ion exchange chromatography system and Chromeleon LE 7.0 software as described in Chapter II. Standard preparation protocols, properties and results can all be found in the previous chapter.

D. Results

i. Initial Experiments

a. Slurry and enrichment incubations

Slurries established from the on-site aquifer and vadose zone sediments as well as those from the off-site location yielded macroscopic growth evidence (turbidity) after 24 hours of incubation. Each selective media enrichment culture continued to demonstrate macroscopic growth after three transfers from slurry (**Figure 3.5**) and microscopic evidence verified the presence of bacteria (**Figure 3.6**).

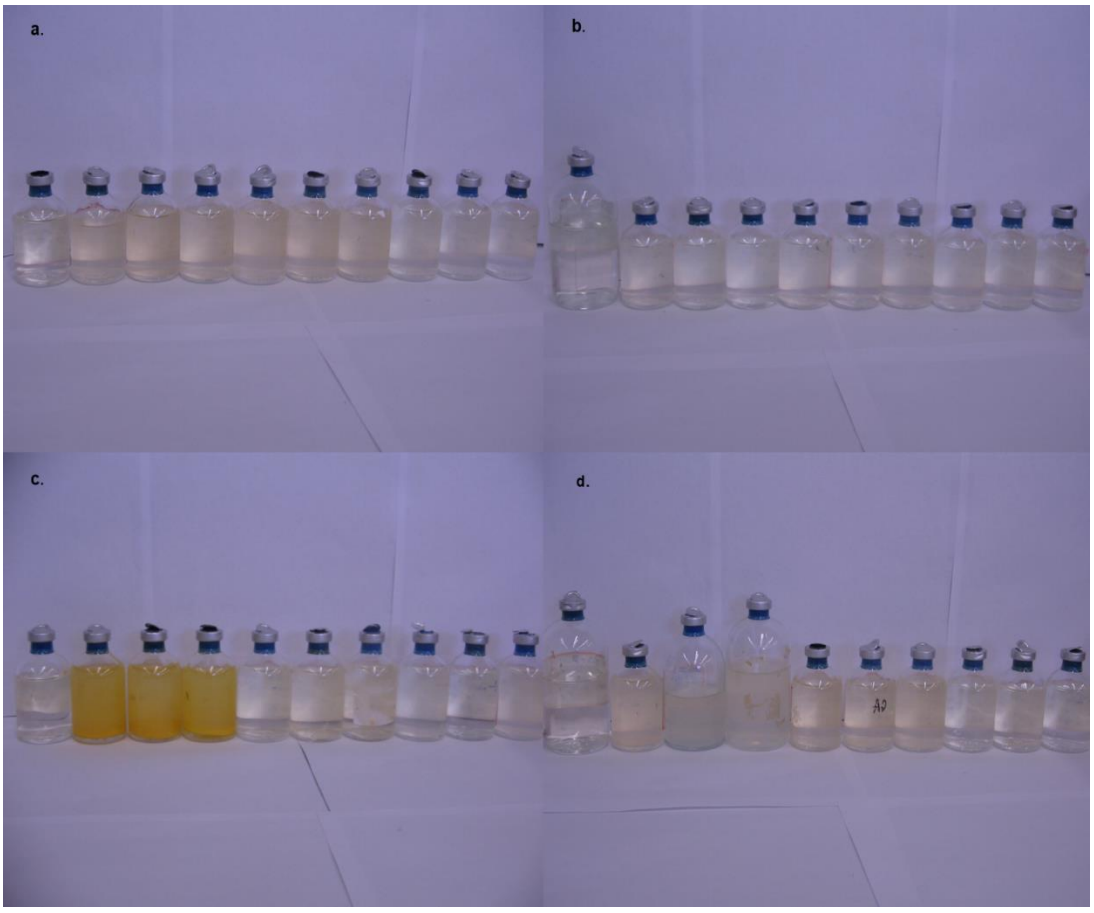

Figure 3.5. Photos of a. 5 mM DMA and 20 mM nitrate; b. 5 mM DMA and 10 mM lactate; c. 5 mM As(V) and 10 mM lactate and d. 5 mM As(III) and 20 mM nitrate enrichments (3 transfers from slurry) after 3 days of incubation. Bottles from left to right: 1. Abiotic; 2-4. Vadose; 5-7. Aquifer; 8-10. Off-site.

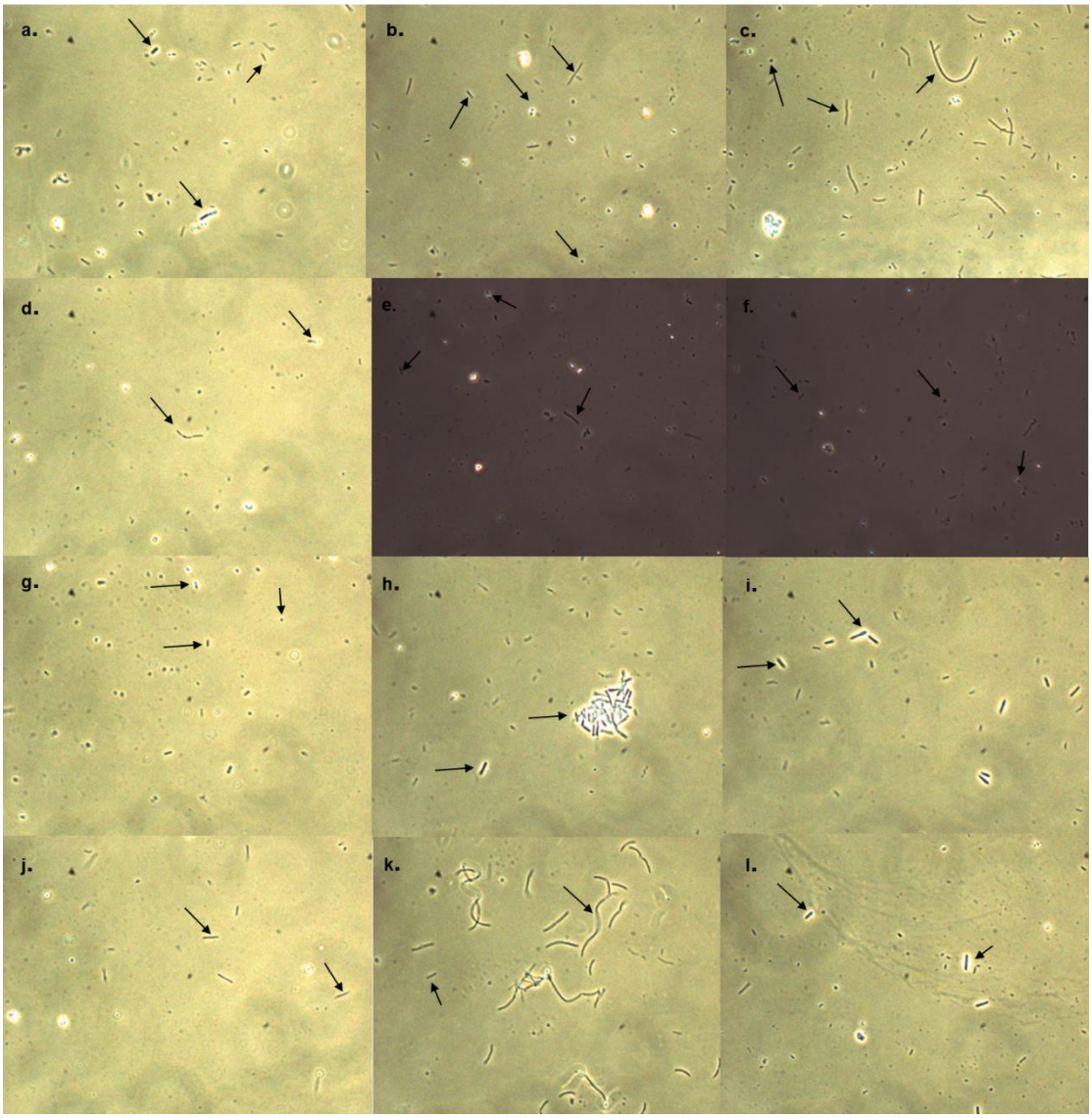

Figure 3.6. Micrographs of enrichment cultures at 430x magnification. Row 1 (a-c): DMA/nitrate amendments; Row 2 (d-f): DMA/lactate amendments; Row 3 (g-i): As(V)/lactate amendments; Row 4 (j-l): (III)/nitrate amendments. Column 1 (a-j): off-site; Column 2 (b-k): aquifer; Column 3 (c-l): vadose. Arrows indicate the presence of cells. Many cells possessed endospores.

Each culture consisted of complex heterogeneous bacterial communities with varying sizes of rod-shaped and coccus-shaped bacteria. Some of the rod shaped cells contained endospores or exospores (**Figure 3.6**). When grown on 5 mM As(V) and 10 mM lactate, the vadose enrichment set generated a fluffy, yellow-colored precipitate (**Figure 3.5 c**.) presumed to be the As(III) containing mineral known as orpiment (As_2S_3) which has proved to be a useful indicator of biological As(V) reduction [4,110]. **Table 3.16** shows a qualitative assessment of growth that occurred in each enrichment set based on macroscopic and macroscopic observations.

b. Time-course experiments

In the enrichment cultures amended with DMA and nitrate, the greatest growth yield occurred in the aquifer enrichment (**Figure 3.7 b.**), followed by the vadose (**Figure 3.7 c.**) and off-site enrichments (**Figure 3.7 a.**). While nitrate reduction did occur in the vadose and aquifer enrichments, there was unfortunately no evidence of DMA degradation nor the appearance of MMA, As(III) or As(V) in any of the cultures (**Figure 3.7 d.**). Bearing this observation in mind, it is most likely that the bacteria within the aquifer and vadose cultures are using organic acids, which occur at elevated concentrations in yeast extract (data not shown) to undergo dissimilatory nitrate reduction and achieve growth. The off-site enrichment apparently grew solely via a fermentation pathway involving yeast extract organic acids. The DMA/lactate amended cultures showed no evidence of the appearance of inorganic As (data not shown). This finding, coinciding with the results of the DMA/nitrate time-course experiment suggests the bacteria selected for in the methylarsenic enrichment cultures are not capable of anaerobic demethylation under these conditions.

Sample/Transfer number	1	2	3
5 mM DMA(V) 20 mM Nitrate			
Off-Site	+	+	+
Vadose	++	++	++
Aquifer	++	++	++
5 mM DMA(V) 10 mM Lactate			
Off-Site	+	+	+
Vadose	+	+	+
Aquifer	+	+	+
5 mM As(III) 20 mM Nitrate			
Off-Site	+	+	+
Vadose	++	++	++
Aquifer	++	++	++
5 mM As(V) 10 mM Lactate			
Off-Site	++	++	++
Vadose	++	++	++
Aquifer	++	++	++

Table 3.16. Initial enrichment culture set growth log. Growth was qualitatively assessed based on macroscopic and microscopic growth using a + and ++ scale, with ++ representing greatest growth.

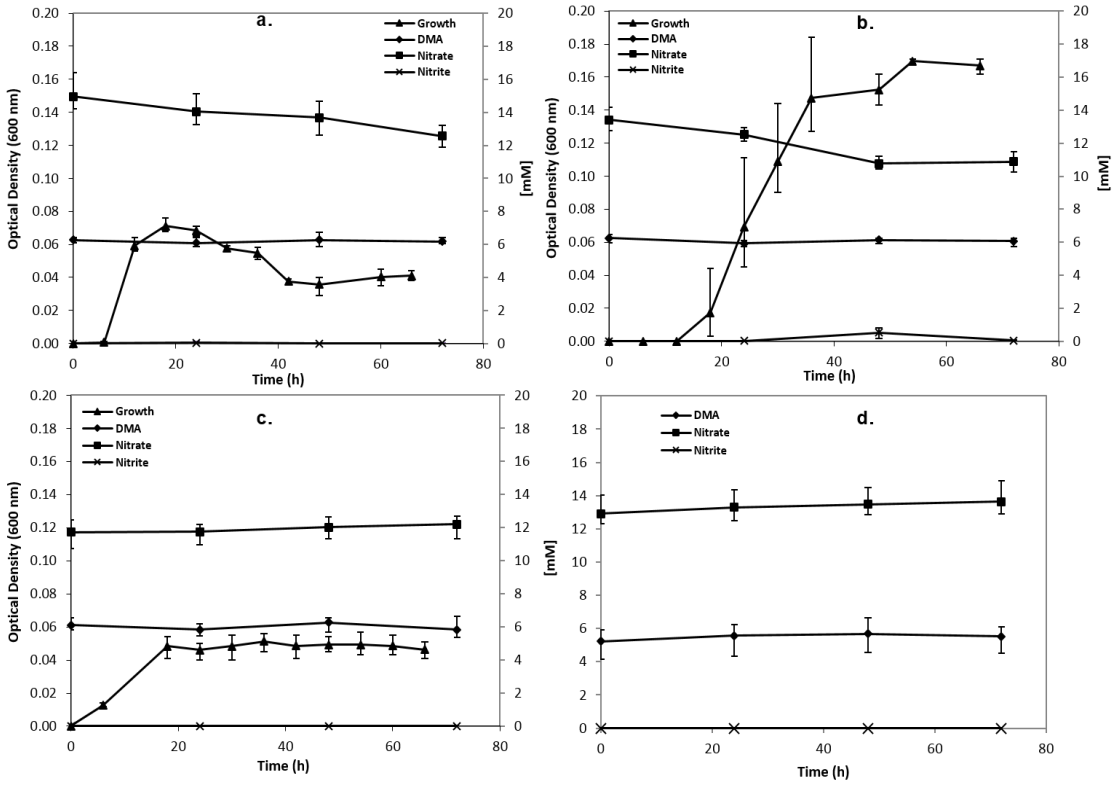

Figure 3.7. Time course plot showing growth of a. Vadose; b. Aquifer; and c. Off-site Vineland enrichments as well as an abiotic control (d.) grown on SES-3 media amended with 5 mM DMA and 20 mM nitrate.

In the cultures amended with As(V) and /lactate, preliminary data demonstrated significant loss of As(V) and the appearance of As(III), notably in the on-site vadose and aquifer enrichments, potentially due to a respiratory mechanism of As(V) reduction (data not shown). However, there was no evidence of As(III) oxidation to As(V) in the As(III)/nitrate cultures (data not shown), making it unlikely that an anaerobic subsurface bacterial "cycling" pathway wherein As(V) reduction and As(III) oxidation were occurring at different depths was operating. However, similar to the findings in the DMA/nitrate time-course studies, nitrate reduction to nitrite transpired in these cultures, most likely due to the action of the organic acid-rich yeast extract.

c. Ribosomal intergenic spacer analysis (RISA)

Total genomic DNA was successfully extracted from duplicate sets of the vadose enrichments under each selective media condition (**Figure 3.8**). RISA performed on the DMA/nitrate amended enrichments demonstrated bacterial community diversity, as ~8 bands were present on the resulting gel **(Figure 3.9**).

ii. Second experiments

a. Slurry and enrichment incubations

The slurries generated from each subsurface sediment sample demonstrated bacterial growth following 24 hours of incubation. After one transfer from slurry, each selective media enrichment culture demonstrated macroscopic and microscopic bacterial growth (**Table 3.17**).

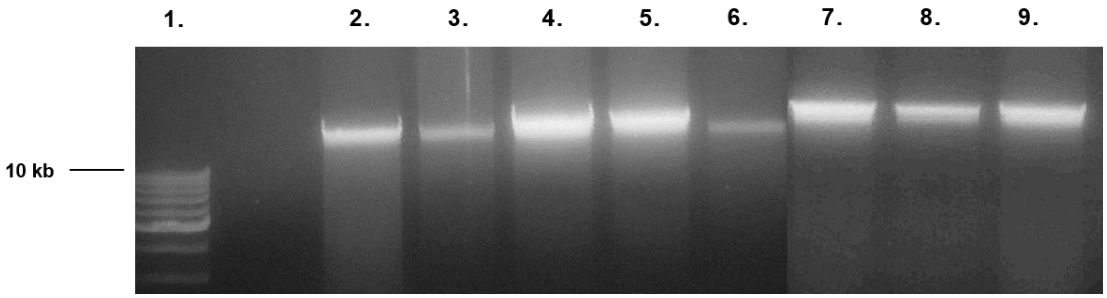

Figure 3.8. Agarose gel (0.8%) of total genomic DNA extracted from Vineland vadose enrichment cultures. Lanes: 1. 10 kb ladder; 2,3: As(V)/lactate amended cultures; 4,5: As(III)/nitrate amended cultures; 6,7: DMA/nitrate amended cultures; 8,9. DMA/lactate amended cultures.

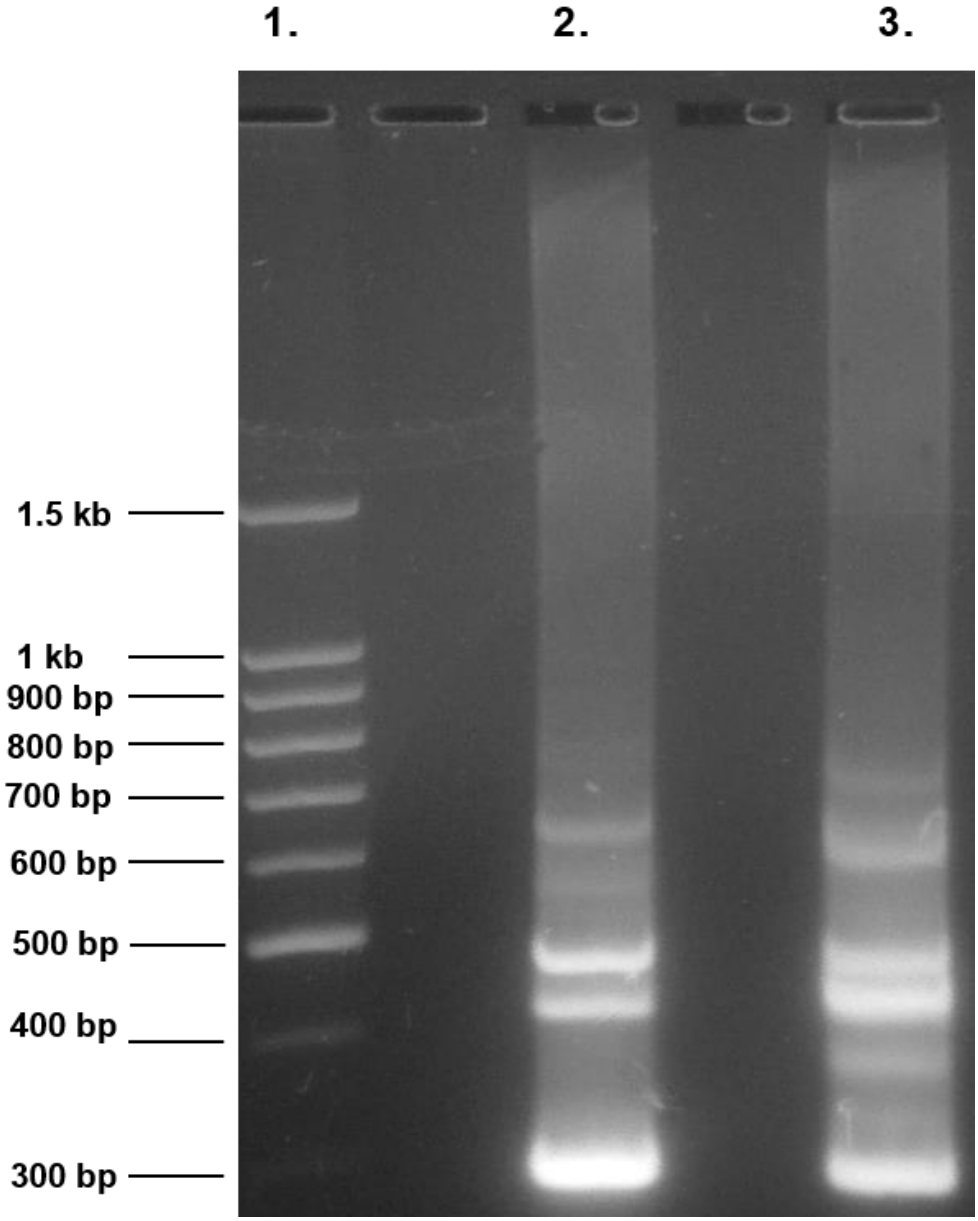

Figure 3.9. Agarose gel (2%) of RISA amplicons from DMA/nitrate amended Vineland vadose enrichment cultures. Lanes: 1. 100 bp ladder; 2,3: Vadose amplicons.

However, the DMA containing enrichments as well as the As(III) containing enrichments failed to grow after another successive transfer. A likely explanation for this is the inability of the bacteria to grow under these conditions without being supplemented with yeast extract, which appeared to be the nutrient source facilitating growth in the initial enrichment culture sets. The inability to grow heterotrophically on DMA as the sole carbon source and autotrophically using As(III) as the terminal electron donor under anaerobic conditions provides further evidence that the yeast extract was indeed supporting growth of the initial enrichment set, rather than the exogenous arsenical electron donors and acceptors provided. All three enrichments successfully grew after multiple transfers from slurry on SES-3 HAO media amended with to 5 mM As(III) (**Figure 3.10 a.).** The vadose enrichment culture, after roughly 24 hours of growth, produced a yellow pigment appearing to be orpiment **(Figure 3.10 a.; second bottle from left**). This is likely from sulfide production (sulfidogenesis) and the chemical bonding of the resulting sulfide with As(III). This process may be an indirect arsenic resistance mechanism, as the vadose enrichment demonstrated much greater macroscopic turbidity than the off-site and aquifer enrichments**.** However, the sulfide production likely occurring in this culture did not appear to occur via sulfate reduction, as the precipitate readily formed even when the bacteria were grown on As(III) amended modified SES-3 HAO media with very minimal sulfate levels (data not shown). Microscopically, the cells grown under these conditions demonstrated cocci and rod morphologies (**Figure 3.11 d-f.**)

Sample/Transfer	1	2	3	4	5
SES-3 DARP Media					
5 mM As(V) 10 mM Lactate					
Off-Site	++	++	++	++	++
Vadose	++	++	++	++	++
Aquifer	++	++	++	++	++
SES-3-CAO Media					
5 mM As(III) 5 mM Nitrate					
Off-Site	+	-			
Vadose	+	-			
Aquifer	+	-			
SES-3-HAO Media					
5 mM As(III)					
Off-Site	++	++	++	++	++
Vadose	+++	+++	+++	+++	+++
Aquifer	+	+	+	+	+
SES-3-Dem Media					
10 mM DMA					
Off-Site	+	-			
Vadose	+	-			
Aquifer	+	-			
10 mM DMA 5 mM Nitrate					
Off-Site	+	-			
Vadose	+	-			
Aquifer	+	-			

Table 3.17. Second enrichment culture set growth log. Growth was qualitatively assessed based on macroscopic and microscopic growth using a +, ++ and +++ scale, with +++ representing greatest growth.

Figure 3.10. Photos of enrichment cultures grown on a. SES-3 HAO media with 5 mM As(III) and b. SES-3 DARP media with 5 mM As(V) and 10 mM lactate after 3 days of incubation (3 transfers from slurry). Bottles from left to right: a. Uninoculated, vadose, aquifer, off-site; b. Uninoculated, aquifer, vadose off-site.

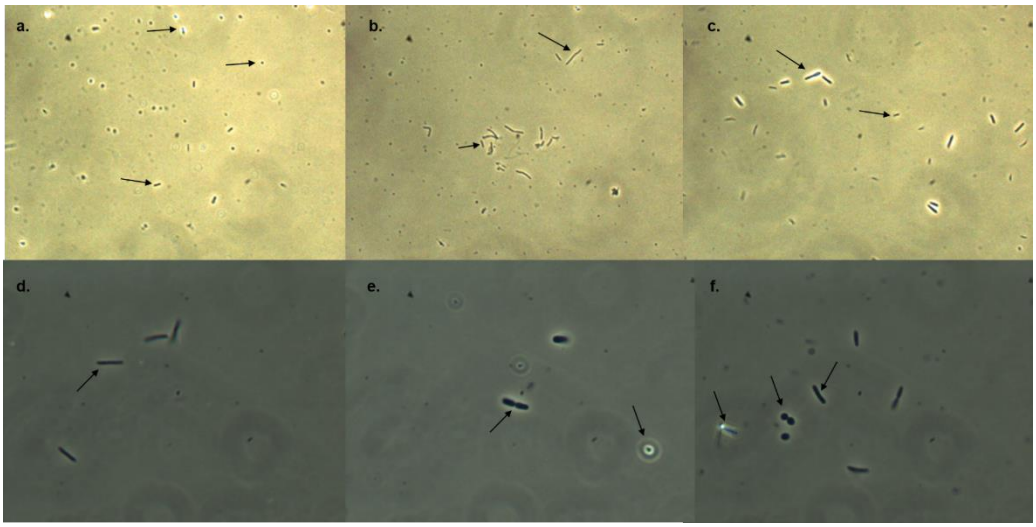

Figure 3.11. Micrographs of enrichment cultures grown on a-c. SES-3 DARP media with 5 mM As(V) and 10 mM lactate and d-f. SES-3 HAO media with 5 mM As(III). a,d. Off-site; b,e. Aquifer enrichments; c,f. Vadose enrichments. Top row: 430x magnification; bottom row: 1000x magnification.

Each enrichment grew on SES-3 DARP media with 5 mM As(V) and 10 mM lactate, with the vadose culture precipitating what is presumably orpiment (**Figure 3.10 b.; second bottle from right**). Microscopically these enrichments consisted of rod-shaped and coccus-shaped bacteria of varying sizes (**Figure 3.11 a-c**), with many of the rods forming endospores or exospores.

b. Time course experiments

When grown on SES-3 HAO media with 5 mM As(III), the vadose enrichment showed significantly greater As(III) resistance when compared to controls lacking the addition As(III) than the aquifer and off-site enrichments (**Figure 3.12**). When assessed in terms of maximum recorded average growth yield values, the vadose enrichment was inhibited by only 30.6% in the presence of the 5 mM As(III) in comparison to the control, while the off-site and aquifer enrichments suffered inhibitions of 82.6% and 91.2%, respectively.

It was initially hypothesized that sulfidogenesis and orpiment production was precipitating substantial amounts of As(III) out of solution, thereby creating an indirect "tolerance" mechanism resulting in the escalated growth yields observed in the vadose enrichment. However, there did not appear to be any noticeable decrease in As(III) over time, nor was there any evidence of oxidation to As(V) (**Figure 3.13 c**). As(III) oxidation evidence was absent in the off-site (**Figure 3.13 a.**) and aquifer (**Figure 3.13 b.**) enrichments.

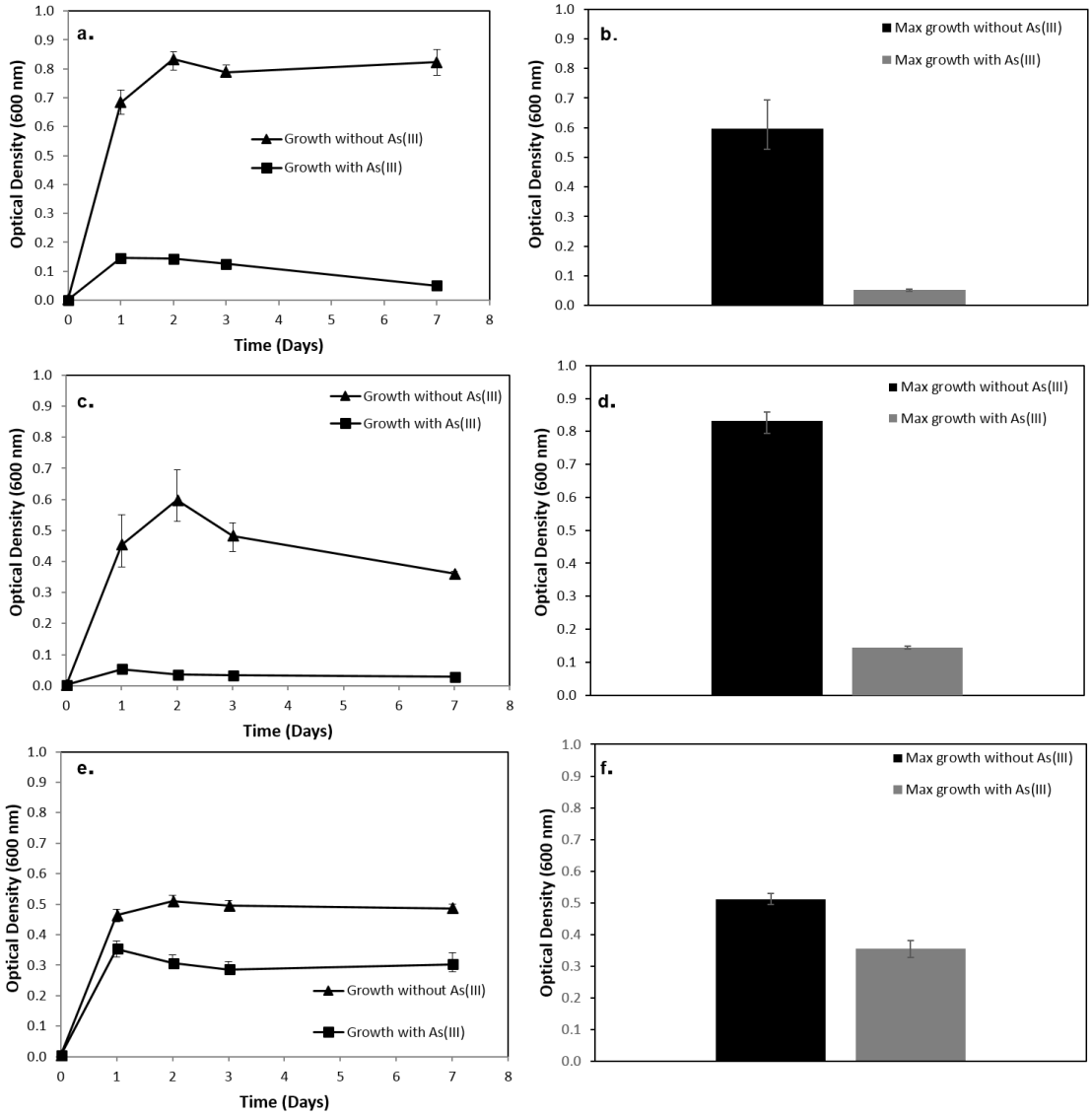

Figure 3.12. Time course plots and bar graphs showing growth yields with and without 5 mM As(III) of off-site (a. and b.), aquifer (c. and d.) and vadose (e. and f.) enrichments on SES-3-HAO media.

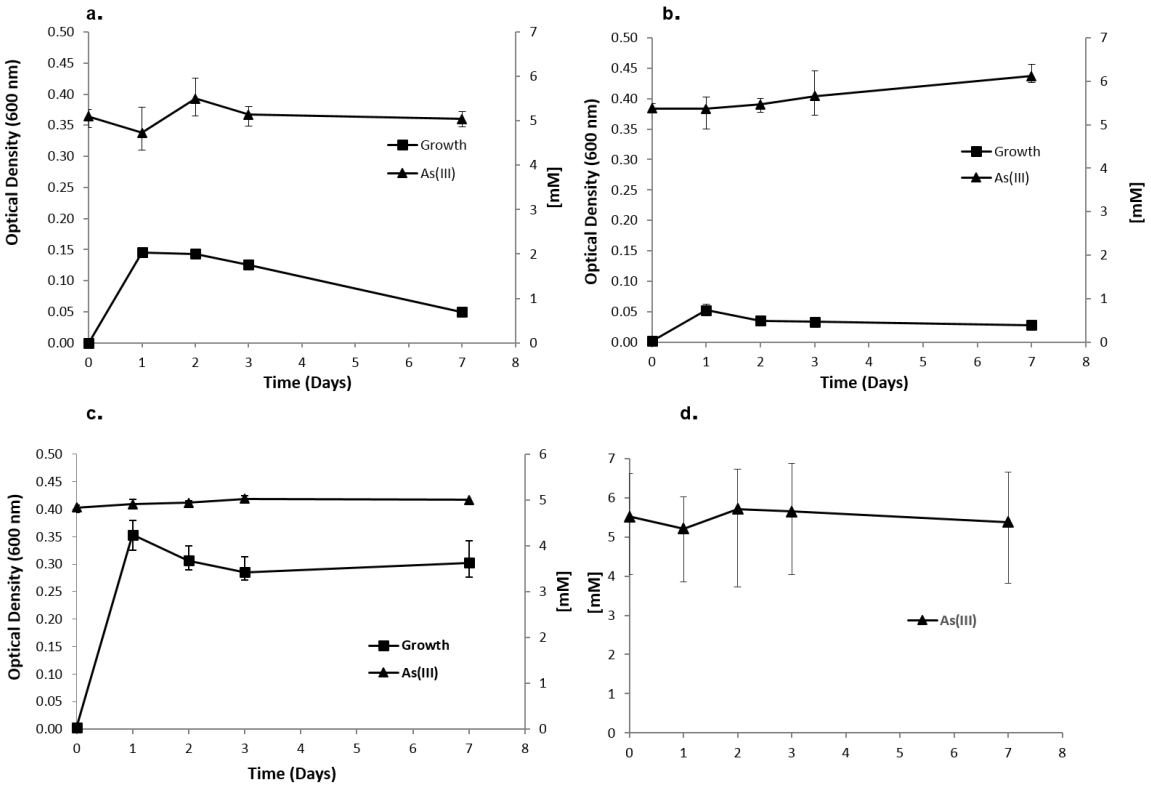

Figure 3.13. Time-course growth plot showing a. Off-site; b. Aquifer; and c. Vadose Vineland enrichments as well as an abiotic control (d) grown on SES-3 HAO media amended with 5 mM As(III). Primary axis quantifies growth (O.D. 600 nm) and secondary axis quantifies As(III) concentration (mM).

When grown on SES-3 DARP media 10 mM lactate and 5 mM As(V), each enrichment culture demonstrated the ability to reduce As(V) to As(IIII). The vadose (**Figure 3.14 c**.) and aquifer (**Figure 3.14 b**.) enrichments achieved complete conversion of As(V) to As(III), with the latter culture displaying more rapid reduction kinetics (within 24 hours). The aquifer enrichment showed evidence supporting a respiratory mechanism, as its growth appeared to cease following the complete conversion of As(V) to As(III). The vadose enrichment did not show a similar trend, as growth persisted following the full reduction of As(V) to As(III). During the course of a more rigorous time-course growth experiment performed in triplicate, the aquifer enrichment demonstrated a roughly 1:1 recovery of As(III) from As(V) after only 22 hours of incubation (**Figure 3.15**). However, due to overlapping retention times, lactate oxidation to acetate could not be quantified under these conditions. All enrichments successfully grew on SES-3 DARP with 5 mM As(V) and 2.5 mM lactate after five transfers from the original 5 mM As(V) and 10 mM lactate amended cultures. When grown under these conditions, the aquifer enrichment once again displayed elevated growth with the addition of As(V) (**Figure 3.16 b**). The off-site enrichment (**Figure 3.16 c**) showed a minimal difference when grown with or without As(V) and the vadose enrichment grew better without it (**Figure 3.16 a**). As(III) was recovered from As(V) in each culture in a relatively balanced 1:1 stoichiometric fashion (**Figure 3.17**). The on-site vadose (**Figure 3.17 a**.) and aquifer (**Figure 3.17 b.**) enrichments greatly exceeded the off-site enrichment (**Figure 3.17 c.**) in the total amount of As(V) transformed as well as the reduction rate, suggesting dissimilatory As(V) reduction occurred only in the on-site cultures.

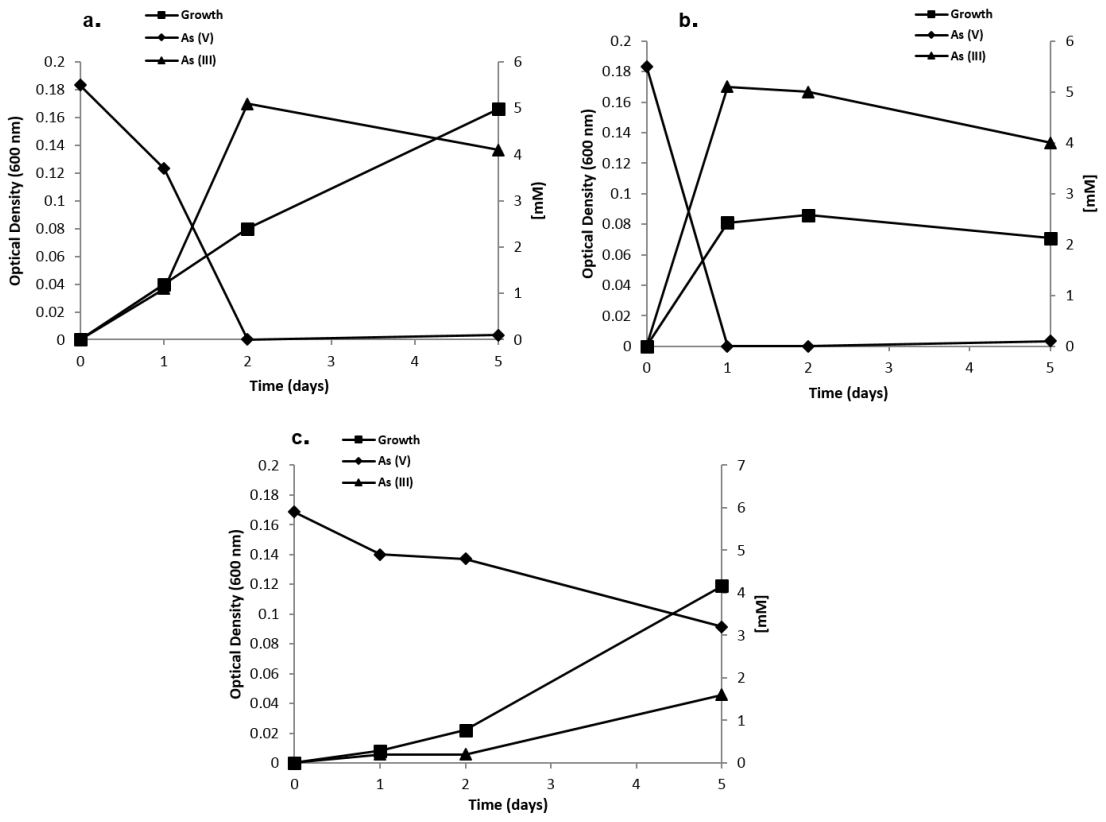

Figure 3.14. Preliminary time-course plot showing a. Vadose; b. Aquifer; and c. Off-site Vineland enrichments grown on SES-3 DARP media amended with 5 mM As(V) and 10 mM lactate. Primary axis quantifies growth (O.D. 600 nm) and secondary axis quantifies arsenic concentrations (mM).

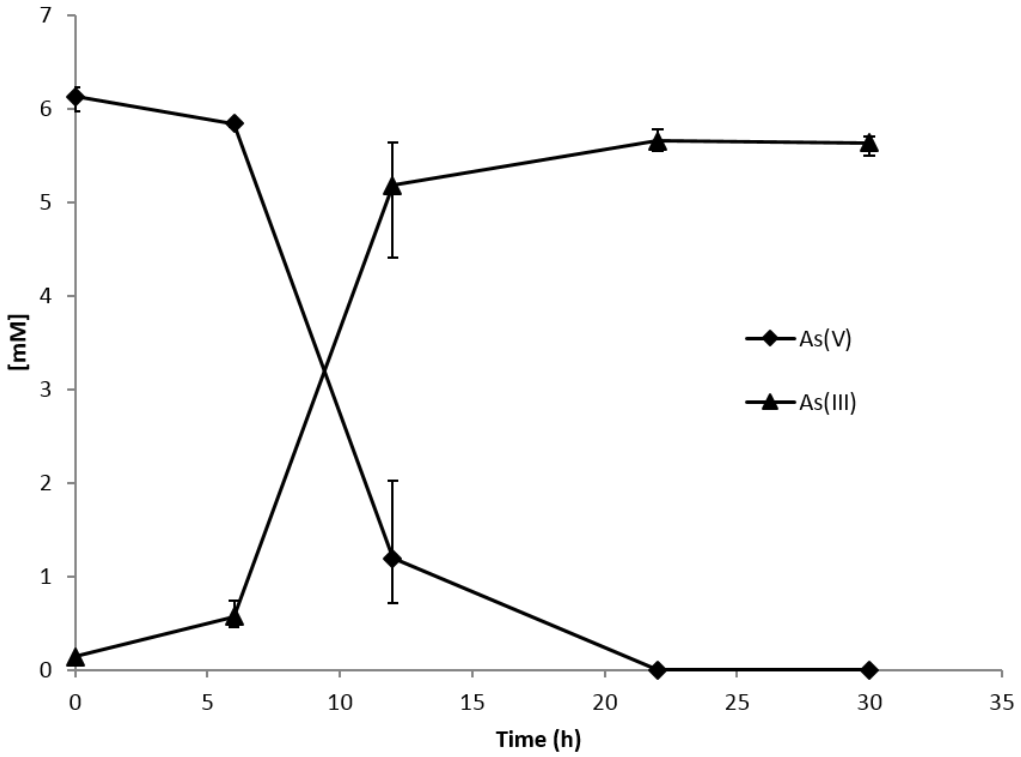

Figure 3.15. Time-course plot showing aquifer enrichment grown on SES-3 DARP media amended with 5 mM As(V) and 10 mM lactate. Data points represent averages of triplicate data sets and error bar represent the range of values collected.

Max As(III) generation rates were calculated by measuring appearance of As(III) between 12-24 hours, 24-36 hours, and 0-12 hours in the aquifer, vadose and off-site enrichments, respectively (12-hour time points were selected based on greatest slope of the graph). As(III) was generated at maximum rates of 287.9 and 241.2 µM/hr. in the aquifer and vadose enrichments, respectively, while the off-site enrichment was only capable of As(III) formation at a max rate of 22.1 µM/hr. On average, the off-site, aquifer and vadose enrichments formed 0.35, 4.59 and 4.41 mM As(III), respectively within the 72-hour experimental incubation period.

Lactate was oxidized to acetate in each enrichment culture (**Figure 3.18**). The amount of acetate formed exceeded the expected 1:1 balance with the disappearance of lactate in the on-site vadose (**Figure 3.18 a.**) and off-site cultures (**Figure 3.18 c.**), whereas this balance was achieved in the aquifer culture (**Figure 3.18 b.**). It has been hypothesized that the elevated acetate formed may have been the result of acetogenic bacteria being present. In the on-site vadose and aquifer enrichments, the lactate disappearance achieved an appropriate 1:2 balance with the loss of As(V) and formation of As(III), suggesting a respiratory mechanism is operable. The off-site enrichment showed no such trend, further supporting the notion that the As(V) reduction occurring is a result of a resistance mechanism. Uninoculated media treated identically to biotic cultures showed little to no chemical As(V) reduction (**Figure 3.17 d.**) and the absence of acetate recovery from lactate (**Figure 3.18 d.**).

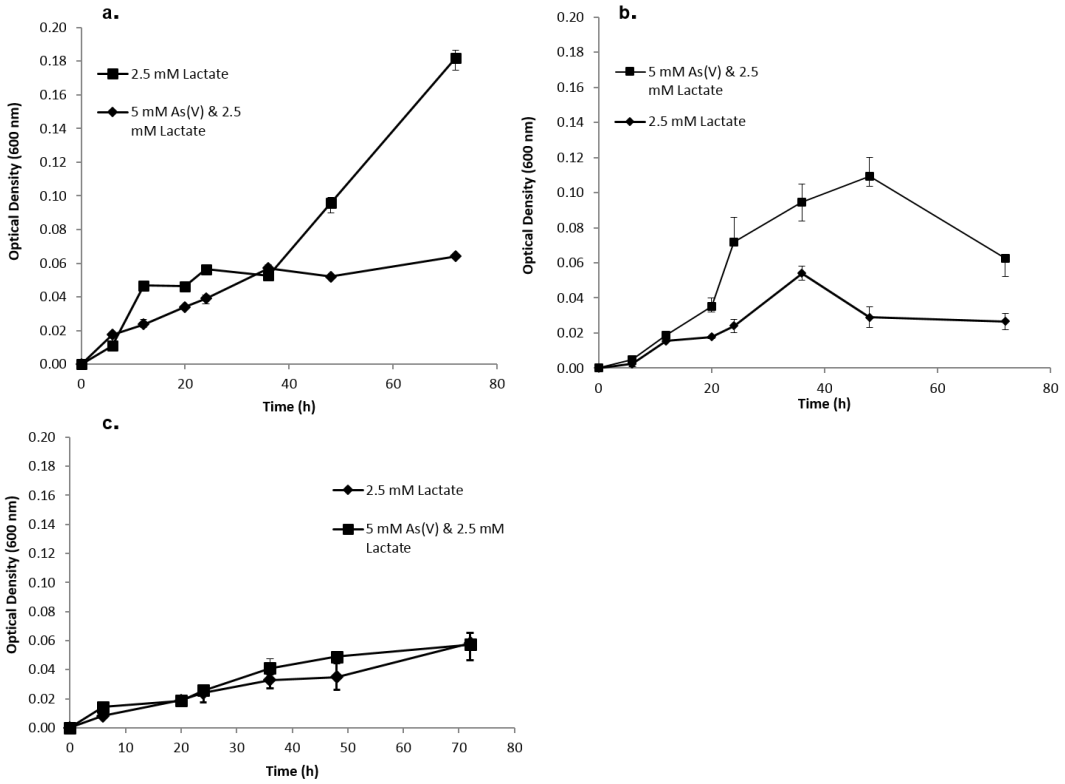

Figure 3.16. Time-course growth plot showing a. Vadose; b. Aquifer; and c. Off-site Vineland enrichments grown on SES-3 DARP media with 2.5 mM lactate +\- 5 mM As(V). Data points represent averages of triplicate data sets and error bars represent the ranges of values collected.

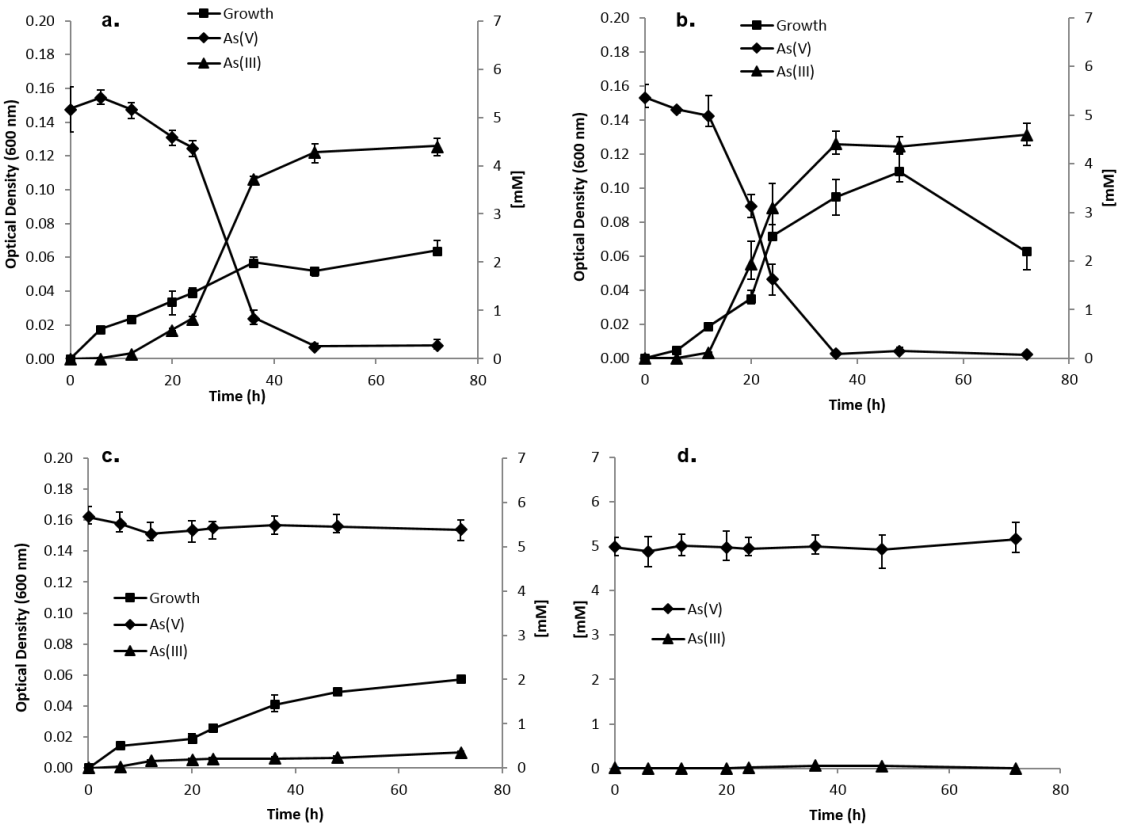

Figure 3.17. Time-course growth plot showing a. Vadose; b. Aquifer; c. Off-site Vineland enrichments as well as an abiotic control (d) grown on SES-3 DARP media with 2.5 mM lactate and 5 mM As(V). Data points represent averages of triplicate data sets and error bars represent the ranges of values collected. Primary axis quantifies growth (O.D. 600 nm) and secondary axis quantifies arsenic concentrations (mM).

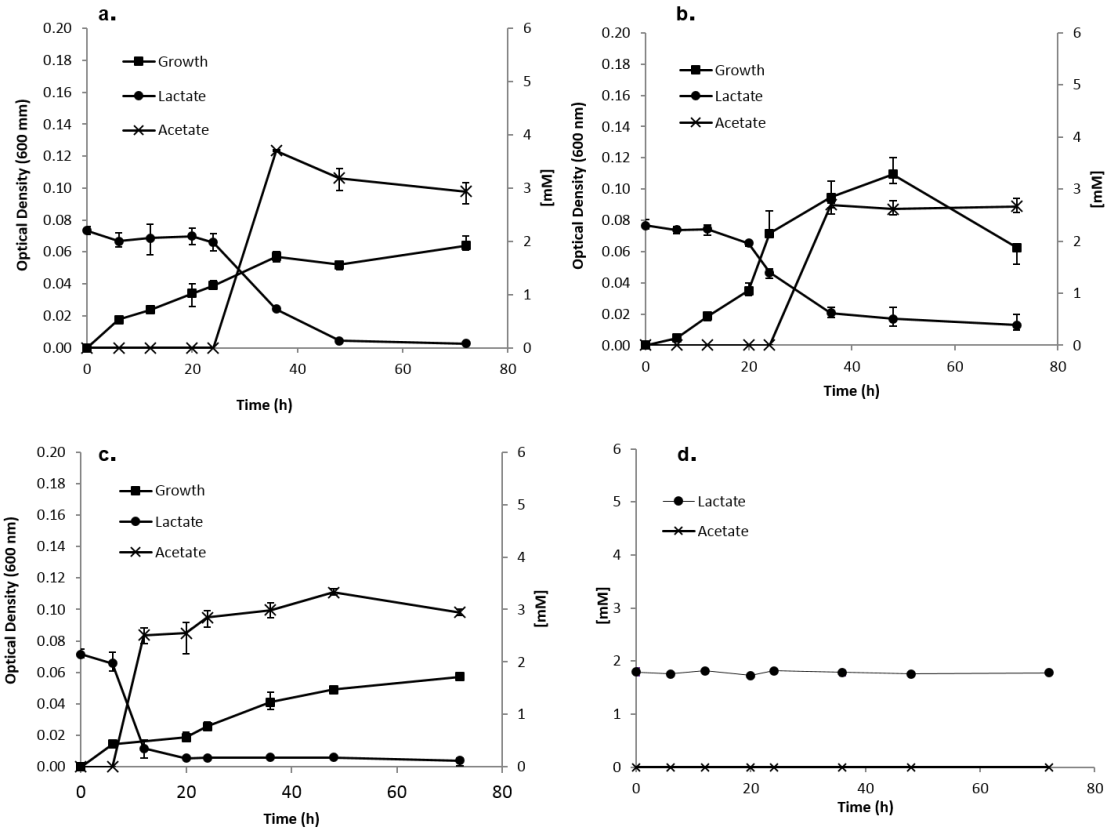

Figure 3.18. Time-course growth plot showing a. Vadose; b. Aquifer; c. Off-site Vineland enrichments as well as an abiotic control (d) grown on SES-3 DARP media with 2.5 mM lactate and 5 mM As(V). Data points represent averages of triplicate data sets and error bars represent the ranges of values collected. Primary axis quantifies growth (O.D. 600 nm) and secondary axis quantifies organic acid concentrations (mM).

iii. Molecular Analyses

a. arrA probing

Genomic DNAs were successfully extracted from each As(V)/lactate amended SES-3 DARP enrichment culture, as well as a *Pseudomonas aeruginosa* strain 1244 culture (used for *arsC* probing control) **Figure 3.19**). Previously extracted genomic DNAs from S. barnesii SES-3 and *B. selenitireducens* MLS-10 (both used for *arrA* probing controls) also generated bands of expected genomic DNA length (>10 kilobases) when electrophoresed, indicating their viability (**Figure 3.19**). PCR amplification using all of the previously described combinations of *arrA*F and *arrA*R primers failed to produce any bands when off-site, aquifer and vadose enrichment culture genomic DNAs were used as template, nor was there any evidence of amplification when *S. barnesii* SES-3 genomic DNA was used (data not shown). The "Initial PCR I" reactions generated bands of various lengths as well as those at the expected 625-630 bp length in the aquifer and vadose samples (**Figure 3.20; Table 3.18**). A smear was found in this range when SES-3 DNA was used. The "Initial PCR II" reactions previously described failed to amplify any DNA of expected length with only a 1 kb band being present when aquifer enrichment template DNA was used. The nested reactions failed to further "purify" any *arrA* fragments, aside from a faint band at the expected 625-630 bp length in the vadose PCR I reaction. Due to the extensive non-specific amplification in the initial PCR I reactions and the lack of product formation in the nested reactions, the protocol was repeated using standard PCR mixture conditions, as previously described in the methods section.

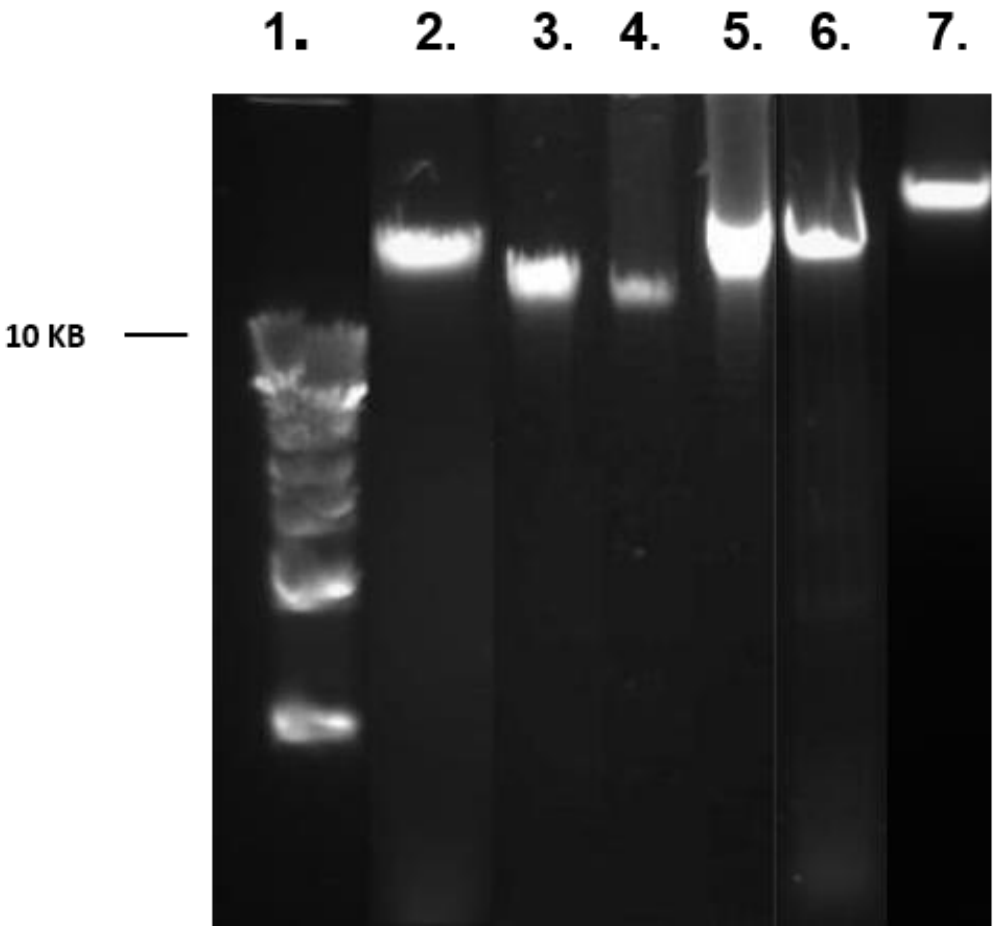

Figure 3.19. Agarose gel (0.8%) of genomic DNAs extracted for DARP enrichment culture molecular analyses. Lanes: 1. 1 Kb Step Ladder, 2. Vineland Off-site DARP enrichment; 3. *Sulfurospirillum barnesii* SES-3; 4. Vineland On-site Vadose DARP enrichment; 5. Vineland on-site aquifer DARP enrichment; 6. *Bacillus selenitireducens* MLS-10; 7.

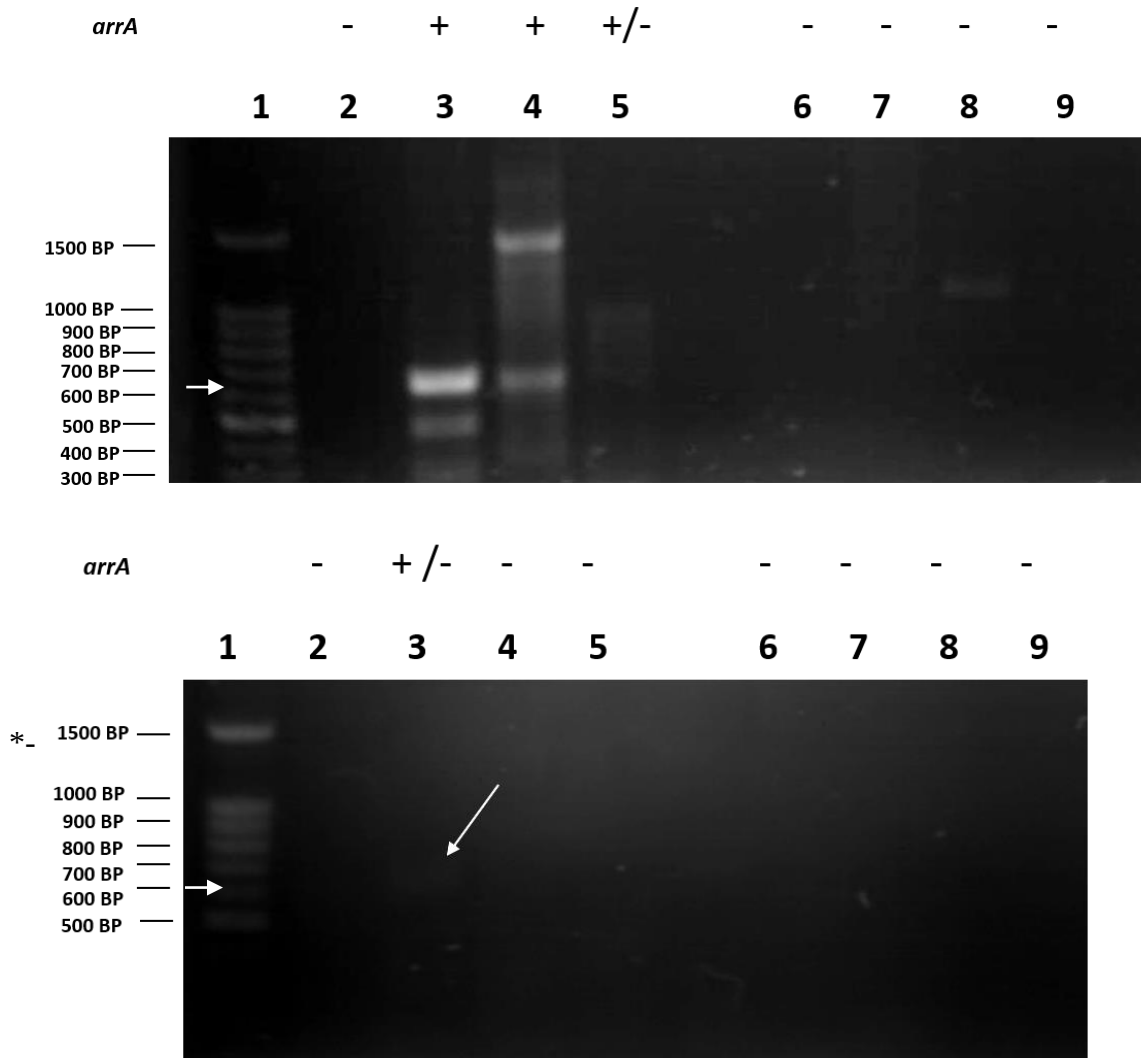

Figure 3.20. Agarose gels (1.5%) of amplicons resulting from DARP enrichment *arrA* probing. Lanes: 1. 100 bp ladder; 2, 6. Off-site enrichment; 3, 7. Vadose enrichment; 4, 8. Aquifer enrichment; 5, 9. *S. barnesii* SES-3. TOP GEL Lanes 2-5: Initial PCR I reactions; Lanes 6-9: Initial PCR II reactions. BOTTOM GEL Lanes 2-5: Nested PCR I reactions; Lanes 6-9: Nested PCR II reactions. The white slanted arrow indicates a faint band. White horizontal arrows indicate the expected *arrA* fragment length of 625-630 bp. The presence (+) or absence (-) of expected *arrA* amplicons are indicated above the lane

Primer Pair (F/R)	Expected *arrA* fragment length	Genomic DNA	Band at expected length?	Other bands
AS1F/AS1R (Initial PCR I)	**625-630 bp**	SES-3	Y/N (smear)	Y/N - smear between 630-1000 bp
		Off-site enrichment	N	N
		Aquifer enrichment	Y	Y – 350 bp, 1500 bp, >1500 bp, smear between 900-1500 bp
		Vadose enrichment	Y	Y – 300 bp, 500 bp
AS1F/AS2R (Initial PCR II)	**625-630 bp**	SES-3	N	Y – between 1-1.5 kb
		All enrichments	N	N
AS2F/AS1R (Nested PCR)	**625-630**	SES-3, off-site and aquifer PCR I/II products, vadose PCR II product	N	N
		Vadose PCR I product	Y/N (faint band)	N

Table 3.18. Summary of first attempt at *arrA* probing using the initial and nested PCR approach.

Under these conditions, the initial PCR I reaction generated bands around the expected 625-630 bp length in the SES-3 control (a faint band) and the aquifer and vadose enrichments, while the off-site enrichment failed to generate any visible DNA amplicons (**Figure 3.21, Table 3.19**). The SES-3 control also showed non-specific amplified DNA fragments at 275, 750 and 100 bp. The aquifer enrichment showed non-specific amplicons around 400, 1250, 1400, and 1500 bp as well as a few faint bands exceeding 1.5 kb. The vadose enrichment demonstrated non-specific amplification at 500, 325 and 275 bp. The nested PCR I reactions again generated a faint band at 625-630 bp in the SES-3 control. However, rather than further purifying this band and limiting the amount of non-specific amplicon generation, a series of new bands emerged around 900, 800, 550, 400 and 300 BP. The aquifer amplification reaction resulted in non-specific amplicons only at 1250 and 300 bp, with a visibly prominent band at the expected *arrA* fragment length of 625-630 bp. The vadose enrichment showed a very prominent band at this length as well, with only one other DNA fragment around 350 bp in length. The off-site reaction yielded faint DNA bands around 350 and 200 bp with no band in the expected *arrA* region. When the PCR I initial and nested PCR reactions were performed again under standard PCR conditions as previously described, there were once again various non-specific band formations that resulted (**Figure 3.21, Table 3.19**). While the vadose and aquifer enrichments demonstrated bands at 625-630 bp in the initial and nested reactions (indicative of the *arrA* gene fragment), they also generated several other bands at the lengths indicated in Figure 3.20 and Table 3.19.

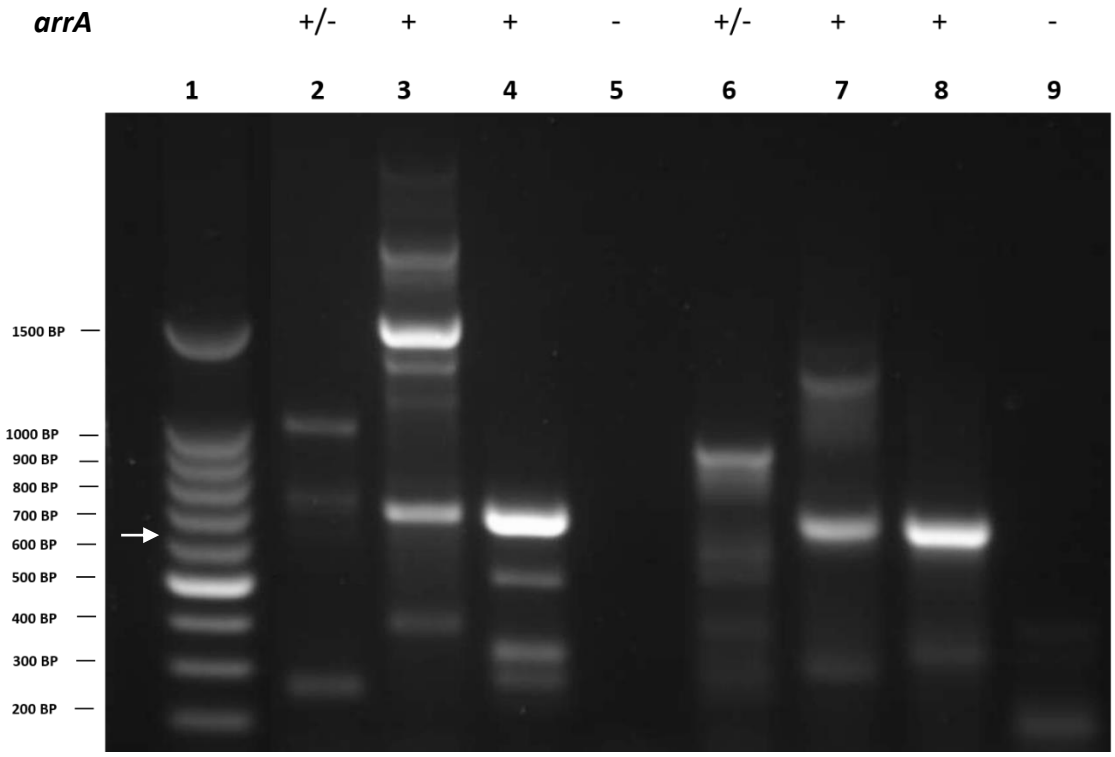

Figure 3.21. Agarose gel (1.5%) of *arrA* PCR I initial (Lanes 2-5) and nested (Lanes 6-9) results under standard PCR reaction mixture conditions. Lanes 2-5 correspond to the initial PCR I reactions while lanes 6-9 correspond to the nested PCR I reactions. Lanes: 1. 100 bp ladder; 2, 6. SES-3; 3, 7. Vadose DARP enrichment; 4, 8**.** Aquifer DARP enrichment; 5, 9. Off-site DARP enrichment Expected *arrA* fragments can be found at 625-630 bp. The white horizontal arrow indicates the expected *arrA* fragment length of 625-630 bp. The presence (+) or absence (-) of expected *arrA* amplicons is indicated above the lane denominations.

Primer Pair (F/R)	Expected *arrA* fragment length	Genomic DNA	Band at expected length?	Other bands (bp)
AS1F/AS1R (Initial PCR I)	**625-630 bp**	SES-3	Y/N	Y – 250, 1000
		Off-site enrichment	N	N
		Aquifer enrichment	Y	Y – 400, 1200, 1300, 1400; 2 > 1500
		Vadose enrichment	Y	Y – 275, 325, 500
AS2F/AS1R (Nested PCR I)	**625-630**	SES-3	Y/N	Y – 300, 350, 500, 600, 900, 1000
		Off-site enrichment	N	Y – 200, 300, 350
		Aquifer enrichment	Y	Y – 300, 1200, 1300
		Vadose enrichment	Y	Y – 350

Table 3.19. Summary of 2nd attempt at *arrA* probing using the initial and nested PCR approach under standard PCR conditions.

The off-site enrichment did not generate any bands in the initial reaction and demonstrated a few smears following the nested reaction. The SES-3 sample appeared to form bands in the vicinity of the 625-630 bp range in both the initial and nested reactions, but demonstrated a similar trend as that shown by the aquifer and vadose enrichments, with various non-specific bands being generated.

When the PCR amplifications were performed using the ArrAfwd/ArrArev primer pair previously described, single bands around 175 bp in length resulted for the on-site vadose and aquifer enrichments, which falls in the 160-200 bp range expected for positive *arrA* amplicons using these primers [105] **(Figure 3.22; Table 3.20).** The off-site enrichment did not show a band in this length range, but generated a smear at 150 bp as well as multiple other bands at lengths of 275-900 bp. The SES-3 and MLS-10 positive control *arrA* amplicons ran at their expected 1engths of 200 and 160 bp, respectively [105].

Ligations and transformations were successfully performed on the ArraF/ArrARev primer pair amplicons, following their purification. Colony PCR amplification using the M13F/M13R primer pair yielded many amplicons consistent in length with those from the original amplification, bearing in mind that an additional 170 bp of plasmid DNA is amplified along with the cloned DNA when the M13/M13R primer set is used (330-370 bp). As shown in **Figure 3.23,** all four of the SES-3 and MLS-10 colony PCR *arrA* positive controls generated bands only at the expected *arrA* lengths of 370 and 330, respectively. The first off-site amplicon appeared to be slightly smaller, but nearly the same size, as the expected *arrA* amplicon length, while clones 2-4 were of varying sizes consistent with those seen in Figure 3.22.

The colony PCR *arrA* clones 1-4 for both the aquifer and vadose enrichments ran at the expected *arrA* fragment length of 330-370 bp. Off-site clones 5-10 all ran at varying lengths consistent with the original gel shown in Figure 3.22, with none appearing to be of a length indicative of the presence of *arrA* (**Figure 3.24**). Vineland vadose and aquifer enrichment clones 5-10 generated only amplicons at the expected *arrA* length.

Sequencing was successfully performed on most of the purified colony PCR products, with the best sequences being named and subjected to nucleotide BLAST. The names of each unique sequence and their BLAST results can be found in **Table 3.21** (the sequenced clones are also labeled on the gels shown in **Figures 3.23** and **3.24**). The positive controls as well as the aquifer and vadose enrichments possessed fragments with high similarities to *arrA*. The off-site enrichment did not generate any fragments significantly similar to *arrA*. The nomenclature of each clone was devised by combining the name of the template DNA, putative gene and clone number (i.e. VAA-1 means Vineland Aquifer *arrA* clone 1; i.e. VOSA-1 means Vineland off-site *arrA* clone 1; VVA-1 means Vineland Vadose *arrA* clone. These results further support the initial hypothesis of a respiratory mechanism of As(V) reduction only in the on-site enrichment cultures.

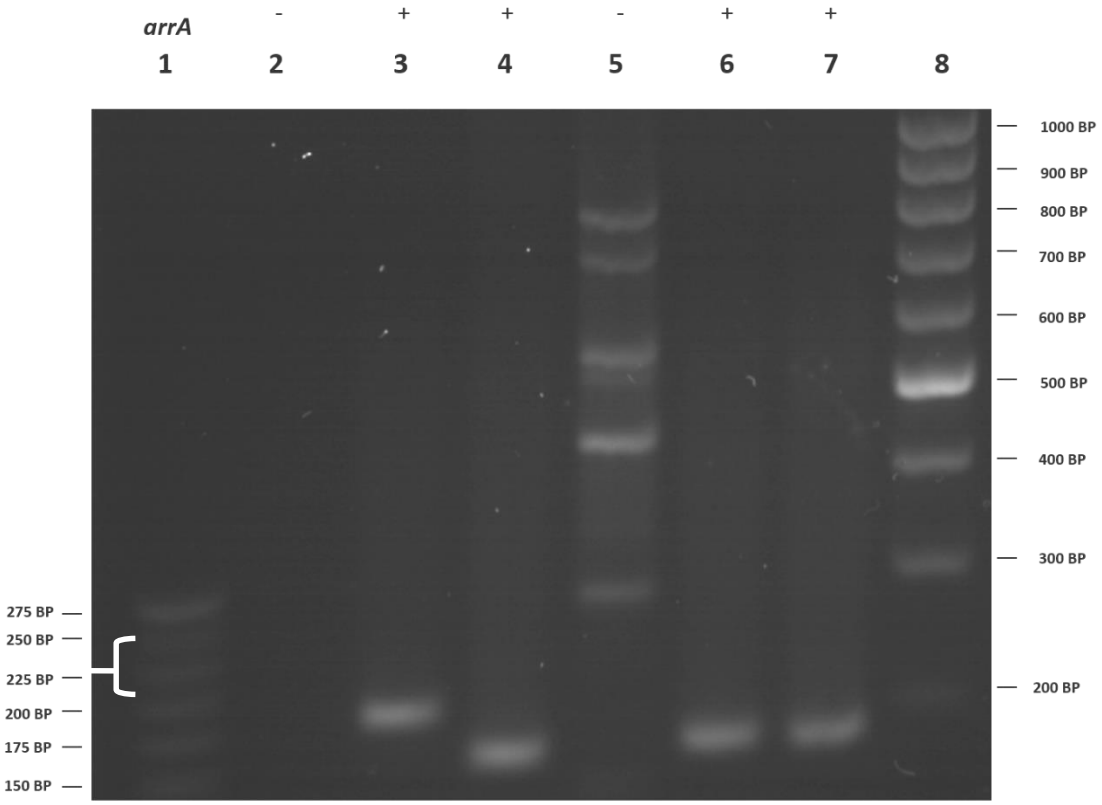

Figure 3.22. Super fine resolution (SFR) agarose (2%) gel of amplicons resulting from *arrA* PCR probing using ArrAfwd and ArrArev primers with +/- to indicate presence/absence of expected *arrA* fragment. Lanes: 1. 25 BP Step Ladder, 2. No template, 3. *Sulfurospirillum barnesii* SES-3 , 4. *Bacillus selenitireducens* MLS-10, 5. Vineland Off-site DARP enrichment, 6. Vineland On-site Aquifer enrichment, 7. Vineland On-site Vadose enrichment, 8. 100 BP Step Ladder. White bracket indicates expected *arrA* fragment length of 160-200 bp.

Primer Pair (F/R)	Expected *arrA* fragment length	Genomic template DNA	Band at expected length?	Other bands?
ArrAfwd/ArrArev	**160-200 bp**	SES-3	Y	N
		Bacillus selenitireducens MLS-10	Y	N
		Off-site enrichment	N	Y – 275, 425, 500, 550, 700, 800 bp
		Aquifer enrichment	Y	N
		Vadose enrichment	Y	N

Table 3.20. Summary of *arrA* probing using ArrAfwd and ArrArev primers.

``

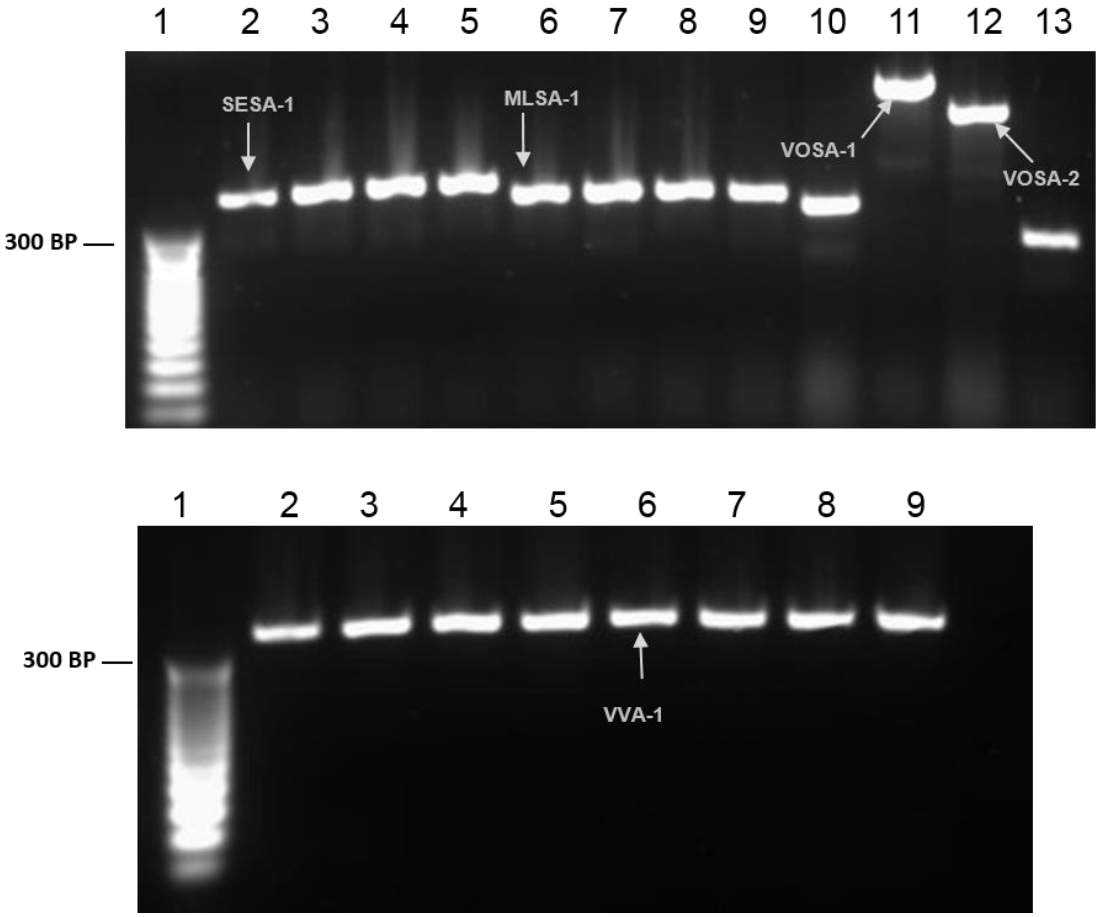

Figure 3.23. SFR 2% agarose gels 1 (TOP) and 2 (BOTTOM) of colony PCR products resulting from *arrA* probing using the ArrAfwd/ArrArev primer pair. Labeled bands indicate the DNA fragments that were successfully sequenced and identified via nucleotide BLAST. Gel 1 Lanes: 1. 25 bp ladder; 2-5. SES-3; 6-9. MLS-10; 10-13. Off-site enrichment. Gel 2 Lanes: 1. 25 bp ladder; 2-5: Aquifer enrichment; 6-9: Vadose enrichment.

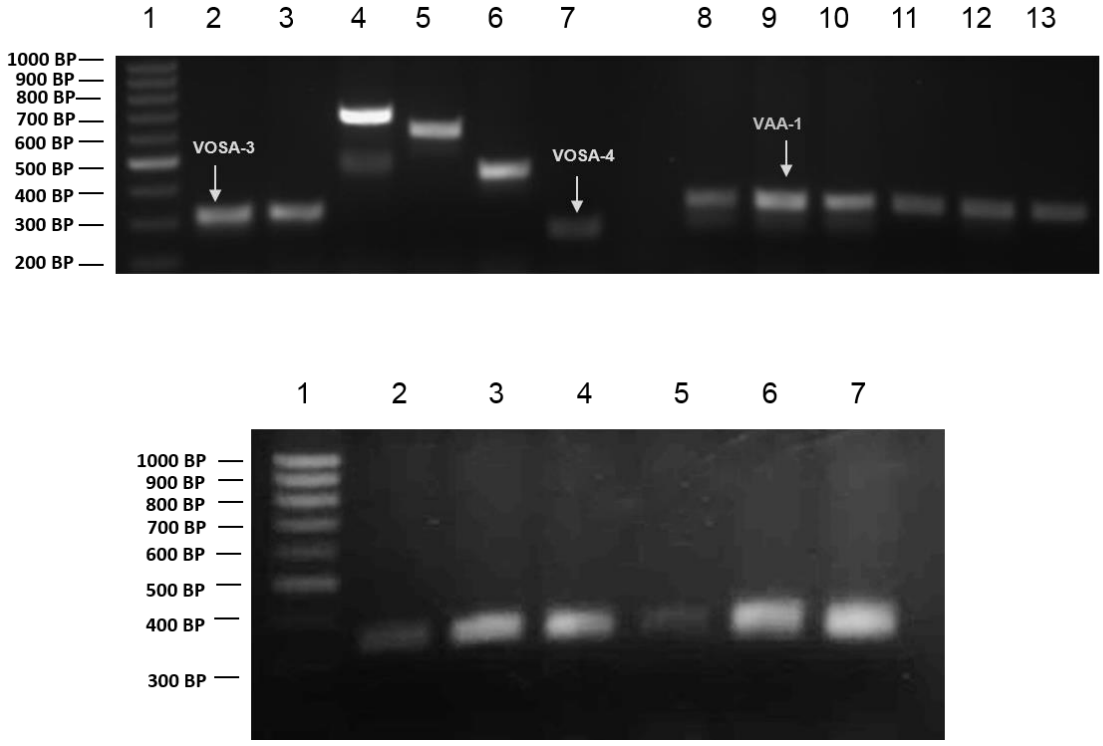

Figure 3.24. SFR 2% agarose gels 3 (TOP) and 4 (BOTTOM) of colony PCR products resulting from *arrA* probing using the ArrAfwd/ArrArev primer pair. Labeled bands indicate the DNA fragments that were successfully sequenced and identified via nucleotide BLAST. Gel 3 Lanes: 1. 100 bp ladder; 2-7. Off-site enrichment; 8-13. Aquifer enrichment. Gel 4 Lanes: 1. 100 bp ladder; 2-7. Vadose enrichment

Culture	Sequence name	Sequence Length (bp)	Top BLAST hit	Max Score	Query cover	Identity	Accession
Off-site enrichment	VOSA-1	580 (incomplete)	*Selenomonas ruminantium* subsp. *lactilytica* TAM6421 DNA, complete genome (putative UDP-N-acetylglucosamine pyrophosphorylase/glucosamine-1-phosphate N-acetyltransferase)	93.3	71%	66%	AP012292.1
	VOSA-2	364	*Tolumonas auensis* DSM 9187, complete genome (uracil-xanthine permease)	82.4	45%	73%	CP001616.1
	VOSA-3	87	*Spirochaeta africana* DSM 8902, complete genome (diguanylate cyclase (GGDEF) domain-containing protein)	59.0	55%	87%	CP003282.1
	VOSA-4	50	*Dothideomycetes* sp. UFMGCB 2143 18S ribosomal RNA gene, partial sequence; internal transcribed spacer 1, 5.8S ribosomal RNA gene, and internal transcribed spacer 2, complete sequence; and 28S ribosomal RNA gene, partial sequence	42.1	42%	100%	HM997113.1
Aquifer enrichment	VAA-1	116	Uncultured bacterium clone HlacAs_arrA_16 dissimilatory arsenate reductase (arrA) gene, partial cds	64.4	53%	83%	JQ890223.1
Vadose enrichment	VVA-1	106	Desulfosporosinus sp. Y5 arsenate respiratory reductase (*arrA*) gene, partial cds	149	95%	93%	DQ220794.1
B. selenitireducens MLS-10	MLS10A-1	101	Bacillus selenitireducens strain MLS10 respiratory arsenate reductase catalytic subunit (arrA) gene, partial cds	145	98%	95%	AY283639.1
S. barnesii SES-3	SES3A-1	126	Sulfurospirillum barnesii arsenate respiratory reductase (arrA) gene, partial cds	197	100%	96%	AY660884.2

Table 3.21. BLAST query results of DNA sequences amplified from DARP enrichment culture genomic DNA using the ArrAfwd/ArrArev primer pair during *arrA* probing. Also included in the table are the results generated from the positive control genomic DNAs from pure cultures of strains MLS-10 and SES-3. Primer sequences were truncated prior to BLASTing. The VOSA-1 sequence was not a full-length amplicon (it was greater than 596 bps).

b. *arsC* probing

PCR amplification using the *arsC*F and *arsC*R primers was unsuccessful, as no clear bands were formed following electrophoresis (data not shown). Therefore, the experiment using those primers was abandoned and other degenerate primer pairs were utilized for attempted *arsC* amplification. The *amlt-42*-f /*amlt-376-r* and *smrc-42-f/smrc-376-r* primers are named using a four-letter abbreviation of the specific gene cluster, the nucleotide position at which annealing occurs, and the direction of amplification (i.e. *amlt-42-f* anneals to position 42 of the *arsC* gene, amplifies in the forward (f) direction and has an abbreviated gene cluster description of "amlt"). Successful amplification using these degenerate primer sets should yield an *arsC* fragment that is 353 bp in length [107]. PCR *arsC* amplification attempts using the *amlt-42*-f and *amlt-376-r* primers and genomic template DNAs from the Vineland enrichments, as well as a control culture of *P. aeruiginosa* 1244 (possesses two separate *arsC* genes in its chromosomal DNA [65]), yielded amplicons approximately of the expected 353 bp length (**Figure 3.25; Table 3.22**). The off-site and aquifer enrichments also generated DNA amplicons of 275 and 800 bp lengths, respectively. Amplification using the *smrc-42-f/smrc-376-r* primer pair failed to produce DNA bands except in the vadose enrichment, which yielded a band at the expected 353 bp *arsC* gene fragment length. An additional smear was formed in the vadose reaction tube that was 300-325 bp in length.

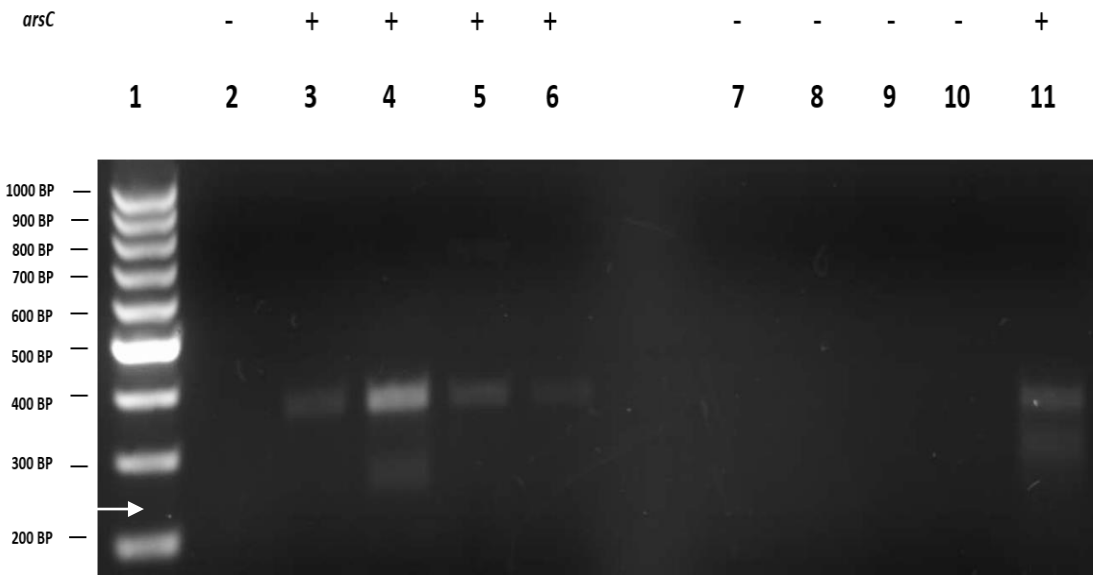

Figure 3.25. SFR agarose (2%) gel of *arsC* probing products with +/- to indicate presence/absence of *arsC*. Amplicons in lanes 2-6 were generated using the *amlt-42-f*/*amlt-376-r* primer pair while those in lanes 7-11 were generated using the *smrc-42-f*/*smrc-376-r* primer pair. Lanes: 1. 100 BP Step Ladder, 2. No template, 3. *Pseudomonas aeruginosa* 1244, 4. Vineland Off-site DARP enrichment, 5. Vineland on-site Aquifer DARP enrichment, 6. Vineland on-site Vadose DARP enrichment, 7. No template, 8. *P. aeruginosa* 1244, 9. Vineland Off-site DARP enrichment, 10. Vineland on-site Aquifer enrichment, 11. Vineland Vadose DARP enrichment. White horizontal arrow indicates expected *arsC* fragment length of 353 bp.

Primer Pair (F/R)	Expected *arsC* fragment length	Genomic template DNA	Band at expected length?	Other bands?
amlt-42-f/amlt-376-r	**353 bp**	*P. aeruginosa* 1244	Y	N
		Off-site enrichment	Y	Y – 275 bp
		Aquifer enrichment	Y	Y – 800 bp
		Vadose enrichment	Y	N
smrc-42-f/smrc-376-r	**353 bp**	1244; off-site and aquifer enrichments	N	N
		Vadose enrichment	Y	Y – 300-325 bp smear

Table 3.22. Summary of *arsC* probing using the *amlt* and *smrc* primer pairs.

Ligations and transformations were successfully performed on the *amlt-42-f/amlt-376-r* primer pair amplicons, following their purification. Colony PCR amplification using the M13F/M13R primer pair yielded amplicons consistent in length with those from the original amplification, bearing in mind that an additional ~170 bp of plasmid DNA is amplified along with the cloned DNA when the M13F/M13R primer set is used (523 bp). All four colony PCR products from the *P. aeruginosa* 1244 DNA template were at the expected *arsC* fragment length of 523 bp (**Figure 3.26**). Of the eleven aquifer colony PCR products, six ran at the expected length of 523 bp (clones 1, 6-10) (clones 2-5, 11), while five ran at around 950 bp. Of the ten vadose colony PCR products, eight (clones 1-4, 6-8, 10) ran at the expected length of 523 bp, while two (clones 5 and 9) failed to generate any amplicons. Of the ten off-site enrichment colony PCR products, nine (clones 1, 3-10) ran at the expected *arsC* length of 523, while one product (clone 2) was only around 275 bp long (**Figure 3.27**). Sequencing was successfully performed on most of the purified colony PCR products, with the best sequences being named and subjected to nucleotide BLAST. All clones successfully sequenced showed extremely high similarities to *arsC*. The names of each unique sequence and their BLAST results can be found in **Table 3.23** (the sequenced clones are also labeled on the gels shown in Figures 3.26 and 3.27**)**. The nomenclature of each clone was devised by combining the name of the template DNA, putative gene and clone number (i.e. PAC-1 means *P. aeruginosa arsC* clone 1; i.e. VOSC-1 means Vineland off-site *arsC* clone 1; VVC-1 means Vineland vadose *arsC* clone 1; VAC-1 means Vineland aquifer *arsC* clone 1).

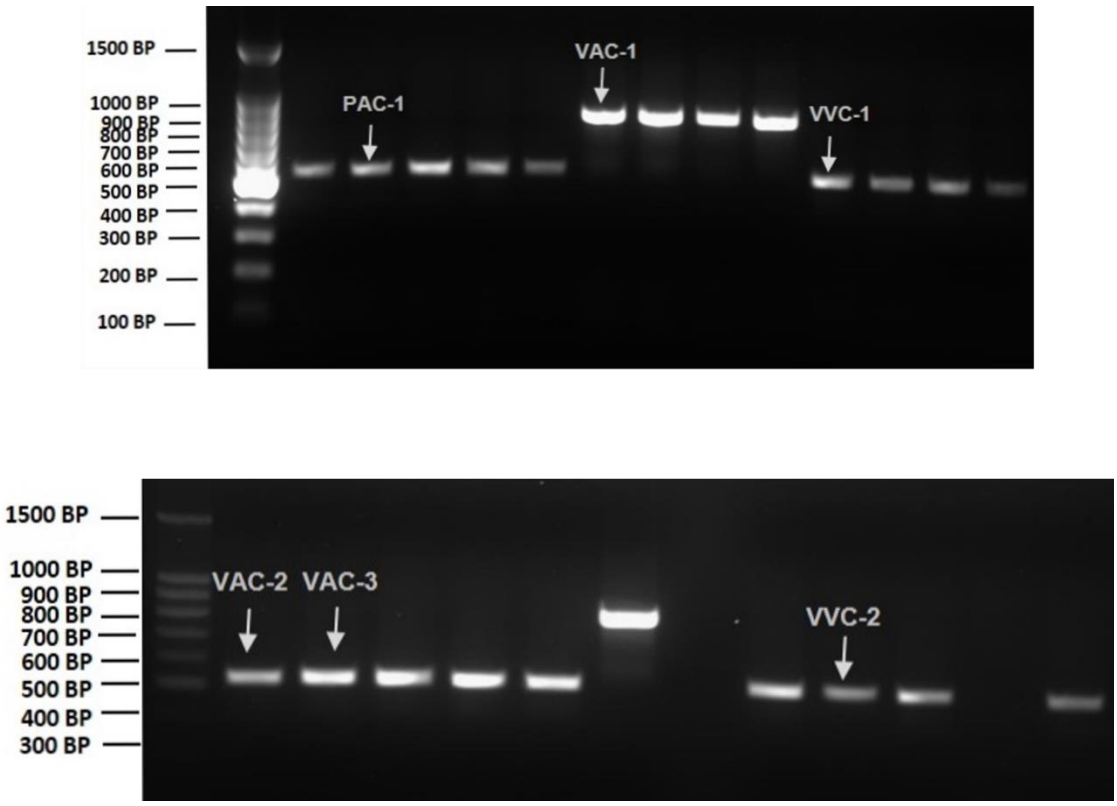

Figure 3.26. SFR agarose (2%) gels 1 (TOP) and 2 (BOTTOM) of colony PCR products resulting from *arsC* probing using the *amlt-42-f*/*amlt-376-r* primer pair. On-gel labels indicate the DNA fragments that were successfully sequenced and identified via nucleotide BLAST. Gel 1 Lanes: 1. 100 bp ladder; 2-5. PA 1244; 6-9. MLS-10; 10-13. Off-site enrichment. Gel 2 Lanes: 1. 25 bp ladder; 2-5: Aquifer enrichment; 6-9: Vadose enrichment.

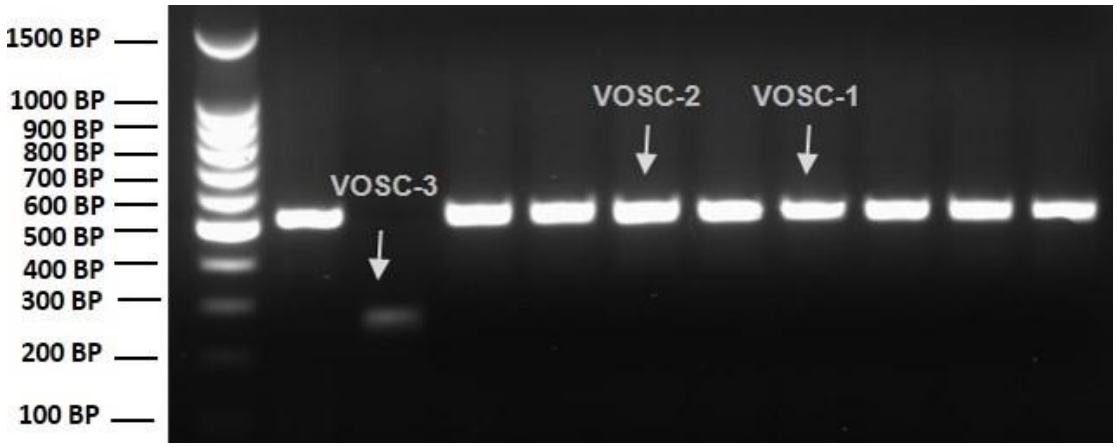

Figure 3.27. SFR agarose (2%) gel 3 of off-site enrichment colony PCR products resulting from *arsC* probing using the *amlt-42-f*/*amlt-376-r* primer pair. On-gel labels indicate the DNA fragments that were successfully sequenced and identified via nucleotide BLAST. Gel 1 Lanes: 1. 100 bp ladder; 2-5. PA 1244; 6-9. MLS-10; 10-13. Off-site enrichment. Gel 2 Lanes: 1. 25 bp ladder; 2-5: Aquifer enrichment; 6-9: Vadose enrichment.

Culture	Sequence name	Sequence Length (bp)	Top BLAST hit	Max Score	Query Cover	Identity	Accession
Off-site enrichment	VOSC-1	300	Providencia sp. VKPM23 arsenate reductase-like (arsC) gene, partial sequence	499	99%	98%	EF581172.1
	VOSC-2	299	Agromyces sp. CH90 arsenate reductase (arsC) gene, partial cds	423	93%	94%	JN609518.1
	VOSC-3	54	Streptococcus equi subsp. zooepidemicus ATCC 35246, complete genome (phosphoenolpyruvate carboxylase gene)	42.8	48%	96%	CP002904.1
Aquifer enrichment	VAC-1	591 (incomplete)	Bacillus megaterium QM B1551, complete genome (DNA-directed RNA polymerase, beta' subunit)	479	81%	82%	CP001983.1
	VAC-2	298	Cronobacter turicensis z3032 plasmid pCTU3, complete sequence (arsC gene)	508	100%	98%	FN543096.1
	VAC-3	298	Providencia sp. VKPM23 arsenate reductase-like (arsC) gene, partial sequence	497	99%	98%	EF581172.1
Vadose enrichment	VVC-1	299	Rhizobiaceae bacterium KAs3-31 arsenate reductase gene, partial cds	515	99%	99%	EF581172.1
	VVC-2	299	Clostridium propionicum DSM 1682 electron transfer flavoprotein subunit beta (acrB) gene, partial cds	405	97%	91%	JN244655.1
P. aeruginosa 1244	PAC-1	290	Providencia sp. VKPM23 arsenate reductase-like (arsC) gene, partial sequence	504	99%	99%	EF581172.1

Table 3.23. BLAST query search results of DNA sequences amplified from DARP enrichment culture genomic DNA using the *amlt-42-f*/*amlt-376-r* primer pair during *arsC* probing. Also included in the table are the results generated from the positive control genomic DNAs from a pure culture of *P. aeruginosa* strain 1244.

c. RISA

RISA analysis of each DARP enrichment culture revealed complex bacterial community structures, consistent with the previous microscopic evidence revealing the presence of multiple cell morphologies. The off-site and aquifer enrichments showed little difference in biodiversity with ~9 and ~8 bands present on the agarose gel, respectively (**Figure 3.28; Table 3.24**). The vadose enrichment revealed the greatest biodiversity with ~13 bands present on the gel. These findings may not be an accurate reflection of the actual number of species present in each enrichment culture, as a single bacterium may have multiple copies of the RIS gene, each bearing a sequence of varying lengths [93]. However, these results suggest that the Vineland subsurface region with the greatest arsenic concentration (vadose zone) has selected for the most diverse bacterial communities.

d. 16S rDNA Analyses

16s rDNA amplicons were successfully amplified in each enrichment culture as well as a control possessing genomic DNA from a pure culture of *P. aeruginosa* (**Figure 3.29**). High-throughput 16S rDNA sequencing was successfully performed on the genomic DNA aliquots of the off-site, aquifer and vadose DARP enrichments, with the results indicating that nearly 100% of the bacteria were *Bacillus* and *Clostridium* species of the *Firmicute*s (Gram positive low G+C) phylum (data not shown).

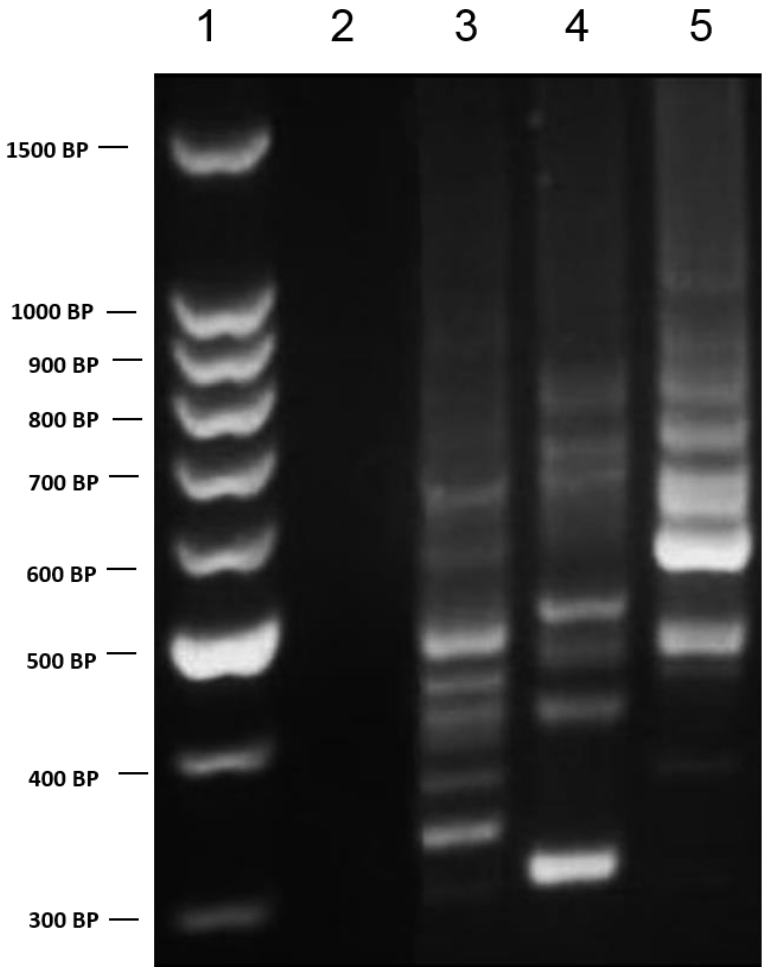

Figure 3.28. SFR agarose (2.5%) gel of RISA amplicons. Lanes: 1. 100 BP Ladder, 2. No template; 3. Vineland off-site DARP enrichment, 4. Vineland on-site aquifer DARP enrichment, 5. Vineland on-site vadose DARP enrichment. Approximate species numbers are estimated by counting each individual band per lane.

DARP Enrichment Culture	Approximate No. of Species
Off-site	9
Aquifer	8
Vadose	13

Table 3.24. Biodiversity in the DARP enrichments as assessed by RISA PCR product electrophoresis on a 2.5% SFR agarose gel. The species numbers were derived from the estimated number of individual RIS bands present in each lane, with each band providing a representation of an individual species. This may not be an accurate representation of the exact numbers of species, as some bacterial strains possess multiple RIS regions of unique lengths; thus one species may produce more than one band [93].

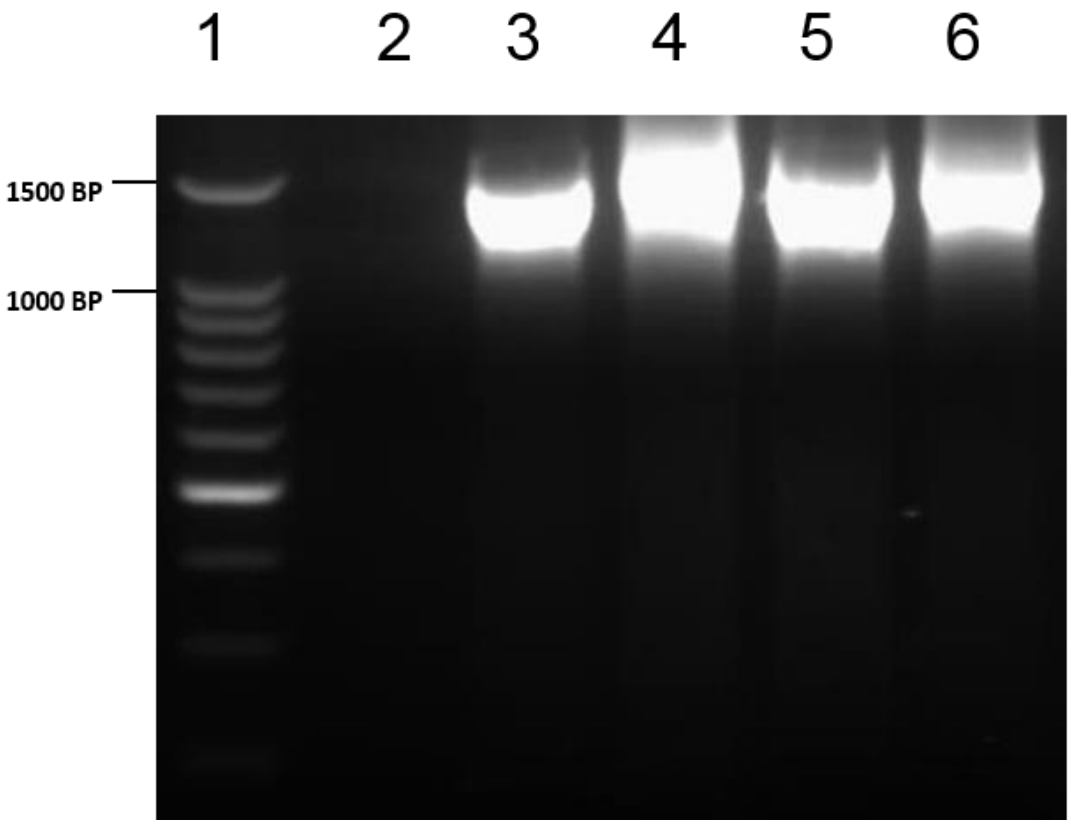

Figure 3.29. Agarose gel (1%) of 16S rDNA amplicons. Lanes: 1. 100 BP Ladder, 2. No template, 3. *P. aeruginosa* strain 1244, 4. Vineland off-site DARP enrichment, 5. Vineland on-site aquifer DARP enrichment, 6. Vineland on-site vadose DARP enrichment.

E. Discussion

The initial goal of the experiments performed on the Vineland subsurface sediments was to demonstrate that communities of anaerobic bacteria have been selected for that are capable of demethylating methylarsenic to a form of the inorganic variety, thus toxifying it in the process. While the initial enrichment cultures experiments demonstrated robust growth in each separate subsurface sediment enrichment set (off-site, aquifer and vadose) the analytical data collected clearly demonstrated that the methylarsenic was not being metabolized, but rather nitrate respiration was likely occurring using the organic acids from the yeast extract as an electron donor or fermentation using aforementioned organics. Thus, the aim of the experiments shifted to investigating the As(V) respiration capabilities of the anaerobic prokaryotic communities within the sediments, which as previously described is a mechanism by which arsenic can be converted to the highly toxic As(III) species and mobilized into groundwater and surface waters, potentially endangering the ecosystems of plants and animals and the health of the surrounding human population. The heavily arsenic-contaminated vadose and aquifer zone subsurface sediment zone enrichments demonstrated strong analytical evidence of As(V) respiration using lactate as an electron donor, while the uncontaminated off-site enrichments showed a dissimilar trend with a probable lactate fermentation pathway with As(V) being reduced to As(III) as a resistance mechanism suggesting based on the stoichiometric ratios achieved.

The enhanced rate of arsenic reduction and near complete recovery of As(III) from As(V) in the aquifer and vadose enrichment sets compared to the retarded As(V) reduction kinetics and lesser total accumulation of As(III) in the off-site set provided strong evidence supporting the notion that the anthropogenic arsenic contamination at Vinland Chemicals selected for potentially environmentally detrimental DARPs. Furthermore, the molecular evidence revealing the presence of both *arrA* and *arsC* gene fragments in the aquifer and vadose enrichments, versus only *arsC* uncovered *i*n the off-site samples, further solidifies these findings.

Since Vineland Chemical Company's former location became an EPA Superfund site on September 1, 1984, various strategies have been implemented in order to clean up the arsenic pollution that resulted from the 44 years of industrial methylarsenic production by the company [31]. Hundreds of thousands of tons of soil and sediments of the area have been processed and replaced by uncontaminated backfill, groundwater has been extracted and treated for arsenic contaminants, and Blackwater Branch has been rigorously cleaned (which will prevent further contamination of Maurice River and Union Lake). While the Vineland location has since been treated for the massive arsenic contamination that once prevailed, the results obtained during these experiments clearly demonstrated that any anthropogenic arsenic pollution resulting from industrial use of arsenic-based herbicides can be highly detrimental to the environment by selecting for DARPs in the subsurface.

Since the 1950's herbicides containing methylarsenicals such as monosodium methylarsonate (MSMA; MMA(V)-based) have been regularly applied to golf courses in southeastern Florida, and, as a result, elevated levels of inorganic arsenic have been detected in groundwater, soils, surface waters as well as lake sediments which demonstrates demethylation as well as mobilization is actively occurring at these locations [32, 140-143]. As previously eluded to, bacteria in simulated golf soil samples treated with MMA(V) are capable of methylarsenic demethylation, liberating inorganic arsenic in the process [33]. Theoretically, subsurface bacterial communities consisting of methylarsenic demethylating species, DARPs, ARMs and DIRBs could be readily selected for due to the continued application of methylarsenic herbicides in southeastern Florida golf courses, which could aid in the speciation and mobilization of arsenic in these locations, potentially aiding in the enrichment of groundwater with highly toxic As(III). Thus, the results obtained during this project can provide insight into the possible environmental consequences that may present themselves after numerous decades of methylarsenic herbicides being applied to the multiple golf courses in Southern Florida.

Chapter IV. Microbial arsenate reduction in sediments from a coal combustion byproduct sludge disposal site

A. Abstract and Hypotheses

Hypothesis: The sediment of a coal combustion byproduct sludge disposal site possess robust communities of arsenic transforming bacteria.

H^1: Bacterial As(III) oxidation is occurring.

H^2: Bacterial As(V) reduction is occurring.

In this study, bacterial arsenic transformation was investigated in the sediments of a coal combustion byproduct (CCB) sludge disposal lake. Initial microcosms were established using specialized anaerobic media formulated based on the water chemistry of the lake, which successfully grew bacteria from the CCB sludge. Once bacterial growth was evident, analytical work was conducted using the previously described anion exchange chromatography method. Initial studies indicated that rapid As(V) reduction was occurring when lactate was included in the microcosms. However, microcosms amended with As(III) and nitrate failed to demonstrate As(III) oxidation to As(V). Therefore, a rigorous microcosm experiment using various coal ash core depths (0-2', 2-4', 4-6', 8-10') was performed under two different conditions: 1) 5 mM As(V) and 10 mM lactate and 2) 5 mM As(V) alone. Microcosms from the 2-4' and 4-6' cores demonstrated much more rapid As(V) reduction under the presence of lactate, suggesting a possible respiratory mechanism. The 0-2' core showed rapid As(V) reduction with or without the inclusion of lactate.

The 8-10' core microcosm demonstrated the slowest As(V) reduction rate and, therefore, did not show evidence of dissimilatory As(V) respiration. Sulfate reduction did not occur in any microcosms. Heat killed controls did not undergo any As(V) reduction.
The findings here suggest that the CCB sludge at this location support robust communities of As(V) reducing bacteria.

B. Coal Combustion Residuals (CCRs) Background

Coal combustion residuals (CCRs) , also referred to as coal combustion byproducts (CCBs), coal combustion products (CCPs) or simply "coal ash" are the residual waste products resulting from the burning of coal for electricity generation [112]. Over 100 million metric tons of CCRs are produced annually in the United States and fall into four distinct categories: (1) fly ash, (2) bottom ash, (3) boiler slag and (4) flue gas desulfurization (FGD) material or residue [113-115]. To use coal combustion to generate electricity, there are currently various methods employed as technology has expanded much in the past two decades. The traditional and predominant method is pulverized-coal combustion, during which the coal is rigorously crushed and passed to a combustion chamber or "boiler" in which the burning occurs [112,116]. While the coal is incinerated, the first three types of CCRs are produced. Fly ash is by far the most abundant type of CCR produced worldwide and represents about 60% of the CCRs generated in the United States annually [117]. It and is generally tan and powdery in appearance, consisting of tiny, glassy, hollow and spherical ferroaluminosilicate (silicon, iron, and aluminum) particles [113]. Fly ash is typically 0.1 - 1 μm which makes it small and light enough to be carried out of the combustion chamber in the flue gas [111,112,118].

To remove the fly ash from flue gas following coal combustion and prevent its emissions, electrostatic precipitators or special filtration methods are utilized [111]. Bottom ash and boiler slag, however, are too coarse and large to be suspended in the flue gas and fall to the bottom of the combustion chamber or stick to the walls [111-113].

Bottom ash is residual non-combusted coal material settling at the bottom of the chamber and makes up about 12% of CCRs [117]; it consists of highly coarse, dark grey to black colored, angular, porous and granular particles that are much larger than fly ash (0.1-10 mm) which explains their inability to exit the chamber in flue gas [111,113,118]. Boiler slag is much less prevalent than fly ash and bottom ash and makes up only about 4% of CCRs generated [117]. Slag results when "operating temperatures exceed ash fusion temperature" [113] and is in a liquefied state prior to being hydrated and drained from the combustion chamber [111,113]. Its size, coarseness and angularness is similar to that observed in bottom ash, but is dark black in color, extremely hard and has a smooth, glassy appearance without pores [111,118]. During the coal firing process, copious amounts of extremely toxic sulfur dioxide gas (SO_2) are liberated into the flue gas due to the elevated sulfur content in many coal types. In 1990, the United States government passed a legislation that further improved the parameters outlined in the original 1970 Clean Air Act known as "The Clean Air Act Amendments of 1990" (CAAA '90 Public Law 101-549) mandating that the United States Environmental Protection Agency (EPA) establish standards for controlling the emissions of six major toxic atmospheric pollutants – sulfur dioxide (SO2), carbon monoxide (CO), particulate matter, ozone (O_3), nitrogen dioxide (NO_2), and led (Pb) – in order to preserve the safety of human health and the environment (The Clean Air Act was also revised in 1977) [112,113,119].

As a result of CAAA '90 Public Law 101-549, all energy companies using coal as their power supply are required to filter gaseous SO_2 from flue gas to prevent harmful atmospheric emissions and acid rain, which results in the production of the type of CCR known as FGD Material [111,113,115].

Many techniques have been developed for flue gas desulfurization, which is referred to as "scrubbing" and can be broken down into two major categories, depending on if the flue gas becomes moisturized or demoisturized, respectively: Wet and dry [112]. While there are over a hundred FGD techniques that have been developed, the overwhelming majority of FGD systems in the United States (roughly 90%) rely on limestone [calcium carbonate or ($CaCO_3$)] or lime [calcium oxide or (CaO)] as the sorbent to which SO_2 is adsorbed [112]. Briefly, using either a wet or dry method, a limestone or lime adsorbent comes in contact with the flue gas and reacts with the gaseous SO_2, forming calcium sulfate ($CaSO_4$, gypsum) or calcium sulfite ($CaSO_3$) [112]. Thus, the majority of FGD material in the United States consists of $CaSO_4$, $CaSO_3$, fly ash and residual sorbent [111-113]. Physically, FGD material is alkaline in nature and physically can appear as sludge or a dry powdery substance, depending on whether the scrubbing process used was wet or dry, respectively [111]. With the implementation of CAAA '90 Public Law 101-549, a major problem is averted in the prevention of SO_2 emissions and acid rain production; however, another is created as the accumulation of FGD materials greatly enhances the total amount of CCRs produced annually [112]. FGD materials are the second most abundant CCR type generated in the US annually and represent about 24% of total CCRs produced [117].

While the chemical nature of CCRs can vary depending on the combustion technique, FGD mechanism, coal type, etc., in general, fly and bottom ashes have chemical compositions comprised mainly of the following eight elements (highest to lowest concentration): Silicon (Si), iron (Fe), aluminum (Al), calcium (Ca), magnesium (Mg), sodium (Na), potassium (K) and titanium (Ti) [113,118,121]. However, CCR ashes also consist of a mixture of trace elements such as zinc (Zn), copper (Cu), molybdenum (Mo), and manganese (Mn) [113,118,121]. However, elements that have been identified as potentially hazardous drinking water contaminants, the levels of which being tightly regulated by the United States EPA, including arsenic (As), selenium (Se), cadmium (Cd), mercury (Hg), lead, (Pb), chromium (Cr) and fluoride (F), also occur in fly and bottom ashes [113,118,121,122]. **Table 4.1** shows the average values of each toxin found in CCR ashes and their maximum contaminant levels (MCL) as commissioned by the United States EPA. A large amount of CCRs (44%) are productively reused industrially for applications such as construction and agriculture [115]. Such a practice greatly alleviates the massive quantity of CCRs fated to lay as dead waste at disposal locations and stimulates the economy as fly ash, bottom ash, boiler slag and FGD materials can be beneficially recycled and sold. In agriculture, CCRs are used as soil amendments to improve plant growth yields and soils by providing essential elements such as phosphorus (P), S, Ca, Mg, and K [121].

Element	Concentration Range (mg/kg) [118]	MCL (mg/l) [122]
Arsenic (As)	0.5-279	0.01
Barium (Ba)	52-5,790	2
Cadmium (Cd)	0.1-18	0.005
Chromium (Cr)	3.4-347	0.1
Fluorine (F)	0.4-320	4
Lead (Pb)	0.4-252	0.015
Mercury (Hg)	0.005-4.2	0.002
Selenium (Se)	0.08-19	0.05

Table 4.1. Heavy metals and metalloids found in fly and bottom ash CCRs.

Recently, plant growth and soil microbial community effects of fly ash application to soil used to grow a rice plant were investigated and indicated that while no acceleration of growth occurs in untreated plants vs. those amended with low concentrations of fly ash (up to 20% at a soil volumetric ratio), growth speed inhibition actually occurred when high levels of fly ash were added (greater than 20% fly ash). Growth of the plant was significantly increased as well at fly ash levels up to 20% with yields significantly decreased higher at concentrations. Thus, while the addition of fly ash to soils can be beneficial if amendments are made at low concentrations, adverse effects (less crop yield, loss of beneficial soil bacteria) might be expected if the fly CCR ash amendments are too concentrated .

The majority of CCRs produced (around 56%) are still disposed of in waste storage sites while 44% are reused productively [115]. The productive and beneficial reuse of CCRs is a growing and popular practice used to limit the mass accumulation of CCRs in waste storage facilities, which can present environmental distress [124]. The two most common applications of CCR productive reuse are in the construction and agricultural industries, respectively [112-114,118,124,125]. Chemically composed primarily of silica and aluminum, fly and bottom ashes are pozzolanic in nature, meaning they form rock-hard cementitious minerals when hydrated and reacted with CaO [118]. This property allows fly and bottom ash to be of appreciable value to a multitude of construction applications. They are used in the creation of cement, concrete, blasting grit, asphalt, bricks, wallboard, fillers, roofing material, etc. [112,114].

The most highly reused CCR in this regard is fly ash, as it accounts for over 90% of the cement and concrete production by all types of CCRs generated, and greater than 60% of total fly ash reused is devoted to this purpose [118]. Boiler slag, while being the most uncommonly produced CCR, is primarily utilized for blasting grit and roofing materials [118]. FGD materials are used to create construction resources such as concrete additives and gypsum ($CaSO_4$) plaster used in drywalls.

FGD generated gypsum is known as "synthetic gypsum" and occurs in almost 1/3 of the gypsum panels produced in the United States, thus contributing to the construction field [117]. In agriculture, CCRs are used as soil amendments for a variety of purposes [118]. FGD materials are utilized to a great extent as agricultural soil amendments in order to alkalinize soil under detrimentally acidic pH conditions, supplement plants with various essential elements for nutrition (i.e. Ca, S), improved water uptake, immobilize soluble phosphorus under elevated levels which may be harmful and cause eutrophication, as well as other purposes [125]. Gypsum, while commonly incorporated into drywalls in the construction industry, is also used agriculturally as a soil amendment to improve water transport by improving the porosity of the soil [125]. Other beneficial reuse applications of CCRs include mining applications, production of sulfur containing chemicals and the stabilization and solidification of hazardous wastes [118]. While there are various beneficial reuse applications associated with the production of CCRs, heavy metals and metalloids within these materials (Table 4.1) may leach into soils, water bodies and groundwater, potentially jeopardizing the safety of plants, animal ecosystems and human beings [116].

C. Materials and Methods

i. Sampling

Samples from a stabilized coal combustion byproduct disposal site were taken from the surface as well as cores from four different depth ranges (0-2', 2-4', 4-6', 8-10'). They were collected and provided by an independent contractor. Both the name of the site and the contractor cannot be disclosed as part of the CREDA agreement.

ii. Media formulation

a. Water chemistry data and calculations

Water chemistry data from the CCB sludge disposal lake was used to convert parts per million (ppm) concentrations of multiple chemicals into averages in mM and M concentrations (**Appendix A**).

b. Basal media formulation

Using the average values from spreadsheet 1, a spreadsheet (**Appendix B**) was created consisting of various calculations used to derive a novel basal salts media formulation which will be referred to as "Basal media." The media consists of the following (g/l): K_2HPO_4 (0.225), KH_2PO_4 (0.225), NaCl (0.44), NH_4Cl (0.225), $MgCl_2$-$6H_2O$ (0.225), Bacto™ yeast extract (0.5), $NaHCO_3$ (0.038), and Na_2S-$7H_20$ (0.569). Also, 2 ml of previously described 500X vitamin and trace element mixes (see page 77) were included. A second medium was also prepared identical to that just described with the exception of adding 5.323 g/l of Na_2SO_4 to mimic the elevated sulfate concentrations present in the lake.

The presence of elevated sulfate in the media may select for sulfate reducing bacteria rather than those respiring As(V), which explains the formulation of "high" and "low" sulfate media types for experimental purposes. The pH was adjusted to 9.70 with NaOH and degassing was performed as previously described (see page 77), but with N_2 alone (No CO_2) for both media formulations.

iii. Initial microcosm preparations

Microcosms were initially prepared in high and low sulfate basal media under the various conditions indicated in **Table 4.2**. Roughly 5 grams of lake bed surface sediments were aseptically added via ethanol sterilized spatula to 100 mL of the previously described high and low sulfate basal media inside of an inflatable, anaerobic glove bag under constant flow of N_2. The bottles were then incubated at 30°C in the dark without shaking. After one week of incubation, using the microcosm listed as "condition 6" (**Table 4.2**) as inoculum, three additional bottles were inoculated to test for electron donor diversity for As(V) respiration as well as respiratory chemolithoautotrophic As(III) oxidation using nitrate as the electron donor (**Table 4.3**).

iv. Second microcosm preparations

A second and final round of microcosms was prepared in triplicate according to the conditions indicated in **Table 4.4**. Roughly 5 grams of sludge from 0-2', 2-4', 4-6' and 8-10' sludge core depths were aseptically added to 100 mL of appropriately amended bottles of basal media, in triplicate, via ethanol sterilized spatula.

Condition	Electron Donor	Electron Acceptor	Added Sulfate
1	10 mM Lactate	As(V)	Y
2	None	As(V)	Y
3	None	None	Y
4	10 mM Lactate	As(V)	N
5	None	As(V)	N
6	None	None	N

Table 4.2. Growth conditions established for initial grab-sample (lake bed surface) microcosms analyses grown on basal media.

Condition	Electron Donor	Electron Acceptor
1	10 mM acetate	5 mM As(V)
2	10 mM pyruvate	5 mM As(V)
3	5 mM As(III)	10 mM nitrate

Table 4.3. Additional growth conditions established for initial grab-sample microcosms grown on basal media with elevated sulfate.

Core Depth	Electron Donor	Electron Acceptor
0-2’	10 mM Lactate	5 mM As(V)
0-2’	None	5 mM As(V)
0-2’ HEAT KILLED	10 mM Lactate	5 mM As(V)
2-4’	10 mM Lactate	5 mM As(V)
2-4’	None	5 mM As(V)
2-4’ HEAT KILLED	10 mM Lactate	5 mM As(V)
4-6’	10 mM Lactate	5 mM As(V)
4-6’	None	5 mM As(V)
4-6’ HEAT KILLED	10 mM Lactate	5 mM As(V)
8-10’	10 mM Lactate	5 mM As(V)
8-10’	None	5 mM As(V)
8-10’ HEAT KILLED	10 mM Lactate	5 mM As(V)

Table 4.4. Growth conditions established for second microcosm set grown on basal media with high sulfate.

Anaerobic conditions were maintained during microcosm preparation by performing all inoculations in a Shel Lab® Bactron IV Anaerobic Chamber according to the manufacturer's instructions. Following inoculations, each microcosm was placed in the dark at 30°C without shaking to stimulate microbial growth. Heat-killed microcosms were established in singlet from each core depth by immediately autoclaving inoculated bottles of basal media with no amendments. Following autoclaving and cooling, the bottles were amended with 5 mM As(V) and 10 mM lactate. Amendments were performed following autoclaving rather than prior to due to the possibility of lactate and As(V) degradation during the heating process.

v. Time-course experiments

During the time-course experiments aliquots were aseptically extracted from each bottle via sterile syringe equipped with a 0.22 µM Fisher Scientific PES filter. Thermo Scientific/Dionex On-guard II M cartridges were attached to the syringes to filter out potential transition metals that could damage the separator column during IC analyses. Following sample extraction, each was placed at -80°C until chemical analyses were performed.

vi. Analytical methods

All analytical work was carried out using the Dionex ICS-1100 system with dual conductivity and UV/Vis detection and the Chromeleon LE 7.0 software as previously described in chapter II. Standard preparation protocols can be found on page 58 of chapter II.

vii. Cell harvesting

Following the one-week incubational period of the second microcosm set, one bottle from each triplicate set amended with both As(V) and lactate was chosen for cell harvesting. The aqueous portion of each culture was carefully withdrawn via sterile pipette, transferred to a 50 ml centrifuge tube, and centrifuged at 7,000 rpm for 10 minutes. The supernatants were discarded and the resulting cell pellets frozen at -80°C for potential further molecular analyses.

D. Results

i. Initial microcosms

a. Microcosm incubations

After 24 hours of incubation, turbidity was visible in each microcosm established. Microscopy revealed the presence of heterogeneous communities of rod-shaped bacteria in each culture (**Figure 4.1**). Microscopic and macroscopic evidence in each bottle suggested that As(V)-amended microcosms receiving lactate grew more robustly than those without the addition of an electron donor (**Table 4.5)**. The least amount of growth was achieved in the microcosms that did not receive As(V) or lactate amendments. There did not appear to be a difference in growth whether additional sulfate was present or not.

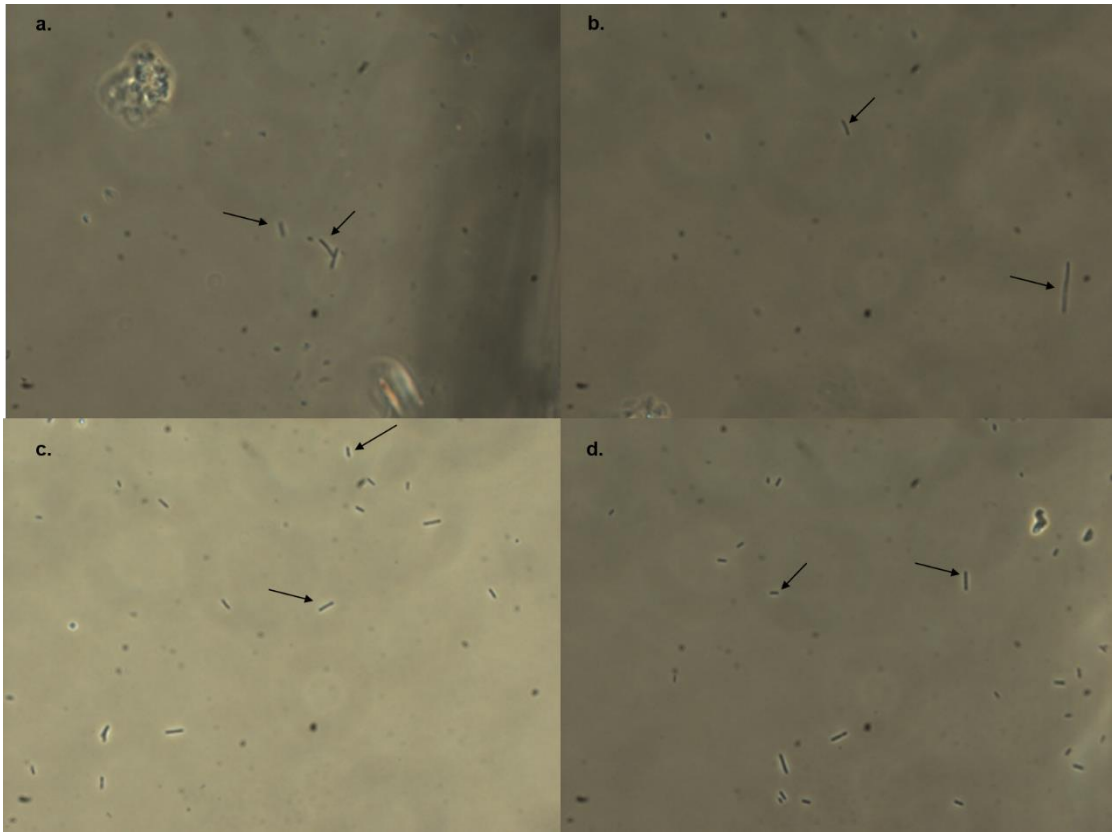

Figure 4.1. Microscopic growth photos of initial microcosms. Photos: a) As(V) + lac + sulfate; b) As(V) + lac – sulfate; c) As(V) – lac + sulfate; d) As(V) – lac – sulfate. Arrows indicate bacterial cells.

Condition	Electron Donor	Electron Acceptor	Sulfate added?	Growth (+++, ++, +)
1	10 mM Lactate	As(V)	Y	+++
2	None	As(V)	Y	++
3	None	None	Y	+
4	10 mM Lactate	As(V)	N	+++
5	None	As(V)	N	++
6	None	None	N	+

Table 4.5. Qualitative (+, ++. +++) assessment of macroscopic growth of initial grab-sample microcosms based on turbidity of each microcosm after 24 hours of incubation at 30°C.

The microcosms receiving As(V) amendments formed the yellow precipitate presumed to be orpiment, with the greatest amount of precipitation appearing to occur in the microcosms received the lactate amendment (data not shown).

b. Time-course experiments

Aliquots taken from the As(V) and lactate amended microcosms (conditions 1 and 4 from Table 4.4) revealed that a significant amount of As(V) reduction had occurred under these conditions (**Figure 4.2**). The presence of sulfate did not appear to inhibit As(V) reduction, with both media types achieving near complete conversion of As(V) to As(III) within two days of incubation (Figure 4.2). Since the actual lake conditions consist of extremely high sulfate levels (37.5 mM), only the basal media with the added sulfate was chosen moving forward with this project, which will now simply be referred to as "basal media." As(V) reduction occurred over the course of two days when acetate or pyruvate was used as the electron donor (data not shown). Chemolithoautotrophic arsenite oxidation was not observed under 5 mM As(III) and 10 mM nitrate (data not shown).

ii. Second microcosm time-course experiments

Each microcosm under the varying selective media conditions showed macroscopic growth evidence in the form of turbidity after roughly 24 hours of incubation. In terms of qualitative assessment of growth based on turbidity alone, the following hierarchy can summarize the growth yields of the microcosms established from each different core depth: 0-2' = 2'4' > 4-6' > 8-10' (**Table 4.6**).

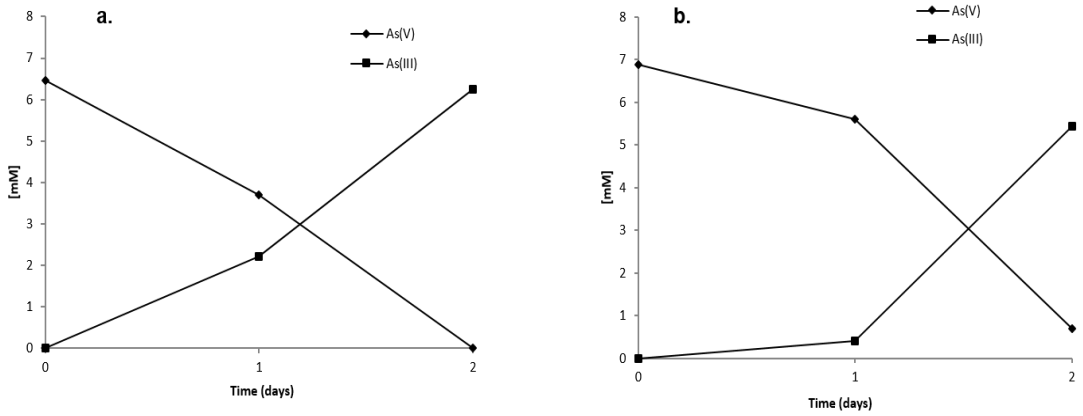

Figure 4.2. Time-course plot of grab sample (bed surface) microcosms amended with 10 mM lactate and 5 mM As(V) a) with and b) without additional sulfate.

It appeared as if total microbial growth shared a negative correlation with increasing core depth, as the greatest growth yield occurred in microcosms amended with sludge closer to the lake bed surface. In the 0-2', 2-4' and 4-6' core, turbidity was greatest in the microcosms amended with As(V) and lactate versus just As(V) alone, suggesting a possible respiratory mechanism in which lactate serves as the electron donor. The 8-10' core microcosms did not share a similar trend, as there was no noticeable difference between cultures grown with or without the lactate amendments. During aliquot extraction at each time point, a bright yellow color was retained in the sample filtrates and transition metal filters that was presumed to be orpiment (**Figure 4.3**). Each microcosm set appeared to generate a brighter yellow coloration during filtration when lactate was present with the As(V), versus simply As(V) alone (**Table 4.6**). Therefore, it appears as if the presence of lactate facilitates greater microbial growth as well as enhanced orpiment production – both observations being highly indicative of a possible respiratory mechanism. Heat-killed bottles showed no evidence of turbidity nor the appearance of yellow coloration during aliquot filtration..

As(V) was reduced to As(III) in each microcosm set during the one week experimental incubation period (Figure). In the 0-2' (**Figure 4.4 a**) and 2-4' (**Figure 4.4 b**) core microcosm sets, whether lactate was present or absent, As(III) was recovered from As(V) in the expected 1:1 stoichiometric ratio up to the 72-hour time point. However, this stoichiometry was not observed at the 7-day mark, as As(III) levels declined gradually between days 3 and 7, suggesting that a significant amount of the soluble form may be precipitating out as orpiment over a period of time.

In the 4-6’ core microcosm set, As(III) was recovered from As(V) in a 1:1 stoichiometric fashion throughout the entire incubation period (**Figure 4.4 c**). The 8-10’ core microcosm set did not demonstrate any As(V) reduction activity until after the 3-day mark, unfortunately meaning the majority of this activity could not be plotted (**Figure 4.4 d**).

Complete As(V) disappearance occurred within one week of incubation along with the emergence of As(III). However, a lack of 1:1 recovery may once again be explained by orpiment mineralization occurring somewhere within the 3- to 7-day mark, during which no data were collected. While the heat-killed controls showed no evidence of As(III) formation and therefore no reduction of As(V), disappearance of As(V) did occur over time in the 0-2’ (**Figure 4.4 b.**) and 4-6’ core microcosms (**Figure 4.4 c.**). A feasible explanation for this observation is that As(V) may have become mineralized in the sediment used as inoculum, as this compound has a strong affinity for solid-state iron and aluminum containing oxides [3]. Each culture set demonstrated more rapid As(III) formation from As(V) when lactate was added in addition to As(V), providing evidence for potential As(V) respiration using lactate as the electron donor. The most rapid As(V) reduction rates were achieved in the 4-6’ and 2-4’ microcosms amended with both lactate and As(V), with observed maximum As(III) appearance rates of 71 and 64 µM/h, respectively. Without the lactate amendments, these microcosm sets were only capable of As(III) formation at max rates of 26 and 16 µM/h, respectively. The 0-2’ core microcosm set generated As(III) at rates of 60 and 27 µM/h with and without lactate, respectively.

Core Depth	Electron Donor	Electron Acceptor	Growth (+,++,+++)	Orpiment (+,++,+++)
0-2’	10 mM Lactate	5 mM As(V)	++	+++
0-2’	None	5 mM As(V)	+++	++
0-2’ HEAT KILLED	10 mM Lactate	5 mM As(V)	-	-
2-4’	10 mM Lactate	5 mM As(V)	++	++
2-4’	None	5 mM As(V)	+++	+
2-4’ HEAT KILLED	10 mM Lactate	5 mM As(V)	-	-
4-6’	10 mM Lactate	5 mM As(V)	+	++
4-6’	None	5 mM As(V)	++	+
4-6’ HEAT KILLED	10 mM Lactate	5 mM As(V)	-	-
8-10 ‘	10 mM Lactate	5 mM As(V)	+	++
8-10 ‘	None	5 mM As(V)	+	+
8-10’ HEAT KILLED	10 mM Lactate	5 mM As(V)	-	-

Table 4.6. Qualitative assessment (+, ++. +++) of growth and orpiment formation in each microcosm after 24 hours of incubation at 30°C. Growth was assessed by visual turbidity while orpiment production was assessed by visual brightness of yellow coloration.

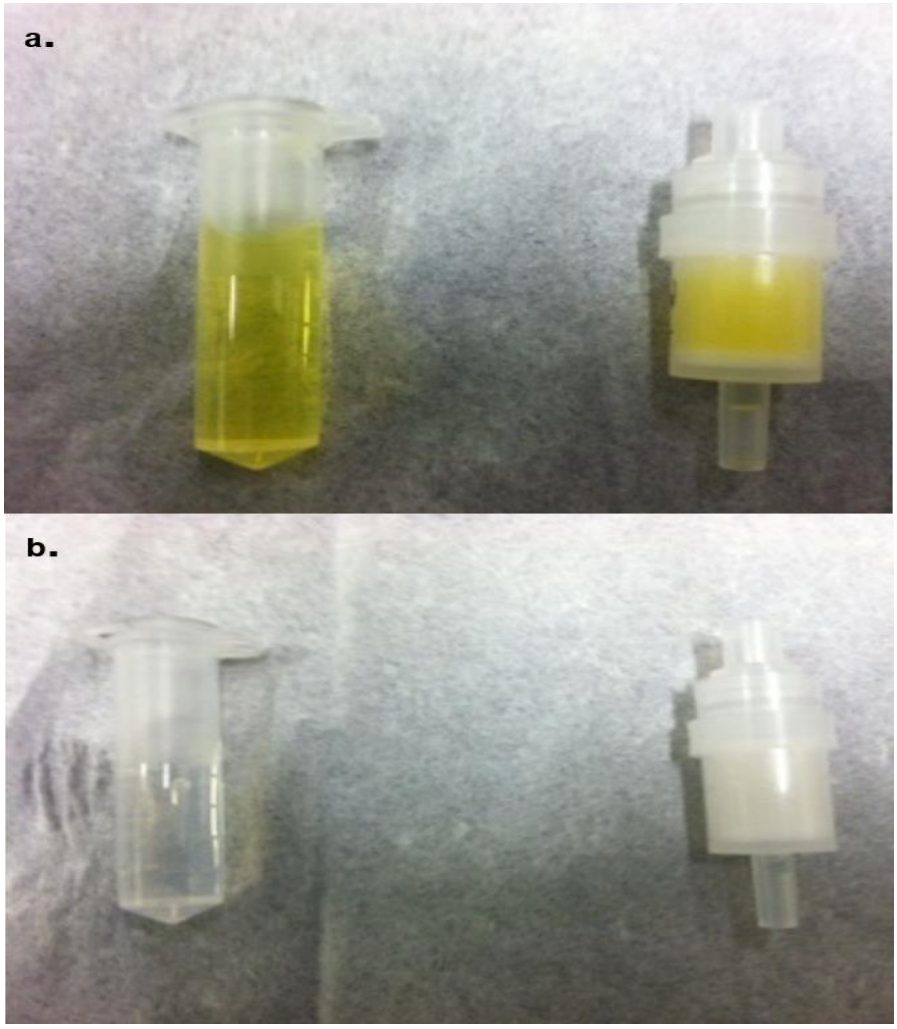

Figure 4.3. Photos taken of biological filtrate tubes (left) and transition metal filters (right) after aliquot extraction during time-course experiments. Shown here are samples from the a. Biotic and b. Heat-killed 2-4' core microcosm sets after one week of incubation.

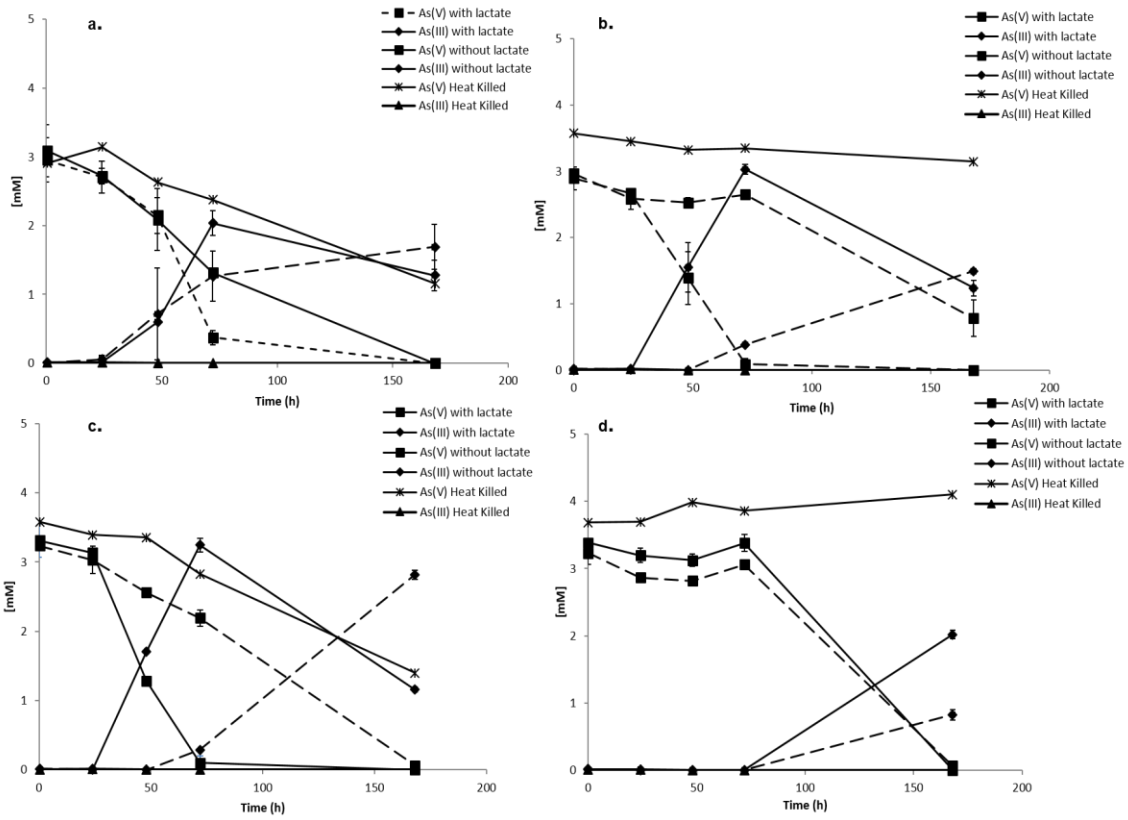

Figure 4.4. Time-course plots of microcosms prepared from core sludge at **a.** 0-2'; **b.** 2-4'; **c.** 4-6' and **d.** 8-10' depths. Data points represent averages of duplicate values and error bars represent ranges of the values.

Considering the extended lag period prior to any As(V) reduction activity that occurred in the 8-10' core microcosms, it isn't possible to obtain accurate and reliable reduction rate calculations, as much activity is unaccounted for between the 3- and 7-day incubation marks. The disappearance of sulfate did not occur in any the microcosm sets or the heat-killed controls, suggesting that sulfate reduction was not utilized as an anaerobic growth mechanism by the bacterial communities cultured (**Figure 4.5**).

iii. Analytical standards

Tables 4.6 and **4.7** and summarize the detection parameters for each standard prepared in basal media and detected via conductivity and UV/Vis, respectively. **Figures 4.6 and 4.7** show the standard curves generated using conductivity and UV/Vis detection, respectively.

E. Discussion

These results demonstrate that bacterial As(V) reduction activity was detected throughout the top 10' of the sediments. This is significant considering the elevated concentrations of other metals and metalloids that might inhibit microbial activity. . Furthermore, As(V) reduction occurred without the addition of exogenous carbon source (e.g., lactate) in the surface sediments (0-2') indicating sufficient autochthonous carbon was present to support this activity.

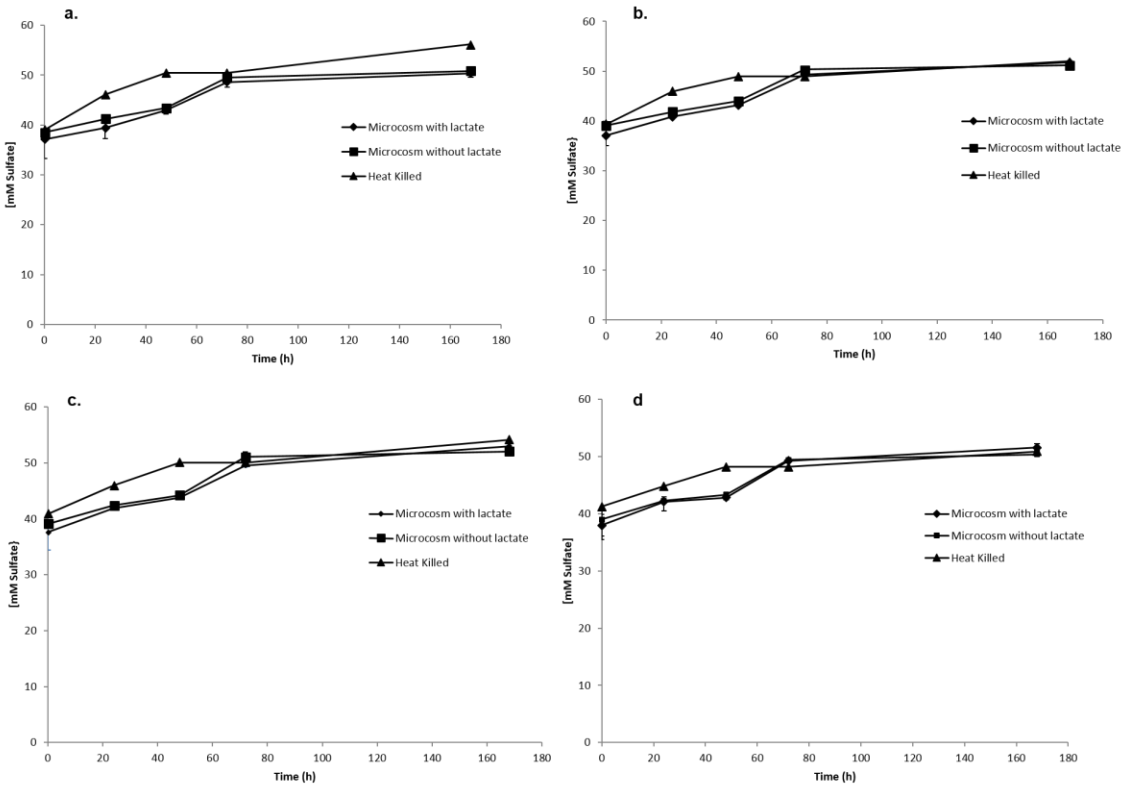

Figure 4.5. Time-course plots of microcosms prepared from core sludge at a. 0-2'; b. 2-4'; c. 4-6' and d. 8-10' depths. Data points represent averages of triplicate values and error bars represent ranges of the values (some error bars are smaller than their data point symbols).

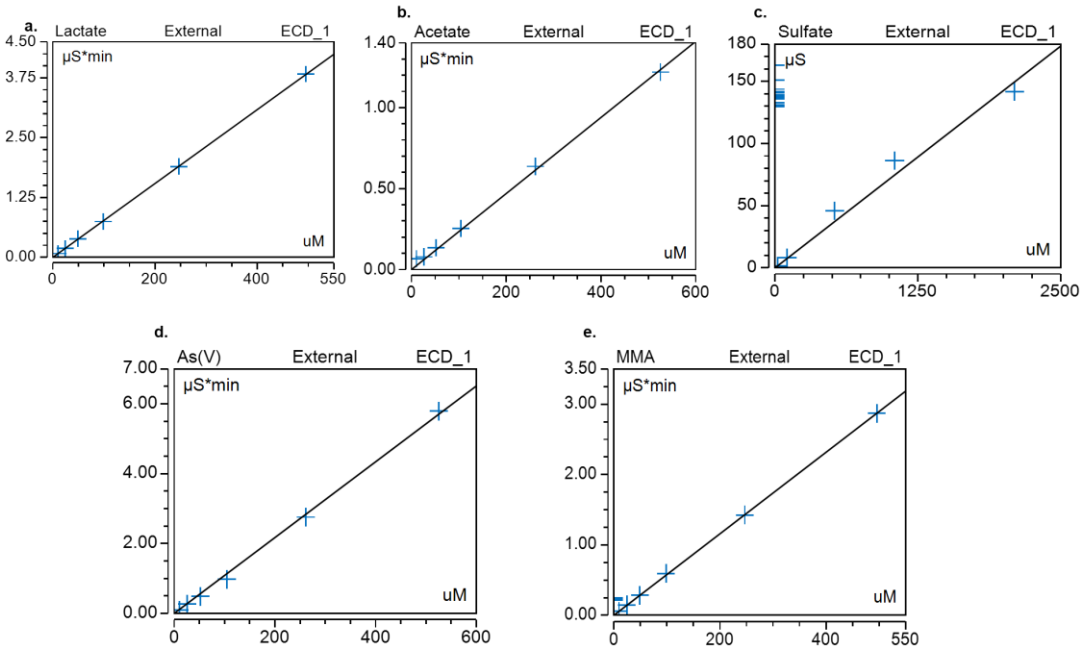

Figure 4.6. Standard curves of: a. Lactate; b. Acetate; c. Sulfate; d. As(V) and e. MMA(V) prepared in basal media and detected with conductivity.

Compound	Optimum UV detection wavelength	Average Retention Time (min.)	UV Detection Limit (DL)
Dimethylarsinic acid (DMA)	200 nm	3.020	~50 µM
Arsenite As(III)	205 nm	3.660	<10 µM
Monomethylarsonic acid (MMA)	200 nm	7.948	~25 µM

Table 4.7. Detection parameters of standards prepared in basal media and detected with the conductivity cell.

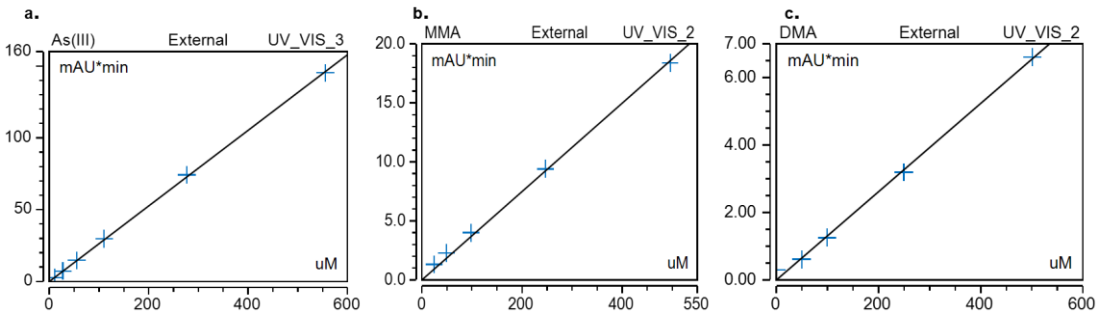

Figure 4.7. Standard curves of: a. As(III); b. MMA(V) and c. DMA(V) prepared in basal media and detected with UV/Vis. UV_VIS_2 is at 200 nm wavelength while UV_VIS_3 is at 205 nm wavelength.

Compound	Optimum UV detection wavelength	Average Retention Time (min.)	UV Detection Limit (DL)
Dimethylarsinic acid (DMA)	200 nm	3.020	~50 µM
Arsenite As(III)	205 nm	3.660	<10 µM
Monomethylarsonic acid (MMA)	200 nm	7.948	~25 µM

Table 4.8. Detection parameters of standards prepared in basal media and detected with UV/Vis.

This was not the case for the sediments from the deeper cores. The rapid As(V) reduction rates also are an indication that respiratory As(V) reduction may be occurring, thus suggesting the presence of DARPs in the sediments. Further biochemical and/or molecular work will need to be carried out to determine whether the bacterial communities present in each sediment microcosm are reducing As(V) via resistance (i.e. ARMs) or respiration (i.e. DARPs).

Although the disappearance of sulfate was not measurable by the methods employed (e.g., ion chromatography), the copious quantities of arsenic trisulfide (as evident by the yellow precipitate) indicate the presence of sulfide in the system. This may preclude the release of As(III) into the groundwater if sufficient quantities of sulfide are available to immobilize the As(III) produced as a result of As(V) reduction.

The lack of growth and activity in the enrichments with As(III) as the electron donor and nitrate as the electron acceptor indicates the probable absence of these organisms in the system. This does not preclude the possibility of heterotrophic (e.g., aerobic) As(III) oxidizing bacteria in the surface sediments. Given the lack of oxygen at depth, however, would preclude the biological oxidation of As(III). Testing additional alternative electron acceptors might be warranted.

Chapter V. *Alkaliphilus oremlandii* sp. strain OhILAs analyses

A. Abstract and Hypotheses

Hypothesis: Arsenic transformation can be demonstrated in pure cultures of *A. oremlandii* sp. OhILAs and *A. ehrlichii* sp. MLHE-1 using the anion exchange chromatography method with dual UV/Vis and conductivity detection. As(V) recovery from roxarsone and As(V) respiration using lactate as the electron donor will be demonstrated in OhILAs using this technique.

In this study, pure cultures of *Alkaliphilus oremlandii* OhILAs, and *Alkalilimnicola ehrlichii* MLHE-1 were cultured in order to demonstrate the broad applications of the anion exchange chromatography method when investigating microbial arsenic transformation. OhILAs, a Firmicute isolated from anoxic sediments of the Ohio River has been shown to liberate inorganic As(V) from the organic compound roxarsone when grown in the presence of lactate, as well as respire As(V) under various conditions [30,92]. Under the media conditions present in this study, OhILAs failed to produce any As(V) or As(III) when grown on roxarsone and lactate. However, As(V) reduction was apparent when lactate was included in the media. Though As(V) reduction did occur, the lack of lactate oxidation and slow kinetics suggest a resistance pathway rather than respiration. The findings here demonstrate the ability of the ICS-1100 system to exhibit both As(V) reduction and As(III) oxidation in anaerobic pure bacterial cultures.

B. Alkaliphilus oremlandii sp. strain OhILAs background

A. oremlandii sp. strain OhILAs (formerly known as *Clostridium* sp. strain OhILAs) is a low G + C gram positive, spore forming, motile, mesophilic bacterium that was isolated from anoxic sediments of the Ohio River (Pittsburgh, PA) [92]. Previous experiments with OhILAs suggested that the strain was capable of dissimilatory As(V) reduction using a variety of organic electron donors including lactate and acetate, with the respiratory As(V) reductase catalytic subunit (ArrA) being detected during biochemical analyses [92]. OhILAs was shown to degrade roxarsone in the presence of lactate when grown in a minimal basal salts medium, yielding inorganic As(V) and 3-amino-4-hydroxybenzene arsenic acid (3A4HBAA) in the process (**Figure 5.1**) [30]. When 1mM roxarsone and 10 mM lactate were amended into the basal salts media, 0.6 mM of 3A4HBAA and 0.3 mM As(V) resulted [30]. Lactate was also oxidized to lactate in the process, suggesting a possible dissimilatory roxarsone respiration mechanism during which lactate is used as the electron donor [30]. The cleavage of As(V) from roxarsone is of environmental significance, as roxarsone is an organoarsenical often added to chicken feed in order to improve growth and pigmentation, promote angiogenesis and prevent microbial pathogen infection (notably coccidiosis) [92]. The improved pigmentation, size and vascularity of the chicken makes the meat more attractive to the consumer, thus leading to greater poultry sales [30]. However, once deposited into the environment in the form of chicken litter, bacterial communities including strains such as OhILAs can lead to the subsurface sediment and contamination of As(V), which as discussed earlier can be transformed to As(III) and mobilized into the groundwater.

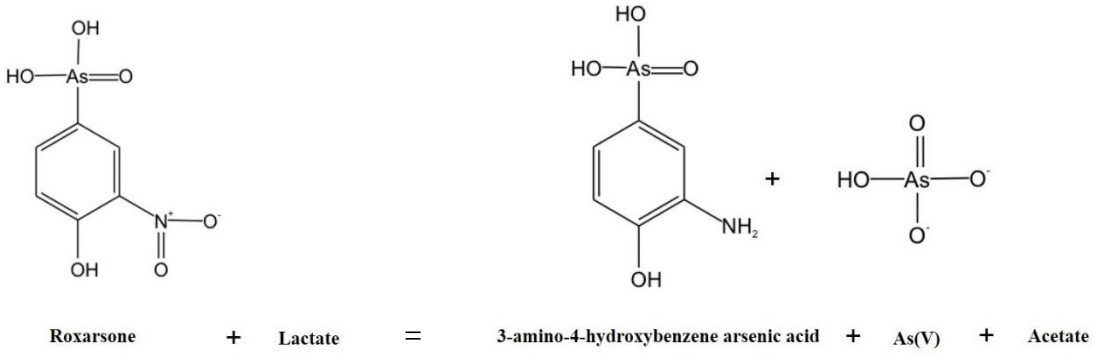

Figure 5.1. Process by which roxarsone is degraded by *A. oremlandii* OhILAs. By an unknown mechanism 3-amino-4-hydroxybenzene arsenic acid and As(V) are liberated from roxarsone when lactate is included in the growth media. Lactate is oxidized to acetate during the process.

Analytical work done during the investigation of roxarsone and As(V) transformation in OhiLAs was previously performed using HPLC, UV/Vis spectrometry and mass spectrometry[30]. However, anion exchange chromatography has never been used for such an experiment involving a pure culture. Therefore, using the anion exchange chromatography method previously described with dual conductivity and UV/Vis detection to examine arsenic transformation in a pure culture (versus the slurries and enrichments previously analyzed) would be novel.

Previous research on OhILAs has suggested that it is capable of respiratory As(V) dissimilatory reduction using a variety of organic electron donors. The electron donors tested and implicated in this process are lactate, acetate, pyruvate, formate, fumarate, glycerol and fructose. No analytical work was carried out to demonstrate respiration is occurring when the electron donors were amended at 20 mM concentrations into media bottles containing 10 mM As(V). Conclusions were drawn that respiration was occurring due to the observation that growth yields were enhanced in each bottle with the addition of As(V) versus just the organic acid alone. If growth yields are improved when a suitable electron acceptor is added it is presumed that respiration is occurring (which generates significantly more ATP than organic acid fermentation, leading to enhanced cell division). Whether or not this presumption can be verified analytically in the case of OhILAs was undetermined. Analyzing OhILAs cultures grown under identical conditions to those previously established will determine if the stoichiometry of As(V) reduction to As(III) and the degradation of the selected organic acid occur in an appropriately balanced fashion, verifying a respiratory growth mechanism.

C. Materials and methods

i. OhILAs media preparations

a. OhILAs basal media

OhILAs basal media was initially prepared with the following components grams per 1000 ml): MgCl2 (0.095), NaHCO3 (4.2), and yeast extract (0.5) [30]. Also included were 2 mL each of 500X trace element and vitamin mixes (see page 80). The pH of the mixture was adjusted to 7.3 by the addition of concentrated HCl and was degassed with N_2 alone [30]. The second round of media of OhILAs basal media was prepared identically to the first, but with Sigma brand yeast extract (for SES-3 and the initial OhILAs media, Fisher brand yeast extract had been used). The third round of OhILAs basal media was prepared identically to the first, but this time with 1 g/l of Bacto Yeast yeast extract with a pH adjustment to 8.0.

b. OhILAs growth media

OhILAs growth media was prepared with the following components [92] (grams per 1000 ml): K_2HPO_4 (0.225), KH_2PO_4 (0.225), NaCl (0.46), NH_4Cl (0.225), $MgCl_2$-$6H_2O$ (0.117), Sigma yeast extract (1), $NaHCO_3$ (4.2), and Na_2S-$7H_20$ (0.1). The solution was adjusted to pH 7.5 with concentrated HCl and degassed under 80:20 N_2:CO_2 [92].

ii. Culture incubations

A stock culture of OhILAs was provided by John Thomas, a Ph.D. student in the Duquesne University Department of Chemistry and Biochemistry.

This stock culture was used as the initial inoculum for all OhILAs pure culture experiments conducted.

Inoculations were performed by transferring one ml of this inoculum anaerobically and aseptically to each of the OhILAs basal media and OhILAs growth media formulations described previously. **Table 5.1** shows the amendments included in the media bottles inoculated. To test for dissimilatory arsenate reduction, lactate was chosen as the electron donor as it is very commonly utilized during such a process. The concentrations ratios of each amendment were consistent with those previously used in literature. However, only 10 mM lactate and 5 mM As(V) were used in the respiration experimental cultures (**Table 5.1**, growth condition 1), as opposed to using 20 mM and 10 mM, respectively (the concentrations used in the published literature [92]). Following inoculations the cultures were incubated at 37°C in the dark without shaking [30]. Growth was monitored by visible macroscopic turbidity and phase-contrast light microscopy. Roxarsone degradation (**Table 5.1**, growth condition 2) was monitored by the disappearance of yellow coloration in the cultures during incubations.

iii. Time-course experiments

Time-course experimentation was carried out using log-phase OhILAs cultures (after ~18 hours of growth) grown on OhILAs growth media under both conditions listed previously after three successive transfers from the original inoculations from stock.

Growth Condition	Electron Donor	Electron Acceptor
1	10 mM lactate	5 mM As(V)
2	10 mM lactate	1 mM Roxarsone

Table 5.1. Growth conditions established for OhILAs incubations. The indicated electron donors and acceptors were amended into 50 ml OhILAs growth media bottles.

This was done to ensure that the stock culture constituents were fully diluted out and growth was stimulated by only the amendments described in both growth conditions. At each time point, 1 ml of culture was taken via sterile syringe for growth analyses while an additional 3 ml was filter sterilized (Fisher Scientific 0.22 um PES) and acidified with 200 µl of 2 M sulfuric acid for analytical work. Growth and analytical aliquots were placed at -80°C until further analyses. Growth analyses were performed by measuring optical density at 600 nm on a Perkin-Elmer Lambda 2 dual-beam spectrophotometer.

iv. Analytical Methods

All analytical work was conducted on the Thermo Scientific/Dionex ICS-1100 system and Chromeleon LE 7.0 software described in chapter II. Standard preparation protocols can be found on page 59 of chapter II. Aliquots taken from cultures grown on 1 mM roxarsone and 10 mM lactate during time-course experiments were diluted only 2-fold in NANOpure water prior to analysis to potentially prevent diluting out low As(V) levels.

v. Molecular Methods

Genomic DNA was extracted using the methods previously described (page 86) from a log-phase OhILAs culture grown under 10 mM lactate and 5 mM As(V).

16S rDNA analysis was performed using the PCR parameters previously described (page 94), with sequencing being performed using the methods previously described (page 105) by Jennifer Rutter, M.S. from the Department of Environmental Sciences, Duquesne University. Sequences were analyzed using BLASTN and GenBANK.

D. Results

i. Culture incubations

The three media formulation of OhILAs basal media described above were incapable of supporting growth of OhILAs on 1 mM roxarsone and 10 mM lactate after the first transfer from stock. The OhILAs growth media described above, which includes a more comprehensive array of inorganic nutrients and a higher concentration of yeast extract (1 g/l), proved to capable of supporting growth after three successive transfers from the stock culture. Macroscopic evidence revealed that the roxarsone, which provides characteristic yellow color to the media upon amendment, was being degraded after 72 hours of incubation, as the media assumed a tannish appearance (**Figure 5.2**). Microscopic analyses of the bacteria grown under both conditions listed in discussed revealed a homogenous culture of rods displaying all of the characteristic morphological features of the OhILAs strain, which verified the purity of both cultures (**Figure 5.3**).

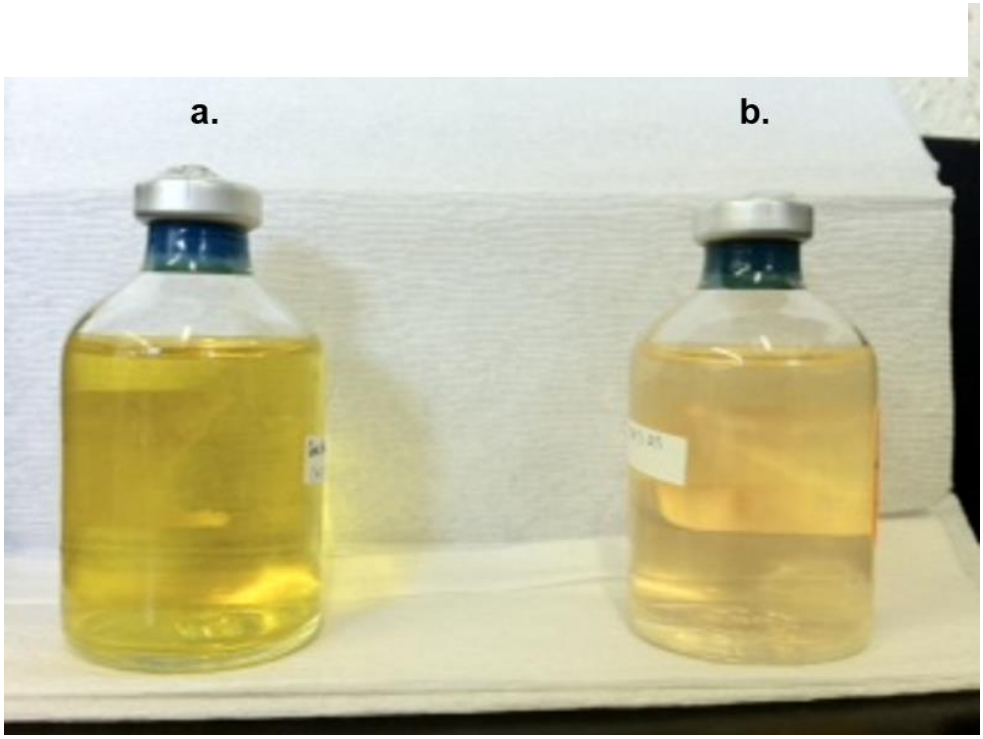

Figure 5.2. Photos of *A. oremlandii* OhILAs culture bottles amended with 1 mM roxarsone and 10 mM lactate at a. 0 hours and b. 72 hours of incubation at 37C in the dark. Roxarsone gives the media bottle a golden coloration. After 72 hours the roxarsone has been degraded, as indicated by the loss of golden coloration.

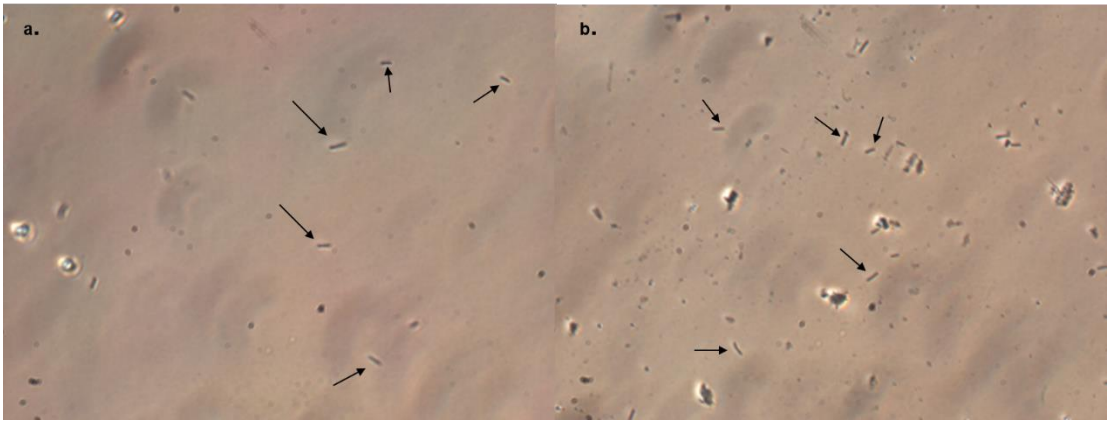

Figure 5.3. Microscopic photos (400x) taken of *A. oremlandii* OhILAs cultures grown on OhILAs growth media with **a.** 5 mM As(V) and 10 mM lactate and **b.** 1 mM roxarsone and 10 mM lactate after 72 hours of incubation.

ii. Time-course experiments

Consistent with the observations previously made of the OhILAs incubations grown on roxarsone and lactate, the yellow coloration initially present in the media bottles gradually disappeared with time during incubation (data not shown). However, while this observation was clearly indicative of roxarsone degradation, no inorganic As(V) was detected during the 2 week incubation period (data not shown), which is contradictory to the previously published data[30]. Consistent with the previously published results, no As(III), MMA or DMA were detected (data not shown)[30]. The cultures grown on lactate and As(V) showed gradual reduction of the latter to As(III) over time but no degradation of lactate (**Figure 5.4 a**). This contradicts previously published data suggesting that, under identical conditions to those present in these experiments, OhILAs undergoes dissimilatory As(V) respiration using lactate as the electron donor. Had this been the case, lactate oxidation to acetate would have occurred. It is possible that respiratory growth did occur during the first few days of incubation, as there appears to be a positive correlation between the rate of As(V) conversion to As(III) and growth (**Figure 5.5**). Between the 12- and 24-hour time points, during which the most rapid growth occurred, As(III) generation was at its most rapid pace, appearing at a rate of 85 μM/h. Throughout the remainder of the incubation period (between 24 and 72 hours) the reduction rate was dwindled five-fold to 17 μM/h. On average, a total of around 3 mM As(V) was reduced after two weeks. Abiotic bottles showed no evidence of As(V) or lactate transformation (**Figure 5.4 b).**

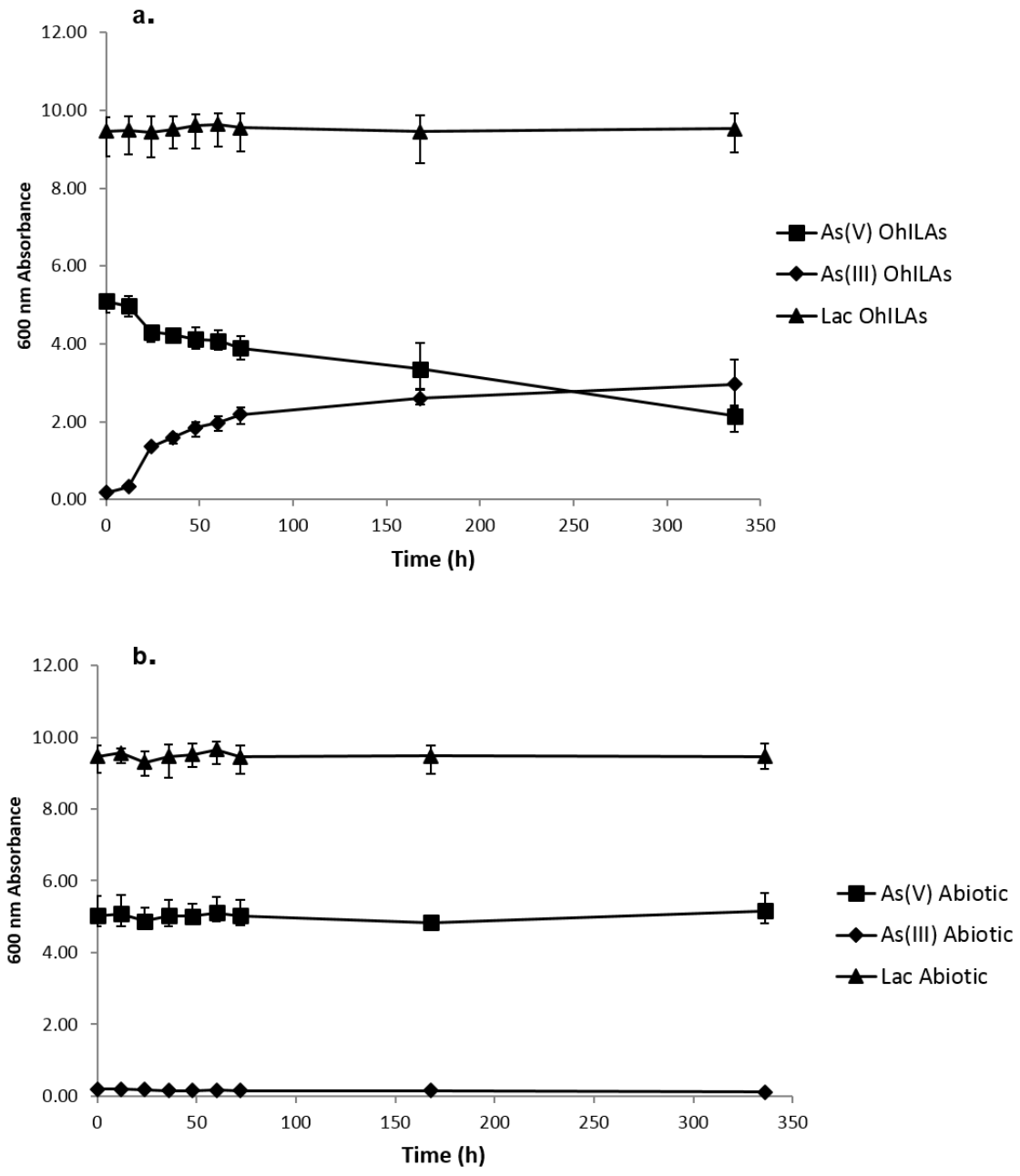

Figure 5.4. Time-course plots of a. *A. oremlandii* OhILAs and b. Uninoculated media amended with 10 mM lactate and 5 mM As(V) incubated 37° C in the dark. Data points and error bars represent averages and ranges of triplicate values, respectively.

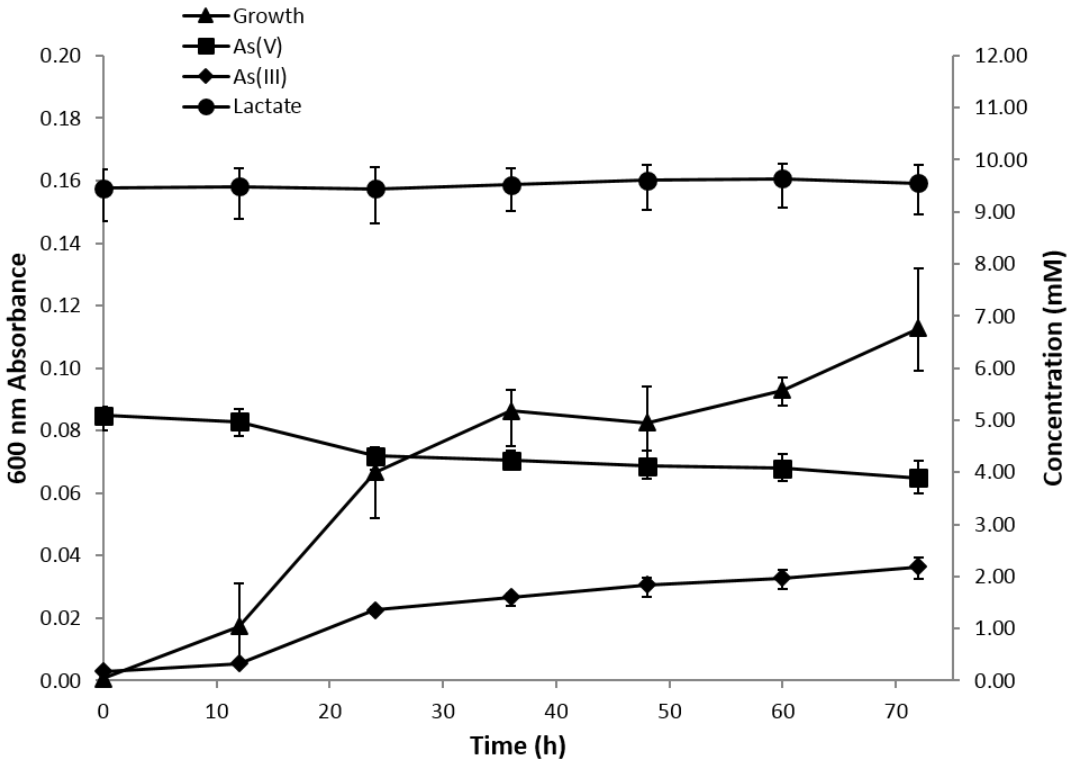

Figure 5.5. Condensed time-course plot of *A. oremlandii* OhILAs grown on 10 mM lactate and 5 mM As(V) incubated at 37° C in the dark. Data points and error bars represent averages and ranges of triplicate values, respectively.

Taking into consideration the elevated concentration of yeast extract included in the growth media used for these experiments (1 g/l), other suitable organic electron donors may have been present at high enough concentrations (acetate, pyruvate, formate, etc.) to serve as electron donor(s) for As(V) respiration early during the incubation period. However, it can be concluded that lactate was not used as an electron donor if any respiratory growth did indeed briefly occur. After 24 hours the reduction kinetics are much more gradual, suggesting that As(V) was reduced in a non-respiratory for resistance after the first day of growth. Provided that OhILAs does indeed have the genes encoding the cytoplasmic non-respiratory As(V) reductase (*arsC*) as well as the periplasmic respiratory As(V) reductase (*arrA*) [92], it is possible that respiratory and non-respiratory mechanisms respectively occurred throughout the 2-week experimental incubation period.

iii. Analytical Standards

Tables 5.2 and **5.3** and show the detection parameters for each standard prepared in OhILAs growth media and detected with conductivity and UV/Vis detection, respectively. **Figure 5.6** and **5.7** show the standard curves generated for each using conductivity and UV/Vis detection, respectively.

E. Discussion

OhILAs was initially grown on 1 mM roxarsone and 10 mM in the OhILAs basal salts media identical to the chemical composition discussed in the previous literature published by Stolz and his associates [30].

Compound	Average Retention Time (min.)	Conductivity Detection Limit (DL)
Lactate	3.84.	<10 µM
Monomethylarsonic acid (MMA)	9.21	~10 µM
Arsenate As(V)	15.61	<10 µM

Table 5.2. Detection parameters of standards prepared in OhILAs growth media and detected with conductivity.

Compound	Optimum UV detection wavelength	Average Retention Time (min.)	UV Detection Limit (DL)
Dimethylarsinic acid (DMA)	200 nm	3.020	~50 µM
Arsenite As(III)	205 nm	3.678	<10 µM

Table 5.3. Detection parameters of standards prepared in OhILAs growth media and detected with conductivity.

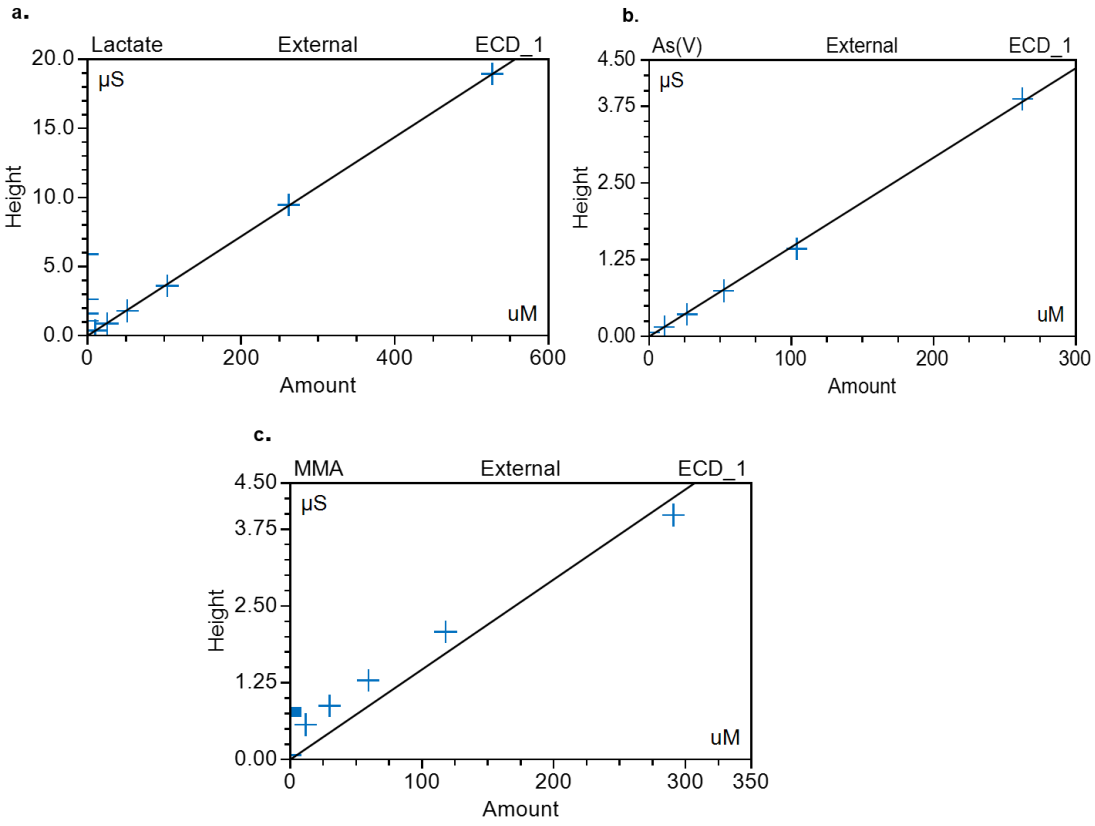

Figure 5.6. Chromeleon LE 7.0 generated standard curves of a. Lactate; b. As(V) and c. MMA prepared in OhILAs growth media and detected with conductivity.

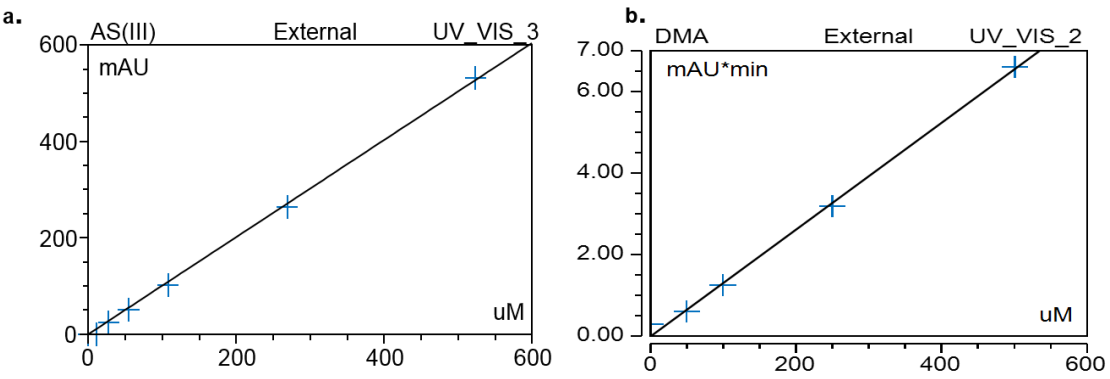

Figure 5.7. Chromeleon LE 7.0 generated standard curves of a. As(III) and b. DMA(V) prepared in OhILAs growth media and detected with UV/Vis. UV_VIS_2 is at 200 nm wavelength while UV_VIS_3 is at 205 nm.

Using the stock solution of pure OhILAs previously mentioned as the inoculum, the strain grew robustly and appeared to completely degrade any available roxarsone after one transfer. However, upon transferring a second time growth was minimal and the yellow coloration persisted. It is hypothesized that the 20 mM fructose used to maintain the strain in the stock culture carried over at a high enough concentration following the initial inoculation to facilitate fermentative growth. Following the second transfer, the strain was incapable of growth on the extremely nutritionally scarce chemical contents included in the OhILAs basal salts media. However, when OhILAs growth media was used, which includes yeast extract to provide nutritional amendments, the culture was capable of sustaining growth and degrading the yellow roxarsone coloration multiple transfers from stock. However, when grown under these conditions there was no indication of inorganic As(V) following incubation, nor was any lactate transformed (data not shown). This is contradictory to the published findings of Stolz et al.[30], as they were able to demonstrate what appears to be respiratory growth using lactate as the electron donor and roxarsone as the electron acceptor, resulting in the liberation of As(V) and the conversion of lactate to acetate. Along with the findings of Stolz et al.[30], Fisher and colleagues[90] published similar results demonstrating that, when grown on OhILAs growth media using the conditions described in the literature, the strain is capable of As(V) respiration using lactate as an electron donor, as well as the conversion of roxarsone to As(V). The growth experiments conducted by Fisher and associates[90] demonstrated that the addition of 10 mM As(V) to 20 mM lactate stimulated growth when compared to a control grown on 20 mM lactate alone, thus respiration was assumed.

However, in these experiments, under identical conditions there was no lactate oxidation and only slightly more than half of the As(V) was reduced to As(III) with kinetics that suggest resistance. It is puzzling that the former experiments involving OhILAs and arsenic transformations are as of yet irreproducible.

Summary and future directions

The specific aims of this dissertation research were to analyze subsurface bacterial communities in anthropogenically contaminated subsurface environments and determine the arsenic transformation capacities of these organisms by developing a novel ion chromatography analytical method. In the former Vineland Chemical Company location in Vineland, NJ, the massive arsenic contamination resulting from industrial production of organoarsenical herbicides appeared to have selected for robust communities of DARPs in the subsurface, notably the aquifer zone, which potentially could have threatened the chemical safeness of the groundwater relied upon for drinking by the surrounding human population. While the EPA has intervened, identifying this location as a Superfund site and investing millions of dollars into its remediation, the bacterial selection phenomenon that occurred here left us with valuable insight into what can occur biogeochemically over time during anthropogenic arsenic contaminations. The results of the CCB disposal site microcosm experiments has demonstrated that the deposition of such waste into the environment can select for arsenic reducing bacteria, many of which potentially being environmentally detrimental DARPs. Provided that organoarsenical herbicides (mainly MSMA) were extensively produced industrially and applied to Floridian golf courses adjacent to waterbodies since the 1950's to treat crab grass, and literature has shown that biogeochemical and geochemical processes have led to the demethylation of the pentavalent methylarsenic to toxic organic and inorganic trivalent species at such locations, it is highly possible that many demethylating and DARPs have been selected for that are potentially hazardous to the environment and human health [32, 141-143].

This is a situation that should be continually monitored by research groups, with groundwater and waterbody arsenic concentrations frequently measured, as arsenic transforming bacteria in the surface and subsurface sediments in these areas may continue to pose a serious threat to the environment and human safety.

During the phase of my research devoted to the development of a reliable analytical method used to quantify arsenic oxyanions and other anions involved in bacterial metabolism, it became clear that common highly sensitive approaches such as HPLC-ICP-MS are not required for such research. While the Thermo Fisher/Dionex ICS-1100 system using conductivity detection alone was only suitable for the quantification of As(V) and MMA(V), the addition of the UV/Vis 4-channel detector provided a two-pronged approach which allowed for the quantification of As(III) and DMA(V). This method can be used to analyze bacterial arsenic transformation in enrichment cultures, microcosms and pure cultures, as indicated by the Vineland, CCB disposal sludge and OhILAs experiments performed. This cost-efficient and effective method for measuring four major arsenic oxyanions as well as a slew of others can be highly useful for research groups in the future. It would be extremely interesting to analyze bacterial communities in surface and subsurface sediments excavated from arsenic contaminated golf courses in Florida using the Thermo-Fisher/Dionex ICS-1100 system with conductivity and UV/Vis detection developed during this research, as the microcosm or enrichment culture approach can be utilized. Furthermore, there is significant potential at these locations for the discovery and isolation of novel species of arsenic transforming bacterial strains (DARPs, CAOs, HAOs, demethylating species, etc.).

References

1. Mandal BK, Suzuki KT. Arsenic round the world: A review. *Talanta*. 2002;58(1):201-235.

2. Oremland RS, Stolz JF. The ecology of arsenic. *Science*. 2003;300(5621):939-944. doi: 10.1126/science.1081903.

3. Oremland RS, Stolz JF. Arsenic, microbes and contaminated aquifers. *Trends Microbiol*. 2005;13(2):45-49. doi: 10.1016/j.tim.2004.12.002.

4. Stolz JF, Oremland RS. Bacterial respiration of arsenic and selenium. *FEMS Microbiol Rev*. 1999;23(5):615-627.

5. Stolz JF, Basu P, Oremland RS. Microbial transformation of elements: The case of arsenic and selenium. *Int Microbiol*. 2002;5(4):201-207. doi: 10.1007/s10123-002-0091-y.

6. Stolz JF, Basu P, Santini JM, Oremland RS. Arsenic and selenium in microbial metabolism. *Annu Rev Microbiol*. 2006;60:107-130. doi: 10.1146/annurev.micro.60.080805.142053.

7. Jomova K, Jenisova Z, Feszterova M, et al. Arsenic: Toxicity, oxidative stress and human disease. *J Appl Toxicol*. 2011;31(2):95-107. doi: 10.1002/jat.1649; 10.1002/jat.1649.

8. Sharma VK, Sohn M. Aquatic arsenic: Toxicity, speciation, transformations, and remediation. *Environ Int*. 2009;35(4):743-759. doi: 10.1016/j.envint.2009.01.005; 10.1016/j.envint.2009.01.005.

9. Sambu S, Wilson R. Arsenic in food and water--a brief history. *Toxicol Ind Health*. 2008;24(4):217-226. doi: 10.1177/0748233708094096; 10.1177/0748233708094096.

10. Frankenberger WT, ed. *Environmental chemistry of arsenic.* New York, NY: CRC Press; 2001.

11. Jaafar J, Irwan Z, Ahamad R, Terabe S, Ikegami T, Tanaka N. Online preconcentration of arsenic compounds by dynamic pH junction-capillary electrophoresis. *J Sep Sci*. 2007;30(3):391-398.

12. Dopp E, Hartmann LM, von Recklinghausen U, et al. Forced uptake of trivalent and pentavalent methylated and inorganic arsenic and its cyto-/genotoxicity in fibroblasts and hepatoma cells. *Toxicol Sci*. 2005;87(1):46-56. doi: 10.1093/toxsci/kfi218.

13. Miller WH, Jr, Schipper HM, Lee JS, Singer J, Waxman S. Mechanisms of action of arsenic trioxide. *Cancer Res*. 2002;62(14):3893-3903.

14. Hughes MF, Beck BD, Chen Y, Lewis AS, Thomas DJ. Arsenic exposure and toxicology: A historical perspective. *Toxicol Sci*. 2011;123(2):305-332. doi: 10.1093/toxsci/kfr184; 10.1093/toxsci/kfr184.

15. Marsh J. Account of a method of separating small quantities of arsenic from substances with which it may be mixed. *Edinburgh New Philosophical Journal*. 1836;21:229-236.

16. Jensen WB. The marsh test for arsenic. *Notes from the Oesper Collections*. May/June 2014;26.

17. Webster SH. The development of the marsh test for arsenic. *J Chem Educ*. 1947;24(10):487.

18. Zernike K. Arsenic case is considered homicide, Maine police say. *New York Times.* 2003 May 2.

19. Waxman S, Anderson KC. History of the development of arsenic derivatives in cancer therapy. *Oncologist*. 2001;6 Suppl 2:3-10.

20. Regelson W, Kim U, Ospina J, Holland JF. Hemangioendothelial sarcoma of liver from chronic arsenic intoxication by fowler's solution. *Cancer*. 1968;21(3):514-522.

21. Cuzick J, Evans S, Gillman M, Price Evans DA. Medicinal arsenic and internal malignancies. *Br J Cancer*. 1982;45(6):904-911.

22. Sommers S.C., Mcmanus R.G. Multiple arsenical cancers of skin and internal organs. *Cancer*. 1953;6(2):347-359.

23. Chan PC, Huff J. Arsenic carcinogenesis in animals and in humans: Mechanistic, experimental, and epidemiological evidence. *Journal of Environmental Science & Health Part C*. 1997;15(2):83-122.

24. Antman KH. Introduction: The history of arsenic trioxide in cancer therapy. *Oncologist*. 2001;6 Suppl 2:1-2.

25. Aronson SM. Arsenic and old myths. *R I Med*. 1994;77(7):233-234.

26. Ravandi F. Arsenic trioxide: Expanding roles for an ancient drug? *Leukemia*. 2004;18(9):1457-1459. doi: 10.1038/sj.leu.2403419.

27. Nickson R, McArthur J, Burgess W, Ahmid KM, Ravenscroft P, Mizanur R. Arsenic poisoning of Bangladesh groundwater. *Nature*. 1998;395:338.

28. Harvey CF, Swartz CH, Badruzzaman AB, et al. Arsenic mobility and groundwater extraction in Bangladesh. *Science*. 2002;298(5598):1602-1606. doi: 10.1126/science.1076978.

29. Akter KF, Owens G, Davey DE, Naidu R. Arsenic speciation and toxicity in biological systems. *Rev Environ Contam Toxicol*. 2005;184:97-149.

30. Stolz JF, Perera E, Kilonzo B, et al. Biotransformation of 3-nitro-4-hydroxybenzene arsonic acid (roxarsone) and release of inorganic arsenic by clostridium species. *Environ Sci Technol*. 2007;41(3):818-823.

31. United States Environmental Protection Agency (EPA) [Internet]; 2015. Available from http://www.epa.gov.

32. Pichler T, Brinkmann R, Scarzella GI. Arsenic abundance and variation in golf course lakes. *Sci Total Environ*. 2008;394(2-3):313-320. doi: 10.1016/j.scitotenv.2008.01.046.

33. Yoshinaga M, Cai Y, Rosen BP. Demethylation of methylarsonic acid by a microbial community. *Environ Microbiol*.. 2011;13(5):1205-1215. doi: 10.1111/j.1462-2920.2010.02420.x; 10.1111/j.1462-2920.2010.02420.x.

34. Vega L, Styblo M, Patterson R, Cullen W, Wang C, Germolec D. Differential effects of trivalent and pentavalent arsenicals on cell proliferation and cytokine secretion in normal human epidermal keratinocytes. *Toxicol Appl Pharmacol*. 2001;172(3):225-232. doi: 10.1006/taap.2001.9152.

35. Hughes MF. Arsenic toxicity and potential mechanisms of action. *Toxicol Lett*. 2002;133(1):1-16. doi: 10.1016/S0378-4274(02)00084-X.

36. Guha Mazumder DN. Chronic arsenic toxicity & human health. *Indian J Med Res*. 2008;128(4):436447.

37. Pimparkar BD, Bhave A. Arsenicosis: Review of recent advances. *J Assoc Physicians India*. 2010;58:617-24, 629.

38. Smedley P, Kinniburgh D. A review of the source, behaviour and distribution of arsenic in natural waters. *Appl Geochem*. 2002;17(5):517-68.

39. Naranmandura H, Carew MW, Xu S, et al. Comparative toxicity of arsenic metabolites in human bladder cancer EJ-1 cells. *Chem Res Toxicol*. 2011;24(9):1586-1596. doi: 10.1021/tx200291p; 10.1021/tx200291p.

40. Crane R., Lipmann F. The effect of arsenate on aerobic phosphorylation. *J Biol Chem*. 1953;201(1):235-243. http://europepmc.org/abstract/MED/13044791.

41. Winski SL. Arsenate toxicity in human erythrocytes: Characterization of morphologic changes and determination of the mechanism of damage. *Journal of Toxicology and Environmental Health, Part A*. 1998;53(5):345-355. doi: 10.1080/009841098159213.

42. Shen ZX, Chen GQ, Ni JH, et al. Use of arsenic trioxide (As2O3) in the treatment of acute promyelocytic leukemia (APL): II. clinical efficacy and pharmacokinetics in relapsed patients. *Blood*. 1997;89(9):3354-3360.

43. Soignet SL, Maslak P, Wang Z, et al. Complete remission after treatment of acute promyelocytic leukemia with arsenic trioxide. *N Engl J Med*. 1998;339(19):1341-1348.

44. Soignet SL, Frankel SR, Douer D, et al. United States multicenter study of arsenic trioxide in relapsed acute promyelocytic leukemia. *J Clin Oncol*. 2001;19(18):3852-3860.

45. Mathews V, George B, Lakshmi KM, et al. Single-agent arsenic trioxide in the treatment of newly diagnosed acute promyelocytic leukemia: Durable remissions with minimal toxicity. *Blood*. 2006;107(7):2627-2632. doi: 10.1182/blood-2005-08-3532.

46. Ghavamzadeh A, Alimoghaddam K, Ghaffari SH, et al. Treatment of acute promyelocytic leukemia with arsenic trioxide without ATRA and/or chemotherapy. *Ann Oncol*. 2006;17(1):131-134. doi: 10.1093/annonc/mdj019.

47. Styblo M, Serves SV, Cullen WR, Thomas DJ. Comparative inhibition of yeast glutathione reductase by arsenicals and arsenothiols. *Chem Res Toxicol*. 1997;10(1):27-33. doi: 10.1021/tx960139g.

48. Lin S, Cullen WR, Thomas DJ. Methylarsenicals and arsinothiols are potent inhibitors of mouse liver thioredoxin reductase. *Chem Res Toxicol*. 1999;12(10):924-930.

49. Petrick JS, Ayala-Fierro F, Cullen WR, Carter DE, Vasken Aposhian H. Monomethylarsonous acid (MMAIII) is more toxic than arsenite in chang human hepatocytes. *Toxicol Appl Pharmacol*. 2000;163(2):203-207. doi: http://dx.doi.org/10.1006/taap.1999.8872.

50. Petrick JS, Jagadish B, Mash EA, Aposhian HV. Monomethylarsonous acid (MMAIII) and arsenite: LD50 in hamsters and in vitro inhibition of pyruvate dehydrogenase. *Chem Res Toxicol*. 2001;14(6):651-656. doi: 10.1021/tx000264z.

51. Qin J, Rosen BP, Zhang Y, Wang G, Franke S, Rensing C. Arsenic detoxification and evolution of trimethylarsine gas by a microbial arsenite S-adenosylmethionine methyltransferase. *Proc Natl Acad Sci U S A*. 2006;103(7):2075-2080. doi: 10.1073/pnas.0506836103.

52. Bentley R, Chasteen TG. Microbial methylation of metalloids: Arsenic, antimony, and bismuth. *Microbiol Mol Biol Rev*. 2002;66(2):250-271.

53. Challenger F. Biological methylation. *Chem Rev*. 1945;36(3):315-361. doi: 10.1021/cr60115a003.

54. Paez-Espino D, Tamames J, de Lorenzo V, Canovas D. Microbial responses to environmental arsenic. *Biometals*. 2009;22(1):117-130. doi: 10.1007/s10534-008-9195-y.

55. Challenger F. Biological methylation. *Adv Enzymol Relat Subj Biochem*. 1951;12:429-491.

56. Buchet J, Lauwerys R. Study of inorganic arsenic methylation by rat liver in vitro: Relevance for the interpretation of observations in man. *Arch Toxicol*. 1985;57(2):125-129.

57. Clemens R, Tree HG, Ewing PL, Emerson GA. Conversion by tissues of inorganic arsenicals to forms not recoverable by the usual assay methods. *Tex Rep Biol Med*. 1951;9(1):27-33.

58. Braman RS, Foreback CC. Methylated forms of arsenic in the environment. *Science*. 1973 [accessed 2014 Jul 25];182(4118):1247-1249.

59. Ye J, Rensing C, Rosen BP, Zhu Y-. Arsenic biomethylation by photosynthetic organisms. *Trends Plant Sci*. 2012;17(3):155-162. Accessed 3 July 2014.

60. Hasegawa H, Sohrin Y, Seki K, et al. Biosynthesis and release of methylarsenic compounds during the growth of freshwater algae. *Chemosphere*. 2001;43(3):265-272. Accessed 3 July 2014.

61. Vahter M. Mechanisms of arsenic biotransformation. *Toxicology*. 2002;181:211-217.

62. Vahter M. Methylation of inorganic arsenic in different mammalian species and population groups. *Sci Prog*. 1999;82 (Pt 1):69-88.

63. Yuan C, Lu X, Qin J, Rosen BP, Le XC. Volatile arsenic species released from escherichia coli expressing the AsIII S-adenosylmethionine methyltransferase gene. *Environ Sci Technol*. 2008;42(9):3201-3206.

64. Rosen BP, Tamas MJ. Arsenic transport in prokaryotes and eukaryotic microbes. *Adv Exp Med Biol*. 2010;679:47-55.

65. Mukhopadhyay R, Rosen BP, Phung LT, Silver S. Microbial arsenic: From geocycles to genes and enzymes. *FEMS Microbiol Rev*. 2002;26(3):311-325.

66. Achour AR, Bauda P, Billard P. Diversity of arsenite transporter genes from arsenic-resistant soil bacteria. *Res Microbiol*. 2007;158(2):128-137. doi: 10.1016/j.resmic.2006.11.006.

67. Xu C, Shi W, Rosen BP. The chromosomal arsR gene of escherichia coli encodes a trans-acting metalloregulatory protein. *J Biol Chem*. 1996;271(5):2427-2432.

68. Chen Y, Rosen BP. Metalloregulatory properties of the ArsD repressor. *J Biol Chem*. 1997;272(22):14257-14262.

69. Santini JM, Sly LI, Schnagl RD, Macy JM. A new chemolithoautotrophic arsenite-oxidizing bacterium isolated from a gold mine: Phylogenetic, physiological, and preliminary biochemical studies. *Appl Environ Microbiol*. 2000;66(1):92-97.

70. Oremland RS, Hoeft SE, Santini JM, Bano N, Hollibaugh RA, Hollibaugh JT. Anaerobic oxidation of arsenite in mono lake water and by a facultative, arsenite-oxidizing chemoautotroph, strain MLHE-1. *Appl Environ Microbiol*. 2002;68(10):4795-4802.

71. Zargar K, Hoeft S, Oremland R, Saltikov CW. Identification of a novel arsenite oxidase gene, arxA, in the haloalkaliphilic, arsenite-oxidizing bacterium alkalilimnicola ehrlichii strain MLHE-1. *J Bacteriol*. 2010;192(14):3755-3762. doi: 10.1128/JB.00244-10.

72. Zargar K. *Molecular genetics and physiology of arsenic transforming bacteria.* [Ph.D.]. University of California, Santa Cruz; 2010.

73. Richey C, Chovanec P, Hoeft SE, Oremland RS, Basu P, Stolz JF. Respiratory arsenate reductase as a bidirectional enzyme. *Biochem Biophys Res Commun*. 2009;382(2):298-302. doi: 10.1016/j.bbrc.2009.03.045.

74. Von Endt D,W., Kearney P,C., Kaufman D,D. Degradation of monosodium methanearsonic acid by soil microorganisms. *J. Agric. Food Chem*. 1968;(16):17–20.

75. Maki ,Teruya, Takeda ,Noriko, Hasegawa ,Hiroshi, Ueda ,Kazumasa. Isolation of monomethylarsonic acid-mineralizing bacteria from arsenic contaminated soils of Ohkunoshima Island. *Applied Organometallic Chemistry*. 2006a;(20):538-544.

76. Maki T, Hasegawa H, Watarai H, Ueda K. Classification for dimethylarsenate-decomposing bacteria using a restrict fragment length polymorphism analysis of 16S rRNA genes. *Anal Sci*. 2004;20(1):61-68.

77. Lehr CR, Polischuk E, Radoja U, Cullen WR. Demethylation of methylarsenic species by *mycobacterium neoaurum*. *Applied Organometallic Chemistry*. 2003;(17):831-834.

78. Sierra-Alvarez R, Yenal U, Field JA, Kopplin M, Gandolfi AJ, Garbarino JR. Anaerobic biotransformation of organo-arsenical pesticides monomethylarsonic acid and dimethylarsinic acid. *J Agric Food Chem*. 2006;54(11):3959-3966. doi: 10.1021/jf053223n.

79. Ammann AA. Arsenic speciation analysis by ion chromatography -- A critical review of principles and applications. *American Journal of Analytical Chemistry*. 2011;(2):27-45.

80. Chatterjee A. Determination of total cationic and total anionic arsenic species in oyster tissue using microwave-assisted extraction followed by HPLC-ICP-MS. *Talanta*. 2000;51(2):303-314.

81. Narukawa T, Inagaki K, Kuroiwa T, Chiba K. The extraction and speciation of arsenic in rice flour by HPLC-ICP-MS. *Talanta*. 2008;77(1):427-432. doi: 10.1016/j.talanta.2008.07.005.

82. Suzuki Y, Shimoda Y, Endo Y, Hata A, Yamanaka K, Endo G. Rapid and effective speciation analysis of arsenic compounds in human urine using anion-exchange columns in HPLC-ICP-MS. *J Occup Health*. 2009;51(4):380-385.

83. Komorowicz I, Baralkiewicz D. Arsenic and its speciation in water samples by high performance liquid chromatography inductively coupled plasma mass spectrometry-last decade review. *Talanta*. 2011;84(2):247-261. doi: 10.1016/j.talanta.2010.10.065.

84. Williams R,J. Determination of inorganic anions by ion chromatography with ultraviolet absorbance detection. *Anal Chem*. 1983;(55):851-854.

85. Larsen EH, Hansen SH. Separation of arsenic species by ion-pair and ion exchange high performance liquid chromatography. *Mikrochim Acta*. 1992;(109):47-51.

86. Laverman AM, Blum JS, Schaefer JK, Phillips E, Lovley DR, Oremland RS. Growth of strain SES-3 with arsenate and other diverse electron acceptors. *Appl Environ Microbiol*. 1995;61(10):3556-3561.

87. Macy JM, Santini JM, Pauling BV, O'Neill AH, Sly LI. Two new arsenate/sulfate-reducing bacteria: Mechanisms of arsenate reduction. *Arch Microbiol*. 2000;173(1):49-57.

88. Hoeft SE, Kulp TR, Stolz JF, Hollibaugh JT, Oremland RS. Dissimilatory arsenate reduction with sulfide as electron donor: Experiments with mono lake water and isolation of strain MLMS-1, a chemoautotrophic arsenate respirer. *Appl Environ Microbiol*. 2004;70(5):2741-2747.

89. Cummings DE, Caccavo , Frank, Fendorf S, Rosenzweig RF. Arsenic mobilization by the dissimilatory fe(III)-reducing bacterium shewanella alga BrY. *Environ Sci Technol*. 1999;33(5):723-729. doi: 10.1021/es980541c.

90. Zobrist J, Dowdle PR, Davis JA, Oremland RS. Mobilization of arsenite by dissimilatory reduction of adsorbed arsenate. *Environ Sci Technol*. 2000;34(22):4747-4753. doi: 10.1021/es001068h.

91. Oremland RS, Blum JS, Culbertson CW, et al. Isolation, growth, and metabolism of an obligately anaerobic, selenate-respiring bacterium, strain SES-3. *Appl Environ Microbiol*. 1994;60(8):3011-3019.

92. Fisher E, Dawson AM, et al. Transformation of inorganic and organic arsenic by alkaliphilus oremlandii sp. nov. strain OhILAs. *Ann N Y Acad Sci*. 2008;1125:230-241. doi: 10.1196/annals.1419.006.

93. Gurtler V, Stanisich VA. New approaches to typing and identification of bacteria using the 16S-23S rDNA spacer region. *Microbiology*. 1996;142 (Pt 1):3-16.

94. Borneman J, Triplett EW. Molecular microbial diversity in soils from eastern amazonia: Evidence for unusual microorganisms and microbial population shifts associated with deforestation. *Appl Environ Microbiol*. 1997;63(7):2647-2653.

95. Ranjard L, Brothier E, Nazaret S. Sequencing bands of ribosomal intergenic spacer analysis fingerprints for characterization and microscale distribution of soil bacterium populations responding to mercury spiking. *Appl Environ Microbiol*. 2000;66(12):5334-5339.

96. Ranjard L, Poly F, Combrisson J, et al. Heterogeneous cell density and genetic structure of bacterial pools associated with various soil microenvironments as determined by enumeration and DNA fingerprinting approach (RISA). *Microb Ecol*. 2000;39(4):263-272.

97. Cardinale M, Brusetti L, Quatrini P, et al. Comparison of different primer sets for use in automated ribosomal intergenic spacer analysis of complex bacterial communities. *Appl Environ Microbiol*. 2004;70(10):6147-6156. doi: 10.1128/AEM.70.10.6147-6156.2004.

98. Wilson KH, Blitchington RB, Greene RC. Amplification of bacterial 16S ribosomal DNA with polymerase chain reaction. *J Clin Microbiol*. 1990;28(9):1942-1946.

99. Baesman SM, Stolz JF, Kulp TR, Oremland RS. Enrichment and isolation of bacillus beveridgei sp. nov., a facultative anaerobic haloalkaliphile from mono lake, california, that respires oxyanions of tellurium, selenium, and arsenic. *Extremophiles*. 2009;13(4):695-705. doi: 10.1007/s00792-009-0257-z.

100. Anderson CR, Cook GM. Isolation and characterization of arsenate-reducing bacteria from arsenic-contaminated sites in New Zealand. *Curr Microbiol*. 2004;48(5):341-347. doi: 10.1007/s00284-003-4205-3.

101. Lear G, Song B, Gault AG, Polya DA, Lloyd JR. Molecular analysis of arsenate-reducing bacteria within cambodian sediments following amendment with acetate. *Appl Environ Microbiol*. 2007;73(4):1041-1048. doi: 10.1128/AEM.01654-06.

102. Song B, Chyun E, Jaffe PR, Ward BB. Molecular methods to detect and monitor dissimilatory arsenate-respiring bacteria (DARB) in sediments. *FEMS Microbiol Ecol*. 2009;68(1):108-117. doi: 10.1111/j.1574-6941.2009.00657.x.

103. Baker GC, Smith JJ, Cowan DA. Review and re-analysis of domain-specific 16S primers. *J Microbiol Methods*. 2003;55(3):541-555.

104. Galkiewicz JP, Kellogg CA. Cross-kingdom amplification using bacteria-specific primers: Complications for studies of coral microbial ecology. *Appl Environ Microbiol*. 2008;74(24):7828-7831. doi: 10.1128/AEM.01303-08.

105. Malasarn D, Saltikov CW, Campbell KM, Santini JM, Hering JG, Newman DK. arrA is a reliable marker for as(V) respiration. *Science*. 2004;306(5695):455. doi: 10.1126/science.1102374.

106. Kulp TR, Hoeft SE, Miller LG, et al. Dissimilatory arsenate and sulfate reduction in sediments of two hypersaline, arsenic-rich soda lakes: Mono and searles lakes, california. *Appl Environ Microbiol*. 2006;72(10):6514-6526. doi: 10.1128/AEM.01066-06.

107. Sun Y, Polishchuk EA, Radoja U, Cullen WR. Identification and quantification of arsC genes in environmental samples by using real-time PCR. *J Microbiol Methods*. 2004;58(3):335-349. doi: 10.1016/j.mimet.2004.04.015.

108. Bansal R. *Denaturing gradient gel electrophoresis (DGGE) analysis of microbial diversity in environments impacted with inorganic or organic arsenic.* [dissertation]. [Pittsburgh (PA)]: Duquesne University; 2007.

109. Saltikov CW, Olson BH. Homology of escherichia coli R773 arsA, arsB, and arsC genes in arsenic-resistant bacteria isolated from raw sewage and arsenic-enriched creek waters. *Appl Environ Microbiol*. 2002;68(1):280-288.

110. Newman DK, Beveridge TJ, Morel F. Precipitation of arsenic trisulfide by desulfotomaculum auripigmentum. *Appl Environ Microbiol*. 1997;63(5):2022-2028.

111. Coal combustion residuals. U.S. Environmental Protection Agency; 2015 [accessed 2014 Jul 29]. http://www.epa.gov/solidwaste/nonhaz/industrial/special/fossil/coalashletter.htm

112. Coal combustion byproducts. USGS Mineral Information; 1999 [accessed 2014 Jul 29]. http://minerals.usgs.gov/minerals/pubs/commodity/coal/874499.pdf

113. Sajwan K, Punshon T, Seaman J. Production of coal combustion products and their potential uses. In: *Coal combustion byproducts and environmental issues.* Springer; 2006:3-9.

114. Beneficial use of CCRs. U.S. Environmental Protection Agency; 2014 [accessed 2014 Jul 29] http://www.epa.gov/epawaste/conserve/imr/ccps/benfuse.htm.

115. Yeboah NNN, Shearer CR, Burns SE, Kurtis KE. Characterization of biomass and high carbon content coal ash for productive reuse applications. *Fuel*. 2014;116:438-447.

116. Tishmack JK, Burns PE. The chemistry and mineralogy of coal and coal combustion products. *Energy, waste and the environmental: a geochemical perspective.geological society*. 2004;236:223-246.

117. Goodwin RW. *Combustion ash residue management: An engineering perspective.* New Jersey: Noyes Publications; 2013.

118. Korcak R. Agricultural uses of coal combustion byproducts. *Agricultural uses of municipal, animal, and industrial byproducts. USDA-ARS, Conservation Res.Rep*. 1998(44):103-119.

119. Clean air act requirements and history. U.S. Environmental Protection Agency; 2013 [Accessed 2014 Aug 7]. http://www.epa.gov/air/caa/requirements.html.

120. Wilczynska-Michalik W, Moryl R, Sobczyk J, Michalik M. Composition of coal combustion by-products: The importance of combustion technology. *Fuel Process Technol*. 2014;124:35-43.

121. Nayak AK, Raja R, Rao KS, et al. Effect of fly ash application on soil microbial response and heavy metal accumulation in soil and rice plant. *Ecotoxicol Environ Saf*. 2014;114:257-262.

122. National primary drinking water regulations. U.S. Environmental Protection Agency; 2009 [Accessed 2014 Aug 13]. http://water.epa.gov/drink/contaminants/upload/mcl-2.pdf.

123. Lemly AD. An urgent need for an EPA standard for disposal of coal ash. *Environmental Pollution*. 2014,191:253-255. doi:10.1016/j.envpol.2014.04.029.

124. Ahmaruzzaman M. A review on the utilization of fly ash. *Progress in Energy and Combustion Science*. 2010;36(3):327-363. Accessed 1 August 2014.

125. Clark R, Ritchey K, Baligar V. Benefits and constraints for use of FGD products on agricultural land. *Fuel*. 2001;80:821-828.

129. Caccavo F, Blakemore RP, Lovley DR. A hydrogen-oxidizing, fe(III)-reducing microorganism from the great bay estuary, new hampshire. *Appl Environ Microbiol*. 1992;58(10):3211-3216.

130. Langner HW, Inskeep WP. Microbial reduction of arsenate in the presence of ferrihydrite. *Environ Sci Technol*. 2000;34(15):3131-3136. doi: 10.1021/es991414z.

131. Ahmann D, Krumholz LR, Hemond HF, Lovley DR, Morel FMM. Microbial mobilization of arsenic from sediments of the aberjona watershed. *Environ Sci Technol*. 1997;31(10):2923-2930. doi: 10.1021/es970124k.

132. Polizzotto ML, Harvey CF, Sutton SR, Fendorf S. Processes conducive to the release and transport of arsenic into aquifers of bangladesh. *Proc Natl Acad Sci U S A*. 2005;102(52):18819-18823. doi: 10.1073/pnas.0509539103.

133. Jeanmougin F, Thompson JD, Gouy M, Higgins DG, Gibson TJ. Multiple sequence alignment with clustal X. *Trends Biochem Sci*. 1998;23(10):403-405.

134. Wilgenbusch JC, Swofford D. Inferring evolutionary trees with PAUP*. *Curr Protoc Bioinformatics*. 2003;Chapter 6:Unit 6.4. doi: 10.1002/0471250953.bi0604s00.

135. Inskeep WP, Macur RE, Hamamura N, Warelow TP, Ward SA, Santini JM. Detection, diversity and expression of aerobic bacterial arsenite oxidase genes. *Environ Microbiol*. 2007;9(4):934-943. doi: 10.1111/j.1462-2920.2006.01215.x.

136. Rhine ED, Ni Chadhain SM, Zylstra GJ, Young LY. The arsenite oxidase genes (aroAB) in novel chemoautotrophic arsenite oxidizers. *Biochem Biophys Res Commun*. 2007;354(3):662-667. doi: 10.1016/j.bbrc.2007.01.004.

137. Quemeneur M, Heinrich-Salmeron A, Muller D, et al. Diversity surveys and evolutionary relationships of aoxB genes in aerobic arsenite-oxidizing bacteria. *Appl Environ Microbiol*. 2008;74(14):4567-4573. doi: 10.1128/AEM.02851-07.

138. Hamamura N, Macur RE, Korf S, et al. Linking microbial oxidation of arsenic with detection and phylogenetic analysis of arsenite oxidase genes in diverse geothermal environments. *Environ Microbiol*. 2009;11(2):421-431. doi: 10.1111/j.1462-2920.2008.01781.x.

139. Mailloux BJ, Alexandrova E, Keimowitz AR, Wovkulich K, Freyer GA, Herron M, et al. Microbial mineral weathering for nutrient acquisition releases arsenic. Applied and Environmental Microbiology. 2009;75(8):2558-65.

140. Whitmore TJ, Riedinger-Whitmore MA, Smoak JM, Kolasa KV, Goddard EA, Bindler R. Arsenic contamination of lake sediments in Florida: evidence of herbicide mobility from watershed soils. *J Paleolimnol*. 2008;40(3):869-84.

141. Cai Y, Cabrera JC, Georgiadis M, Jayachandran K. Assessment of arsenic mobility in the soils of some golf courses in South Florida. Sci Total Environ. 2002;291(1):123-34.

142. Feng M, Schrlau JE, Snyder R, Snyder GH, Chen M, Cisar JL, et al. Arsenic transport and transformation associated with MSMA application on a golf course green. *J Agric Food Chem*. 2005;53(9):3556-62.

143. Di Carlo G, Fuentes H. Potential Transport of the Herbicide MSMA and Arsenate (+5) from Golf Courses to Groundwater in Southeastern Florida. WEFTEC 2000; Proceedings of the Water Environment Federation; 2000. 648-75. http://dx.doi.org/10.2175/193864700784608595

Appendix A: Spreadsheet showing CCB disposal lake element concentrations. Recorded ppm values were converted to M and mM concentrations.

Average pH (45 feet)	**9.7325**						
Average Temperature C	**11.35**						
Average ORP (mV)	**-195.75**						
Average Conductivity	**6343.583333**						
Average COD (ppm)	157.5						
Average Alkalinity (CaCO3 ppm)	**90.75**						
Average Alkalinity (HCO3 ppm)	27.66666667						
Average Alkalinity (CO3 ppm)	25.25						
Average TDS (ppm)	6775						
Average TSS (ppm)	115.91	**salinity (ppt) = 0.0018066 • Cl– (mg/L)**					
Salinity (ppt)	0.7994205						
Bold is actual 45 ft. averages							
Italic is elevated values of interest							
	Average ppm						
Oxygen (O2)	**2.523333333**						
Ammonia (NH3)	0.89						
Nitrite (NO2)	0.375						
Nitrate (NO3)	0.375						
Nitrogen (N2)	5						
Phosphate (PO4)	1.9						
Phosphorus (P)	0.1						
Sulfate (SO4)	*3600*						
Sulfide (S)	76						
Calcium (Ca)	*575*				**Bicarbonate atomic mass**	61.0168	**mM**
Magnesium (Mg)	14			**set pH to 9.70**	level: 27.7 mg/l		
Sodium (Na)	*1625*						0.454
Potassium (K)	81		**Chloride atomic mass**		**Mg atomic mass**	24.305	
Chloride (Cl)	*442.5*		35.45				
Arsenic (As)	***0.041366667***		level: 442.5 mg/L (ppm)		level: 14 mg/l		0.576
Barium (Ba)	0.1125						
Berilum (Be)	0.3		0.012844702	**M Cl**	**Potassium atomic mass**	39.098	
Boron (B)	6.175		12.84470247	**mM Cl**			
Cadmium (Cd)	0.3				level: 81 mg/l		2.072
Chromium (Cr)	0.00295		**NaCl molar mass**				
Copper (Cu)	0.00775		58.44		**Sulfide atomic mass**	32.06	
Iron (Fe)	<0.25		0.750644412	**g in 12.8 mM NaCl**			
Lead (Pb)	0.003		**SO4 molar mass**		level: 76 mg/l		2.371
Manganese (Mn)	0.14675		96.06				
Tellurium (Tl)	0.003		level: 3600 ppm (3.6 g/L)		**Sodium atomic mass**	22.9	
Nickle (Ni)	0.0041						
Silver (Ag)	0.003		0.037476577	**M SO4**	level: 1625 mg/l		70.961
Strontium (Sr)	1.65		37.47657714	**mM SO4**			
Valine (V)	0.01675		Ammonium Sulfate (NH4)2SO4	132.14	**Phosphate atomic mass**	94.9714	
Zinc (Zn)	0.015		Magnesium sulfate (MgSO47H20)	246.47			
Antimony (Sb)	0.006		Sodium Sulfate (Na2SO4)	142.04	level: 1.9 mg/l		0.020
Aluminum (Al)	0.09						
Silicon (Si)	*4000*		0.00170274	**M Am Sulfate SES3**	**Ammonia atomic mass**	17.031	
Selenium (Se)	0.1225		1.702739519	**mM Am Sulfate SES3**			
Bromine (Br)	2.85		0.00091289	**M Mag Sulfate SES3**	level: 0.89 mg/l		0.052
Mercury (Hg)	0.0002		0.912890007	**mM Mag Sulfate SES3**			
Methane	<5		2.615629526	**mM Sulfate SES3**			
				Need to add this	**with sodium sulfate**		
				34.85437047	mM		
			4.950714782	**g sodium sulfate**			
			As molar mass				
			74.922				
			5.5213E-07	**M As**			
			0.00055213	**mM As**			
			0.552129771	**uM As**			
			0.00031366	**M As in Sed**			
			0.313659539	**mM As in Sed**			
			313.6595393	**uM As in Sed**			

Appendix B: Spreadsheet showing the formulation of both basal media types using average element concentrations found in the CCB disposal lake.

Basal media (- SO_4^-)	**g * L^{-1}**		**Basal media (+ SO_4^-)**	**g * L^{-1}**							
Pottasium Phosphate (monobasic)	0.225		Pottasium Phosphate (monobasic)	0.225							
Potassium Phosphate (dibasic)	0.225		Potassium Phosphate (dibasic)	0.225							
Sodium Chloride	0.44		Sodium Chloride	0.44							
Ammonium Chloride	0.225		Ammonium Chloride	0.225							
Magnesium Chloride	0.225		Magnesium Chloride	0.225							
Sodium Bicarbonate	0.038		Sodium Bicarbonate	0.038							
Sodium Sulfide	0.569		Sodium Sulfide	0.569							
Yeast Extract	0.5		Sodium Sulfate	5.323							
			Yeast Extract	0.5							
2 mL of 500 X Vitamin Mix											
2 mL of 500 X Trace Elements											
adjust pH to 9.70 with NaOH											
	molar mass	**mM Cl**	g	**mM Na**	**mM Mg**	**mM NH_3**	**mM PO_4**	**mM S**	**mM K**	**mM bicarb**	**mM SO_4**
Sodium Chloride (NaCl)	58.440	7.527	0.440	7.529							
Ammonium Chloride (NH_4Cl)	53.490	4.206	0.225			4.206					
Magnesium Chloride ($MgCl_2.6H_2O$)	203.310	1.107	0.225		1.107						
Sodium Bicarbonate ($NaHCO_3$)	84.010		0.038	0.454						0.454	
Potassium Phosphate d (K_2HPO4)	174.200		0.225				1.292		1.292		
Potassium Phosphate m (KH_2PO4)	136.090		0.225				1.653		1.653		
Sodium Sulfide ($Na_2S.9H_2O$)	240.190		0.569	2.371				2.371			
Sodium Sulfate (Na_2SO_4)	142.04		5.323	37.476							37.476
		12.840		**47.830**	**1.107**	**4.206**	**2.945**	**2.371**	**2.945**	**0.454**	**37.476**
TOTALS											
Average values											
12.84 mM Cl											
0.576 mM Mg											
0.052 mM Ammonium											
2.371 mM sulfide											
70.961 mM sodium											
0.020 mM phosphate											
2.072 mM potassium											
0.454 mM bicarbonate											
37.476 mM Sulfate											